UNIVERSITY OF THE
WITWATERSRAND,
JOHANNESBURG

DISSOLUTION OF COPPER FROM WASTE PRINTED CIRCUIT BOARDS (PCBs) IN ACIDIC CUPRIC CHLORIDE MEDIA (H_2SO_4-$CuSO_4$-NaCl)

MSc (50/50) Research Report

Prepared By

Duduzile Nontobeko Nxumalo

1430668

Submitted to

School of Chemical and Metallurgical Engineering, Faculty of Engineering and the Built Environment, University of the Witwatersrand, Johannesburg, South Africa, *in partial fulfilment of the requirements for the degree of Master of Science in Engineering*

Supervisor(s): **Prof. Vusumuzi Sibanda**

Mr Petrus Basson

October, 2025

ACKNOWLEDGEMENTS

I wish to express my heartfelt gratitude to my supervisor Prof. Vusumuzi Sibanda for his continuous guidance and support.

I owe a great deal of thanks to my former line manager, Mr Petrus Basson, whose expertise and insights were invaluable to the completion of this work.

I am thankful to my colleagues at Mintek's Biometallurgy Division for their encouragement and positive energy throughout this journey. A special mention to Richard Mavhunga and Segofatso Motloutsi for assistance with sample preparation and solution analysis.

To my family, I am grateful for your love, support and encouragement which gave me the strength and courage to finish.

All glory be unto God, the Almighty, who has given me life and strength.

Lastly, I gratefully acknowledge Mintek for the financial support and resources that enabled this research.

DECLARATION

I solemnly declare that the research report titled 'Dissolution of copper from waste printed circuit boards (PCBs) in acidic cupric chloride media' submitted to the University of Witwatersrand in partial fulfilment for the degree Master of Science in Engineering: Metallurgy and Materials is my own work. This work was carried out under the supervision of Prof. Vusumuzi Sibanda and Mr. Petrus Basson. It has not been submitted before for any degree or examination to any other university.

01/10/25

Duduzile Nontobeko Nxumalo

ABSTRACT

This study investigated the dissolution of copper from a high-grade waste printed circuit board (PCB) sample in acidic, cupric chloride media (H_2SO_4-$CuSO_4$-NaCl + Air). The effects of particle size, solids concentration, acidity, temperature, concentrations of cupric ion, chloride and ferrous ion as well as pre-leach calcination were evaluated in agitated reactors. Copper dissolutions of up to 98% were obtained under optimised conditions. The findings revealed that higher solution potential and dissolved oxygen concentrations significantly enhance the dissolution rate, while reducing particle size and solids concentration improved mass transfer efficiency. Calcination as a pre-treatment significantly improved the leaching kinetics, with 93% copper dissolutions achieved after 2 hours. Under the best conditions, comparable results were achieved at both bench and pilot scale, demonstrating potential for large-scale application. Overall, copper dissolution is therefore primarily governed by solution potential, dissolved oxygen concentration, particle size, solids concentration, and acidity. PCB heterogeneity affects mass balance accuracy, highlighting the need for homogenisation procedures to ensure consistent and representative results. A key recommendation is the optimisation of solution potential through enhanced oxygen availability, and higher initial cupric ion concentrations which can substantially improve the rate of copper dissolution.

Keywords: copper dissolution, printed circuit boards, leaching, cupric chloride, waste recycling, hydrometallurgy

TABLE OF CONTENTS

CHAPTER 1: INTRODUCTION 1

1.1. BACKGROUND 1
1.2. RESEARCH PROBLEM AND RATIONALE 2
1.3. RESEARCH OBJECTIVES 3
1.4. RESEARCH QUESTIONS 4
1.5. THESIS OUTLINE 4
1.6. LIMITATIONS 4

CHAPTER 2: LITERATURE REVIEW 5

2.1. OVERVIEW OF E-WASTE AND PCBS 5
2.1.1. PCBs: Materials, Components and Composition 5
2.2. RECYCLING VALUE CHAIN 7
2.2.1. End-Processing of PCBs 7
2.3. LEACHING OF METALS FROM WASTE PCBS 10
2.3.1. Acid Leaching 10
2.3.2. Bioleaching 12
2.3.3. Halide Leaching 13
2.3.4. Oxidants 13
2.4. CUPRIC CHLORIDE LEACHING OF COPPER 15
2.4.1. Chloride Chemistry 15
2.4.2. Application to Ores, Concentrates and Waste PCBs 18
2.5. REACTION KINETICS 20
2.6. PARAMETERS AFFECTING THE RATE AND EXTENT OF LEACHING 22
2.6.1. Particle Size 22
2.6.2. Solids Concentration 22
2.6.3. Temperature 22
2.6.4. Reagent Concentration 23
2.7. SUMMARY 25

CHAPTER 3: EXPERIMENTAL METHODS AND MATERIALS 26

3.1. EXPERIMENTAL PLANNING 26
3.2. RATIONALE 28
3.2.1. Lixiviant Selection 28
3.2.2. Particle Size 28
3.2.3. Solids Concentration 28
3.2.4. Temperature 29
3.3. MATERIALS AND REAGENTS 29
3.3.1. PCB Sample 29
3.3.2. Working Solutions 30

3.4. ANALYTICAL METHODS 31
3.4.1. Solid Head and Residue Samples 31
3.4.2. Solution Samples 31
3.5. EQUIPMENT 32
3.5.1. Bench-Scale Leach Tests 32
3.5.2. Mini-Pilot Leach Test 33
3.5.3. Experimental Procedure 35
3.6. DATA PROCESSING AND INTERPRETATION 36
3.6.1. Statistical Analysis 36
3.6.2. Metal Dissolutions 36
3.6.3. Acid Consumptions 37

CHAPTER 4: RESULTS 38

4.1. HEAD SAMPLE CHARACTERISATION 38
4.1.1. Particle Size Distribution of the Waste PCB Head Samples 38
4.1.2. Chemical Analysis 38
4.2. BENCH-SCALE LEACH TESTS 41
4.2.1. Baseline Conditions 41
4.2.2. Effect of Particle Size 42
4.2.3. Effect of Solids Concentration 43
4.2.4. Effect of Chloride Concentration 45
4.2.5. Effect of Temperature 46
4.2.6. Effect of pH 47
4.2.7. Effect of Initial Cupric Concentration 48
4.2.8. Effect of Initial Ferrous Concentration 50
4.2.9. Effect of Pre-leach Calcination 51
4.2.10. Summary of Results 53
4.3. MINI-PILOT LEACH TEST 54
4.3.1. Recommended Conditions 54
4.3.2. pH, Redox and Dissolved Oxygen Profiles 54
4.3.3. Copper and Iron Dissolution Profiles 56
4.3.4. Acid Consumption Profiles 56
4.3.5. Dissolution of Other Base Metals and Mass Balances 57

CHAPTER 5: DISCUSSION 60

5.1. DISSOLVED OXYGEN CONCENTRATION AND SOLUTION POTENTIAL 60
5.2. EFFECT OF PARTICLE SIZE AND SAMPLE HETEROGENEITY 60
5.3. EFFECT OF SOLIDS CONCENTRATION 61
5.4. EFFECT OF CHLORIDE AND INITIAL CUPRIC CONCENTRATIONS 61
5.5. EFFECT OF TEMPERATURE 61
5.6. EFFECT OF INITIAL FERROUS CONCENTRATION 62
5.7. ACIDITY AND ACID CONSUMPTION 62

5.8. CALCINATION 62
5.9. ELEMENT MASS BALANCES 62
CHAPTER 6: CONCLUSIONS AND RECOMMENDATIONS 63
CHAPTER 7: REFERENCES 64

APPENDIX A: LITERATURE SUPPORTING MATERIAL 71
APPENDIX B: METHODOLOGY SUPPORTING MATERIAL 73
APPENDIX C: EXPERIMENTAL DATA AND RESULTS 79

LIST OF FIGURES

Figure 1.1: Volumes of E-waste Generated in 2022 1
Figure 2.1: Classification of Typical Waste PCBs 6
Figure 2.2: Stages of the E-waste Recycling Value Chain 7
Figure 2.3: Potential Processing Options for E-waste 8
Figure 2.4: Leaching of a low-grade PCB Sample in Sulphuric Acid (No 'Oxidant' Added) 14
Figure 2.5: Potential-pH Diagram for Copper-Chlorine-Water System at 25°C 16
Figure 2.6: Scheme of Possible Steps in the Leaching of Metallic Copper with Cu(II) in Chloride Medium 17
Figure 2.7: Schematic of the Steps in the Dissolution of Metallic Copper in Solutions 20
Figure 2.8: Solubility of Oxygen in Pure and Sea Water 21
Figure 3.1: Preparation of PCB Samples 29
Figure 3.2: PCB Fractions As-Received 30
Figure 3.3: PCB Sample Size Fractions 30
Figure 3.4: Schematic Diagram of the Experimental Set-Up 32
Figure 3.5: Mini-Pilot Experimental Set-Up 34
Figure 4.1: Particle Size Distributions of the bulk PCB Sample 38
Figure 4.2: Leach Profiles at Baseline Conditions 41
Figure 4.3: Leach Profiles at Different Particle Sizes 43
Figure 4.4: Leach Profiles at Different Solids Concentrations 44
Figure 4.5: Leach Profiles at Different Chloride Concentrations 45
Figure 4.6: Leach Profiles at Different Temperatures 47
Figure 4.7: Leach Profiles at Different pH Levels 48
Figure 4.8: Leach Profiles at Different Initial Cupric Concentrations 49
Figure 4.9: Leach Profiles at Different Initial Ferrous Concentrations 51
Figure 4.10: Leach Profiles for Calcined Samples 52
Figure 4.11: pH Profile (Pilot Test) 55
Figure 4.12: Redox and Dissolved Oxygen Profiles (Pilot Test) 55
Figure 4.13: Copper and Iron Dissolution Profiles (Pilot Test) 56

Figure 4.14: Acid Consumption Profiles (Pilot Test) 57
Figure 4.15: Concentrations of Other Metals Over Time (Pilot Test) 58

LIST OF TABLES

Table 2.1: Typical Metal Content in Waste PCBs 6

Table 2.2: Standard Reduction Potentials at 25°C.....14

Table 2.3: Summary of Optimal Cupric Chloride Leaching Parameters from Previous Studies.....19

Table 3.1: Baseline Conditions.....26

Table 3.2: Experimental Matrix for Bench-Scale Leach Tests 27

Table 3.3: Chemical Reagents 31

Table 4.1: Chemical Analysis of the PCB Head Sample by Size (Average Values) 40

Table 4.2: Element Mass Distributions of the PCB Head Sample.....40

Table 4.3: Chemical Analysis of the - 1 mm Head Sample (Statistical Analysis).....40

Table 4.4: A Summary of Cu and Fe Dissolutions.....53

Table 4.5: Experimental Matrix for the Pilot Leach Test 54

Table 4.6: Summary of Dissolutions and Mass Balances for the Pilot Test.....59

CHAPTER 1: INTRODUCTION

1.1. BACKGROUND

The advancements in technology have given rise to our dependence on electrical and electronic equipment (EEE) for everyday life. This has led to an incredible growth in the production and consumption of EEE and subsequently causing a significant increase of waste electric and electronic equipment (WEEE) streams commonly known as e-waste worldwide. In general, e-waste refers to old, end-of life EEE such as televisions, mobile cell phones, computers, washing machines and various other household items which have been discarded by their original users (Nyanjowa and James, 2015). The global volume of e-waste generated in 2022 is presented in Figure 1.1. According to the United Nations Institute for Training and Research (Unitar), e-waste is the fastest-growing waste stream in all the countries around the world, with a record of 62 billion kg of e-waste generated in 2022 globally (Baldé et al., 2024). As a result, many countries are confronted by the considerable environmental and human health risks associated with poorly managed e-waste (Forti et al., 2020).

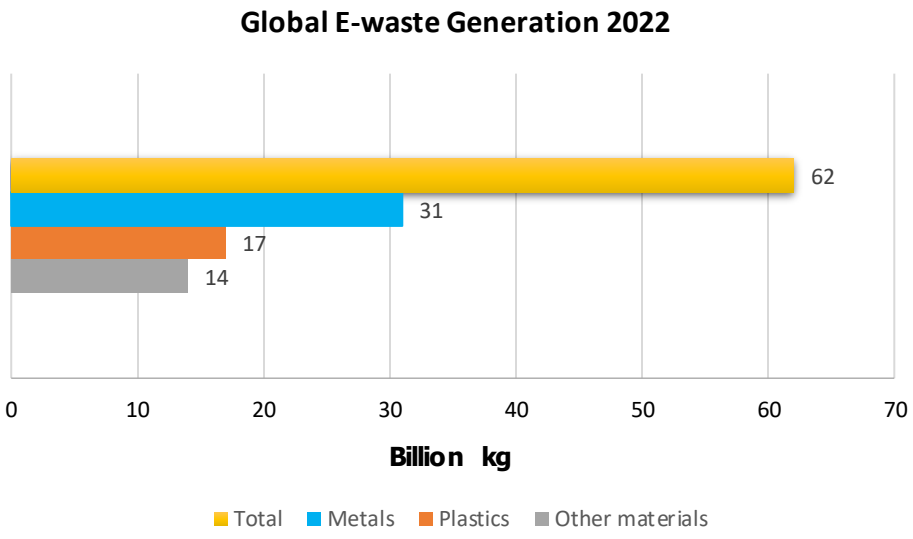

Figure 1.1: Volumes of E-waste Generated in 2022
(Adapted from The Global E-waste Monitor 2024, Baldé et al., 2024)

The presence of toxic elements such as lead and mercury in some components of e-waste has negative effects on human health and the environment. If e-waste is disposed of in landfills, the hazardous elements enter surrounding soil, groundwater and ultimately end up in animals, humans and vegetation. Therefore, specialised

treatment and recovery systems are required to protect the environment and human life.

Some components of e-waste such as the printed circuit board (PCB) are rich in valuable metals and materials. As a result, the large quantities of e-waste have caused a surge of interest in e-waste as a secondary source of valuable metals thus known as an "Urban-mine" (Forti et al., 2020). In 2022, the overall gross value of the metals contained in e-waste was estimated at USD 91 billion (Baldé et al., 2024). Most of the potential value in secondary raw materials in e-waste lies in copper (Cu) (USD 19 billion), gold (Au) (USD 15 billion) and iron (Fe) (USD 16 billion) (Baldé et al., 2024). The waste PCBs represent a significant portion of this value, accounting for over 40% of the total e-waste metal value (Kumar et al., 2018).

Conventional methods for recovering metals from e-waste use extremely high temperatures (pyrometallurgy) to separate and recover valuable metals through processes such as smelting and / or refining. The drawbacks of pyrometallurgical methods such as high energy requirements, gas emissions and potential for dioxin generation has induced an interest in the development and application of hydrometallurgical processes for the recovery of precious, base and rare earth elements from e-waste.

This research focused on the hydrometallurgical recovery of copper from waste PCBs via leaching in acidic chloride media. The study investigated the influence of key process parameters such as solids concentration, chloride concentration, temperature, particle size, acidity, and the concentrations of cupric and ferrous ions. The scalability of the best leach conditions was evaluated at a mini pilot scale. In addition, the potential effect of pre-leach calcination of the waste PCBs on copper dissolution was also evaluated under best conditions.

1.2. RESEARCH PROBLEM AND RATIONALE

The rising volumes of e-waste generated globally make the recovery of metals from waste PCBs an important subject for the preservation of the environment as well as the conservation and recovery of resources. Recovering metals from waste PCBs reduces the volume of e-waste that ends up in landfills, minimising environmental pollution. Waste PCBs contain a significant amount of copper. Copper is a critical material for global energy transition. The recovery and recycling of copper is essential to meet the ever-increasing demand for this raw material. During the last decade, more than 30% of global copper demand was met with recycled copper (International Copper Association, 2024).

Understanding how different parameters influence the efficiency of copper leaching from waste PCBs is a contribution to the advancement of recycling technologies. In

hydrometallurgical processes, the removal of base metals, such as copper, allows for a more selective and efficient recovery of precious metals such as gold in subsequent leaching steps.

Various reagent systems have been studied for the recovery of metals from waste PCBs. These include: sulphate, chloride, nitrate, iodide, ammonia, cyanide, thiourea, thiosulphate, amino acids, ionic liquids and bio-assisted systems. As metals in waste PCBs are present in native and alloy form, an oxidant such as hydrogen peroxide (H_2O_2), oxygen (O_2) and ferric (Fe(III)) is required to effectively dissolve base metals such as copper from waste PCBs (Yazici & Deveci, 2013). There are very limited studies on the leaching of copper from waste PCBs by chloride leaching, particularly in cupric chloride media with sulphuric acid.

One of the shortcomings of previous studies is the focus on micro-scale tests, conducted at very low solids concentrations, with metal dissolutions reported without elemental mass balances and reagent consumptions. These experimental limitations do not allow for the investigations to adequately represent a realistic waste PCB processing environment where the heterogeneity of PCBs and high reagent consumptions can be a challenge. In this study, experiments were conducted at higher solids concentrations, with monitoring of elemental mass balances and reagent consumption, in order to provide more realistic insights into copper recovery from waste PCBs under practical processing conditions.

1.3. RESEARCH OBJECTIVES

This study investigated the leaching of copper from a waste PCB sample in acidic cupric chloride media (H_2SO_4-$CuSO_4$-NaCl) with the following sub-objectives:

a. To determine the chemical composition of the waste PCB sample and compare with literature.
b. To investigate the effect of various parameters on the rate and extent of overall copper dissolution in 2-4 L batch agitated reactors. These include: solids concentration, temperature, chloride concentration, initial concentration of cupric (Cu(II)) and ferrous ions (Fe(II)), pH and pre-leach calcination.
c. To determine the reagent consumptions (sulphuric acid) associated with the metal dissolutions achieved.
d. To perform metal mass balances to assess the accuracy of analytical methods in the characterisation of heterogeneous waste PCB samples.
e. To evaluate the scalability of the best leach conditions in a 23 L, agitated reactor.

1.4. RESEARCH QUESTIONS

The primary question of this study is: what factors govern copper dissolution from waste PCBs in acidic cupric chloride media, and how can these insights guide scalable processing?

Sub-questions:

a. How do key process parameters i.e. solids concentration, chloride concentration, temperature, particle size, acidity, and the concentrations of cupric and ferrous ions affect the rate and extent of copper dissolution, as well as reagent (acid) consumption?
b. Are the best leach conditions scalable?
c. To what extent are the selected analytical methods accurate and reliable for characterizing metals in heterogeneous PCB samples?

1.5. THESIS OUTLINE

This thesis is divided into five chapters as follows:

Chapter 1: Introduction- introduces the research problem and outlines the objectives, significance and scope of the study.

Chapter 2: Literature review- provides a comprehensive overview of e-waste flows, composition and challenges of PCB recycling, different leaching methods, chloride leaching of copper and gaps in the literature.

Chapter 3: Materials and methods- this chapter details the experimental set-up, materials and procedures used in the study.

Chapter 4: Results and discussion- this chapter presents experimental findings, key aspects include: characterisation of the PCB sample, effect of leaching parameters on copper dissolution and other base metals.

Chapter 5: Discussion- provides the interpretation of the findings in relation to fundamental principles and previous studies.

Chapter 6: Conclusions and recommendations- this chapter summarises the key findings of the study and makes recommendations for future research.

1.6. LIMITATIONS

This study focused on the leaching of copper from waste PCBs. Recovery of copper from leach solutions and leaching of other metals were not the focus of this investigation.

CHAPTER 2: LITERATURE REVIEW

2.1. OVERVIEW OF E-WASTE AND PCBS

2.1.1. PCBs: Materials, Components and Composition

PCBs can be defined as rugged, non-conductive boards built on substrate-based structure (Bhunia & Tehranipoor, 2019). The PCBs are integral components of all types of EEE items, and they are mainly used to provide electrical connection and mechanical support to the electrical components of a circuit. A PCB is found in almost all electronic products used in daily life, for example, mobile phones, television sets and computers and can be easily identified as the green-coloured board in most cases. Modern-day PCBs largely vary in complexity, starting from single layer PCBs to complex designs with as many as 20 to 30 layers with hidden vials and embedded components (Bhunia & Tehranipoor, 2019).

The composition of e-waste varies significantly as it depends on the origin, the age of electronic devices and the manufacturer (Khaliq et al., 2014). PCBs vary depending on the type of appliance, *e.g.* cell phone, TV, desktop computers, laptops, etc. PCBs from personal computers and mobile phones contain the highest content of valuable metals (Chehade et al., 2012). Several improvements in electronic devices have occurred over the years; resulting in the decrease of value metal content in these devices. There is no standard composition for PCBs, even the so-called typical values only reflect PCBs from specific manufacturers and time periods (Cui & Zhang, 2008). PCBs consist of metallics, organics or plastics and ceramics. Typical compositions of PCBs quoted in literature are 28-40% metallics, 23-30% plastics and 19-30% ceramics (Kamberovic et al., 2011; Jha et al., 2012; Montero et al., 2012).

While there is no international standard grading of PCBs, waste PCBs are generally classified into three main categories that essentially indicate their precious metal content, *i.e.* high-grade PCBs (200-400 ppm gold), medium-grade PCBs (minimum 100 ppm gold) and low-grade (less than 50 ppm gold) (Nyanjowa & James, 2015). A typical classification of waste PCBs by Desco Electronic Recyclers is presented in Figure 2.1.

Several studies have shown that more than 70% of the contained value in PCBs lies in gold, silver, palladium and copper, with copper being the major metal in PCBs. These metals are seen as the economic drivers for e-waste recycling processes (Cui & Zhang, 2008; Tuncuk et al., 2012; Khaliq et al., 2014).

Table 2.1 shows some of the metal content of waste PCBs reported in previous studies.

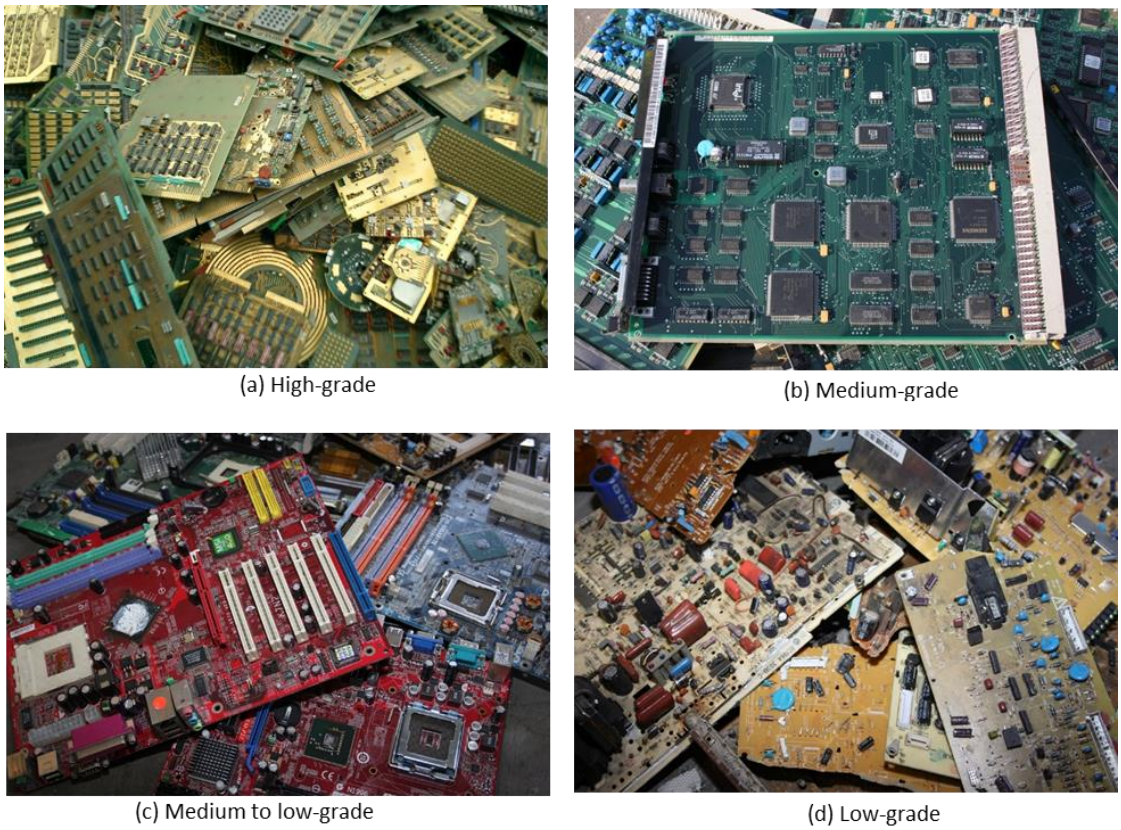

(a) High-grade (b) Medium-grade

(c) Medium to low-grade (d) Low-grade

Figure 2.1: Classification of Typical Waste PCBs

(Source: Desco Electronic Recyclers - Identify E-Waste - What We Recycle, 2017)

Table 2.1: Typical Metal Content in Waste PCBs

Metal	Metal Content (%)						
	A	B	C	D	E	F	G
Ag*	110-3301	1490	1907	800	1000	688	694
Al	-	0.47	0.69	4.7	5	11.69	1.33
Au*	80-1000	440	890	800	250	238	86
Cu	10-26.8	27.99	25.24	23.73	20	30.57	18.5
Fe	-	1.18	0.98	7.47	7	15.21	2.05
Ni	-	1.23	0.93	3.32	1	1.58	0.43
Pb	0.99-4.19	2.17	2.22	4.48	1.5	6.7	2.66
Pd*	10-294	50	47	210	110	-	97
Pt*	4.6-30	57	17	-	-	-	-
Sb	-	-	-	1.82	-	-	-
Sn	-	3.26	3.17	3.65	-	7.36	4.91
Zn	0.16-2.17	2.01	2.05	-	-	1.86	-

* Metals quoted in ppm, A : (Montero et al., 2012); B and C: (Kamberovic et al., 2011b); D and E: (Zhang et al., 2012); F: (Eng et al., 2016); G: (Yazici & Deveci, 2015a)

2.2. RECYCLING VALUE CHAIN

The four main stages of the e-waste recycling value chain are summarised in Figure 2.2. These include collection, dismantling, pre-processing and end-processing (Lydall et al., 2017). The volume of valuable materials recovered from e-waste is contingent on the efficiency of each stage as well as the regional e-waste management systems.

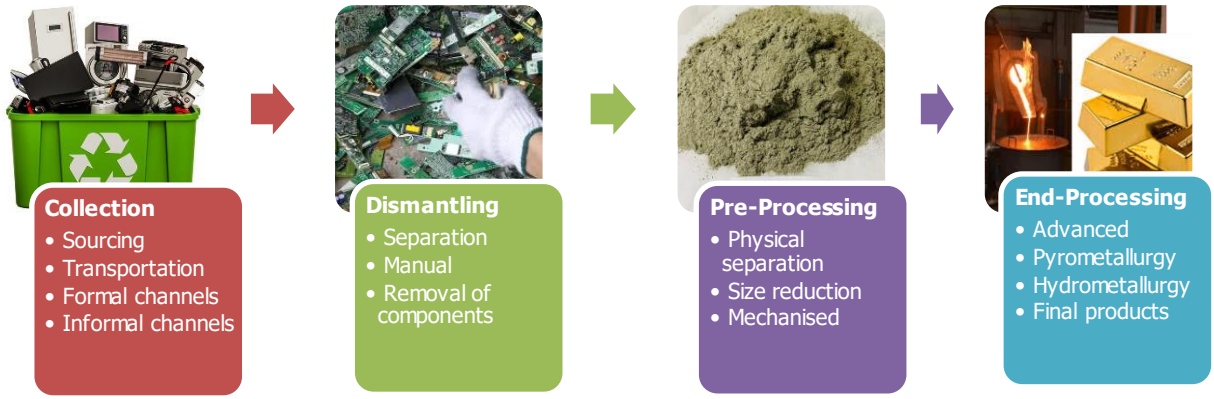

Figure 2.2: Stages of the E-waste Recycling Value Chain

E-waste is collected through formal and informal channels, and these vary by region and country. Common approaches include municipal collection points, retailers, pick-up services, drop-off at specialised treatment facilities, etc.

The recycling of PCBs starts with dismantling, which involves the removal of electronic components (*e.g.* capacitors), toxic components (*e.g.* batteries) and separation of metallic and non-metallic fractions into distinct recyclable streams. The dismantling of PCBs is typically performed manually using tools like screw drivers, pliers, drills, hammers, chisels and grinders (Lydall et al., 2017).

Pre-processing of PCBs varies depending on the chosen method for processing and metal recovery. The pre-processing stage generally focuses on size reduction and upgrading the valuable materials (Lydall et al., 2017; Moyo et al., 2020). The size reduction is carried out by impacting, shearing, milling and pulverising using equipment such as shredders, hammer mills, knife mills, etc. Common physical processes include gravity, magnetic and electrostatic separation.

2.2.1. End-Processing of PCBs

Processing is the last stage of the e-waste recycling value chain. Following metal upgrading by physical separation, the valuable metal fraction can be recovered either by the traditional pyrometallurgical route or by a direct hydrometallurgical route or a combination of both methods as shown in Figure 2.3.

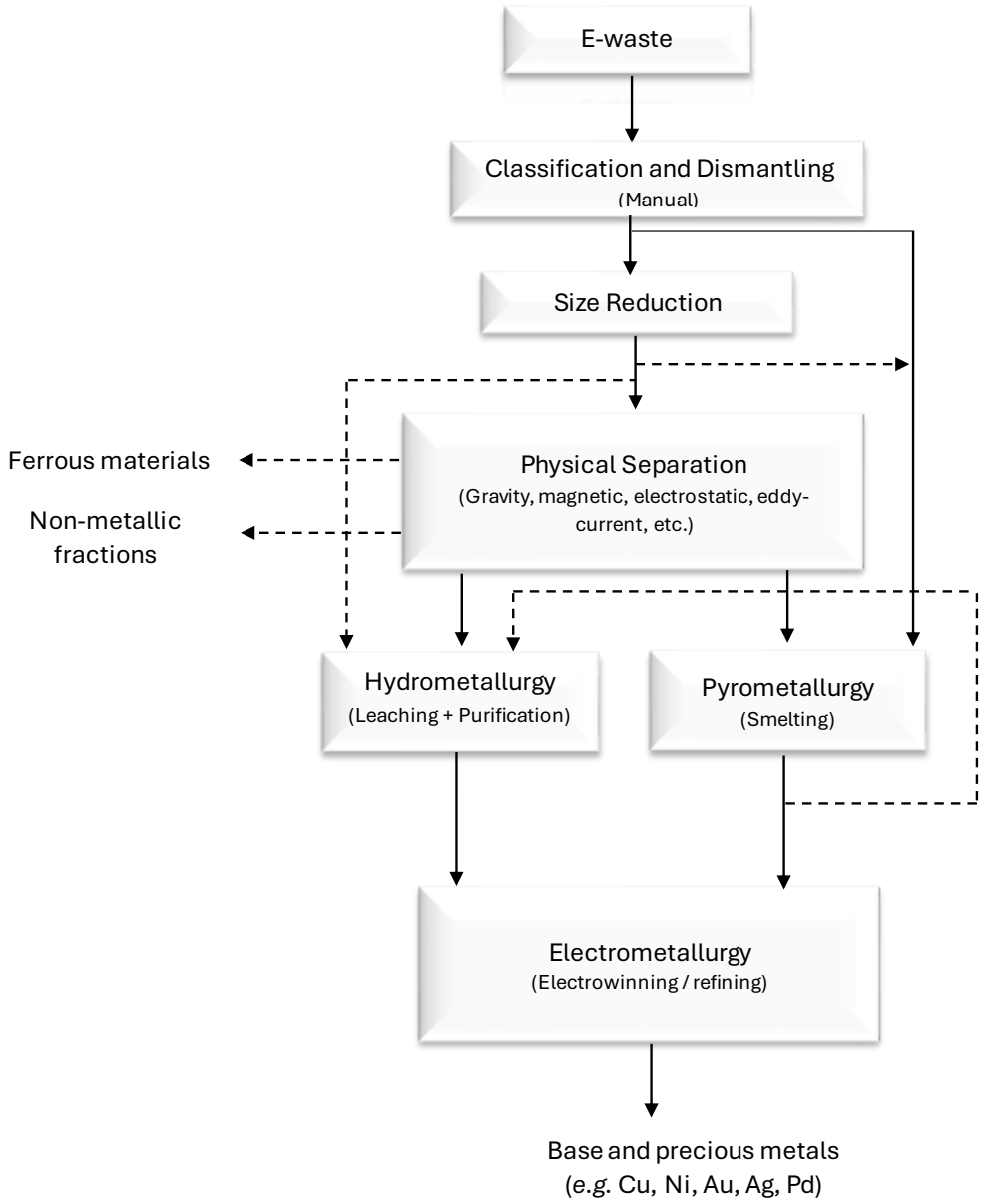

Figure 2.3: Potential Processing Options for E-waste
(Adapted from Tuncuk et al., 2012)

2.2.1.1. Pyrometallurgical Processing

Pyrometallurgical methods for recovering metals from PCBs use high-temperature processes to extract valuable metals through processes such as calcination, drossing, smelting and pyrolysis. Pyrometallurgical processing is currently the main industrial process used to treat waste PCBs (Fazari et al., 2024; Kaya, 2016) and is often integrated with other technologies such as hydrometallurgy to further improve the efficiency of metal recovery. Well-established technologies for co-smelting include ISASMELT™ used by Umicore (Belgium) and Aurubis (Germany) and Ausmelt top

submerged-lance (TSL) smelters used by Dowa mining (Japan) and GRM (Korea). Tetronics International uses plasma-enhanced (plasma arch furnace) processes to recover metals from e-waste as primary feedstock (Tetronics, 2024).

One of the key advantages of pyrometallurgy is its ability to recover a wide range of metals from complex materials including base metals (*e.g.* copper, lead and tin) and precious metals (*e.g.* gold, silver and platinum) (Khaliq et al., 2014). For instance, Umicore's integrated metals smelter and refinery recovers Cu, Ni, As, Ag, Au, Pt, Pd, Rh, Ru, Ir, Pb, Sn, Sb, Bi, In, Se and Te from concentrates and e-waste streams (Umicore, 2024). The Rönnskär smelters (Boliden Ltd, Skelleftehamn, Sweden) recovers various metals from e-waste scrap including Cu, Ag, Au, Pt, Pd, Ni, Se and Zn (Khaliq et al., 2014) and the Noranda process in Quebec recovers Cu, Au, Ag, Pt, Pd, Se, Te and Ni (Khaliq et al., 2014) from a blend of copper concentrates and e-waste feed material.

Pyrometallurgical processes have been widely adopted for recovering valuable metals from e-waste; however, they have certain limitations. These include (Gu et al., 2019; Khaliq et al., 2014; A. Kumar et al., 2017; Sohaili et al., 2012):

a. Generation of harmful emissions including toxic gases (*e.g.* dioxins, particulate matter, etc).
b. Production of large volumes of hazardous solid residues such as slag, sludge, ash and other products.
c. Energy intensive and require reliable high-voltage power supply.
d. Inability to recover plastics as they partially replace coke as an energy source
e. Require large capital investment.
f. Low purity of precious metals, requiring subsequent treatment by hydrometallurgical methods.

2.2.1.2. Hydrometallurgical Processing

Hydrometallurgical processes involve the use of aqueous solutions to selectively dissolve and recover metals from PCBs. These methods are widely used due to their ability to extract metals with high selectivity and efficiency. Typical hydrometallurgical processes consist of the following steps: (i) pre-treatment (*e.g.* sorting, size reduction and chemical pre-treatment), (ii) leaching (metal dissolution), (iii) purification and separation (*e.g.* ion exchange, solvent extraction and precipitation) and (iv) metal recovery (*e.g.* electrowinning, precipitation and cementation).

Compared to pyrometallurgical processing, hydrometallurgy has been proven to be more cost-effective, with high selectivity allowing for production of high purity metals. Hydrometallurgical processes are less energy intensive with low emissions, reducing their impact to the environment (Tuncuk et al., 2012). However, these processes

have certain limitations that hinder their application on the industrial scale. These include (Fazari et al., 2024; Khaliq et al., 2014; Kumar et al., 2017):

a. Difficulty in processing heterogenous and complex materials like e-waste streams.
b. Requirement for fine grinding for efficient leaching.
c. Complex separation of dissolved metals from polymetallic feeds.
d. Risk of metal losses during multiple dissolution steps.
e. High reagent consumptions (operating costs).
f. Slower metal dissolution rates.

2.3. LEACHING OF METALS FROM WASTE PCBS

Leaching is a process in which a solvent, mostly a liquid, is used to solubilise constituents of interest from a solid material. The leaching of PCBs entails the use of acidic or alkaline solutions to dissolve and recover metals.

Various leaching reagent systems have been studied for the recovery of base and precious metals from waste PCBs. These include: sulphate, chloride, nitrate, iodide, ammonia, thiourea, cyanide, thiosulphate, aqua regia, amino acids, ionic liquids and bioleaching systems (Birloaga & Vegliò, 2016; Khatri et al., 2018; Kim et al., 2011; Ping et al., 2009; Tuncuk et al., 2012; Yazici & Deveci, 2013, 2015b).

This section describes some of the leaching reagents that have been investigated for the recovery of metals from waste PCBs, with a focus on base metals.

2.3.1. Acid Leaching

Sulphuric acid is the main reagent in most hydrometallurgical processes and the sulphate solution chemistry is well-established (Winand, 1991). However, other acidic reagents have been investigated for the leaching of base metals from waste PCBs, for example, nitric acid (HNO_3), hydrochloric acid (HCl), aqua regia (HNO_3 + 3HCl), and halides (chloride, iodide, bromide).

Sulphate-based leaching systems with oxidants such as H_2O_2, O_2 and Fe(III) have been proven to be effective for leaching copper and other base metals from waste PCBs. The leaching of copper in sulphuric acid with oxygen, ferric sulphate and hydrogen peroxide is shown in Equations (1), (2) and (3), respectively.

$$Cu_{(s)} + 0.5O_{2(aq)} + H_2SO_{4(aq)} \rightarrow CuSO_{4(aq)} + H_2O_{(l)} \quad (1)$$

$$Cu_{(s)} + Fe_2(SO_4)_{3(aq)} + H_2SO_{4(aq)} \rightarrow CuSO_{4(aq)} + H_2O_{(l)} + 2FeSO_{4(aq)} \quad (2)$$

$$Cu_{(s)} + H_2O_{2(aq)} + H_2SO_{4(aq)} \rightarrow Cu^{2+}_{(aq)} + SO_4^{2-}{}_{(aq)} + 2H_2O_{(l)} \quad (3)$$

Several studies have investigated the leaching of copper from waste PCBs with sulphuric acid and hydrogen peroxide (Birloaga & Vegliò, 2016; Hao et al., 2022; Kamberović et al., 2010; Kumar et al., 2014; Wang et al., 2016). Studies by Kamberović et al. (2010), as part of the HydroWee project, achieved up to 100% copper dissolution in 5 hours with 1.5-2 M H_2SO_4, 50-100 g/L solids-liquid ratio at 75-80°C with 16 L/h O_2 and 40 mL/h H_2O_2 as oxidants at lab-scale. The copper dissolution was strongly influenced by the acid concentration, H_2O_2 addition and temperature. The H_2SO_4-H_2O_2 system has been proven effective to leach copper from waste PCBs but the high H_2SO_4 and H_2O_2 consumptions are some of the drawbacks.

Nitric acid is a strong oxidising acid and has the ability to leach most base metals without the addition of an oxidant. Dissolution of copper dissolution from 2 to 4 mm waste PCB samples was shown to increase with an increase in HNO_3 concentration, with up to 96% dissolution achieved with 4 M HNO_3, at 90°C in 2 hours (Kumar et al., 2014). The reaction for the leaching of copper with HNO_3 is as follows :

$$Cu_{(s)} + 4HNO_{3(aq)} \rightarrow Cu(NO_3)_{2(aq)} + 2H_2O_{(l)} + 2NO_{2(g)} \quad (4)$$

Kumar et al. (2014) found that at higher HNO_3 concentrations, the acid fumes were significant; hence a lower agitation speed was used. The study concluded that HNO_3 achieved higher copper extractions (96%) compared to H_2SO_4 with H_2O_2 (76%). However, H_2SO_4 was identified as the preferred leaching medium. This is because HNO_3 is highly corrosive, requiring costly construction materials, and is generally more expensive than H_2SO_4.

Several studies have reported high recoveries of base and precious metals from PCBs with hydrochloric acid (HCl) or aqua regia (1HNO_3 : 3HCl) (Jadhav & Hocheng, 2015). HCl has also been proven effective for the leaching of Sn which is poor in H_2SO_4. Unlike HNO_3, HCl is a non-oxidising acid and requires an oxidant such as oxygen for effective leaching of copper.

Several studies have investigated the use of acidic ionic liquids (IL) for the leaching of base metals from e-waste. For example, the use of acidic ionic liquids such as 1-butyl-3 methylimidazole hydrogen sulphate ([Bmim]HSO_4) and 1-H-3-methylimidazole hydrogen sulphate ([Hmim]HSO_4) to leach base metals from PCBs was investigated by Barrueto et al (2021). The findings demonstrated the ability of ionic liquids to leach metal ions as the primary reagent in the leaching solution, with up to 86% Cu and 99.5% Co dissolution achieved (Barrueto et al., 2021). While the potential of ILs to leach metals from PCBs has been demonstrated, they have some drawbacks such as high cost, limited availability, recycling and disposal challenges.

Some researchers have investigated the alkaline leaching of copper and other base metals from PCBs using reagents such a glycine (Broeksma, 2018). Glycine is the most viable amino acid, due to its relatively low cost and bulk availability. The main advantage of alkaline leaching is that both base and precious metals can be recovered in the same media without the need for the neutralisation step.

2.3.2. Bioleaching

Bioleaching is a process that uses microorganisms to aid solubilisation of metals from their various sources (*e.g.* ores, concentrates, PCBs, etc). Bioleaching using sulphur and iron oxidising bacterial and archaea is currently applied in commercial operations to process base metal (copper, nickel, cobalt, zinc), and uranium ores and concentrates. Similar to bioleaching is a process called bio-oxidation in which iron sulphide minerals associated with but not necessarily part of the mineral of interest are oxidised or dissolved which in turn liberates the mineral of interest for further processing, *e.g.* bio-oxidation of refractory gold. Advantages of bioleaching include rapid oxidation of Fe(II) to Fe(III) (oxidant), lower capital costs and environmentally friendly.

The common application of bioleaching for non-sulphidic, metallic materials such as PCBs is the regeneration of the oxidant, iron(III), by iron oxidising bacterial / archaea, which oxidise the iron(II) leached from PCBs to iron(III) in the presence of oxygen. The copper is then mobilised by the consumption of Fe(III) which is evident in Equations (5) and (6) (Sodha et al., 2020a; Yang et al., 2014).

$$4Fe^{2+}_{(aq)} + O_{2(aq)} + 4H^{+}_{(aq)} \xrightarrow{\text{bacteria}} 4Fe^{3+}_{(aq)} + 2H_2O_{(l)} \quad (5)$$

$$Cu_{(s)} + 2Fe^{3+}_{(aq)} \rightarrow 2Fe^{2+}_{(aq)} + Cu^{2+}_{(aq)} \qquad \Delta G = -82.90 \text{ kJ/mol} \quad (6)$$

Studies conducted on the bioleaching of PCBs have focused on (i) direct leaching where metal leaching is achieved in the presence of microorganisms and (ii) indirect or hybrid leaching where the metabolic leach medium is harvested and used in the leaching of metallic fractions in the absence of microorganisms. The use of indirect leaching is considered more appropriate as it offers greater flexibility in the optimisation of the process (Valix, 2017) and limits the exposure of microorganisms to toxins or conditions that can inhibit microbial activity.

Several studies have investigated the bioleaching of metals from waste PCBs using different microorganisms (Khatri et al., 2018; Valix, 2017; Yang et al., 2014). A study by Yang et al (2008) concluded that direct bioleaching of copper from PCBs using *Acidithiobalillus ferrooxidans* was feasible, with up to 99% dissolution of copper

achieved from a -0.5 mm PCB sample at initial ferric concentrations of 6.66 g/L at 30°C. The copper leaching rate was strongly influenced by the concentration of ferric, pH and volume of stock culture (Yang et al., 2009). Sodha et al. (2020) successfully optimised the indirect bioleaching of copper from 6 cm x 19 cm PCB plates (non-pulverised) following pre-treatment with sodium hydroxide. About 99% copper was leached by ferric which was bio-generated by *leptospirillum ferriphilum (Sodha et al., 2020b)*.

Although the potential application of bioleaching to recover copper from waste PCBs has been demonstrated, the process has some disadvantages including slow kinetics, high sensitivity to process variations (temp, air, poisons) and limited solids content (less than 20%).

2.3.3. Halide Leaching

Halide leaching involves the use of halogen ions (*e.g.* Cl^-, Br^-, I^-) to solubilise metals from PCBs. Halide leaching has been studied extensively and proven effective as an alternative to cyanide for the leaching of gold and silver. The process involves the formation of metal-halide complexes which are stable in solution. For example, in bromine leaching, gold forms complexes such as $AuBr_4^-$, while copper forms $CuBr_2^-$ complexes (Cui & Anderson, 2020). Similarly in chloride-based copper leaching systems, copper forms Cu(I) and Cu(II) chloride complexes such as $CuCl_2^-$ and $CuCl^+$ depending on the chloride concentration. Halides are commonly known to offer high leaching rates, yet only chlorine/chloride has been applied industrially at a commercial scale (Zhang & Xu, 2016). Effective halide leaching involves the use of acids such a HCl, H_2SO_4 or HNO_3 and oxidants such as air/oxygen and H_2O_2. The chloride leaching of copper with cupric and air as oxidants is discussed in detail in Section 2.4.

2.3.4. Oxidants

As metals in waste PCBs are present in native and / alloy form, an oxidant such as H_2O_2, O_2 and Fe(III) is required to effectively dissolve base metals such as copper from waste PCBs (Yazici & Deveci, 2013). The choice of oxidant can significantly impact the efficiency, economic viability and environmental impact of a leaching process. The standard reduction potentials (E°) of some of the elements found in PCBs are presented in Table 2.2.

The dissolution of Cu requires a stronger oxidant with a standard redox potential higher than 0.34 V (vs SHE); the common oxidants in descending oxidation strength include: ozone (2.07 V) > hydrogen peroxide (1.78 V) > hypochlorite (1.63 V) > chlorine gas (1.36 V) > oxygen (1.23 V) > ferric ion (0.77 V) > $CuCl^+$ (0.54 V). The two strongest oxidants, *i.e.* ozone and hydrogen peroxide are expensive while the chlorides are usually not preferred for base metals leaching due to the expensive materials of construction required because of the corrosive nature of chlorides.

Therefore oxygen/air and ferric salts are generally used as these oxidants are cost effective and readily available (Jackson, 1986). Oxygen gas can be used as an oxidant over a wider pH range as compared to the ferric ion, which is limited to pH less than 2, to avoid precipitation as ferric hydroxide ($Fe(OH)_3$).

Table 2.2: Standard Reduction Potentials at 25°C

Reduction Half Reaction	E° (V, vs SHE)	Reduction Half Reaction	E° (V, vs SHE)
$H_2O_{2(aq)} + 2H^+_{(aq)} + 2e^- \rightarrow 2H_2O_{(l)}$	1.78	$Cu^{2+}_{(aq)} + 2e^- \rightarrow Cu_{(s)}$	0.34
$Au^{3+}_{(aq)} + 3e^- \rightarrow Au_{(s)}$	1.50	$2H^+_{(aq)} + 2e^- \rightarrow H_{2(g)}$	0
$O_{2(g)} + 4H^+_{(aq)} + 4e^- \rightarrow H_2O_{(l)}$	1.23	$Pb^{2+}_{(aq)} + 2e^- \rightarrow Pb_{(s)}$	-0.13
$Pt^{2+}_{(aq)} + 2e^- \rightarrow Pt_{(s)}$	1.10	$Sn^{2+}_{(aq)} + 2e^- \rightarrow Sn_{(s)}$	-0.14
$Pd^{2+}_{(aq)} + 2e^- \rightarrow Pd_{(s)}$	0.95	$Ni^{2+}_{(aq)} + 2e^- \rightarrow Ni_{(s)}$	-0.26
$Ag^+_{(aq)} + e^- \rightarrow Ag_{(s)}$	0.80	$Fe^{2+}_{(aq)} + 2e^- \rightarrow Fe_{(s)}$	-0.44
$Fe^{3+}_{(aq)} + e^- \rightarrow Fe^{2+}_{(aq)}$	0.77	$Zn^{2+}_{(aq)} + 2e^- \rightarrow Zn_{(s)}$	-0.76
$Cu^+_{(aq)} + e^- \rightarrow Cu^{2+}_{(aq)}$	0.52	$Al^{3+}_{(aq)} + 3e^- \rightarrow Al_{(s)}$	-1.66

Figure 2.4 shows the dissolution profiles of some of the base metals from a low-grade PCB sample in sulphuric acid solution at 10% (w/w) solids concentration, pH 1.0 and 50°C without the addition of an oxidant and no aeration.

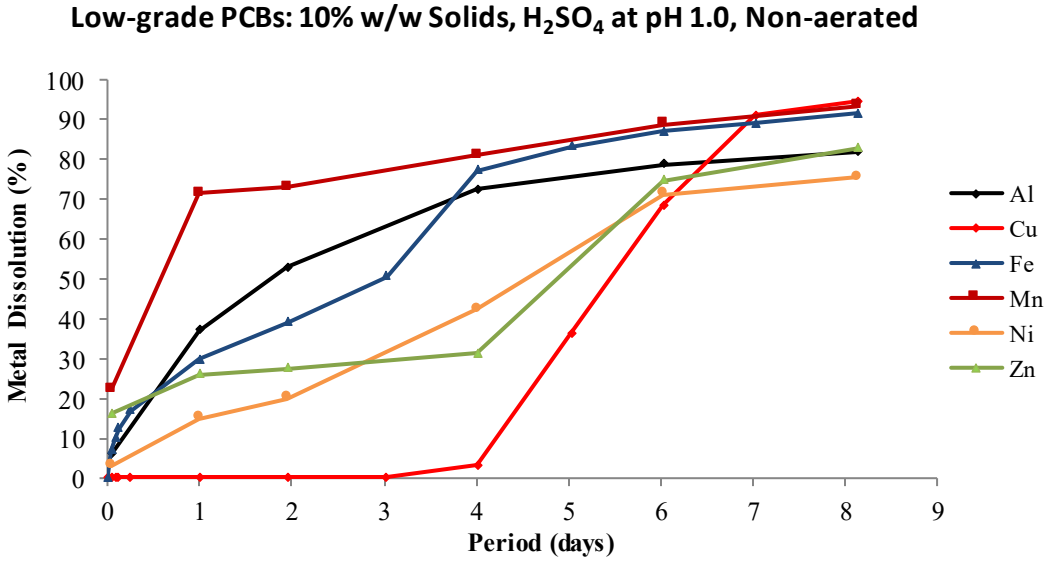

Figure 2.4: Leaching of a low-grade PCB Sample in Sulphuric Acid (No 'Oxidant' Added)
(Source: Nxumalo, 2016)

Although up to 97% dissolution of copper was achieved (probably aided by the slow ingress of oxygen from surrounding air), the leaching kinetics were very slow due to low initial solution potentials during the leaching of relatively high quantities of Al and Fe (in conjunction with minor quantities of manganese, magnesium, nickel and zinc). This suggests the need for an oxidant to increase solution potentials in order to enhance the rate of dissolution of desired metals like copper (Nxumalo, 2016).

A comparison of commonly used oxidants in hydrometallurgical processes is presented in Appendix A.

2.4. CUPRIC CHLORIDE LEACHING OF COPPER

Chloride leaching is one of the most promising hydrometallurgical methods for recovering copper from refractory sulfidic copper minerals such as chalcopyrite (Watling, 2014). Chloride solutions offer several advantages such as higher solubility and activity of metals than in sulphate media (Yazici & Deveci, 2013). One of the key characteristics of the chloride system for copper hydrometallurgy is that the cuprous (Cu(I)) ion becomes stable through complexation with chloride ions. In contrast, Cu(I) is not stable in pure water or sulphate solutions and the cupric (Cu(II)) predominates. As a result, both the ferric/ferrous (Fe(III) / Fe(II)) and cupric/cuprous (Cu(II) / Cu(I)) as well as O_2 / H_2O redox couples are present in chloride solutions compared to only the former redox couple in sulphate solutions. The Cu(II) / Cu(I) couple is highly reversible compared to the Fe(III) / Fe(II) couple, and it is well-known that the O_2 / H_2O couple is far less reversible.

2.4.1. Chloride Chemistry

In cupric chloride leaching, Cu(I) forms very strong complexes with chloride ions, thus increasing Cu(II) activity (Lundström, 2009). The ability of chloride ions to form complexes is very important. Most metals are highly soluble in chloride salt solutions due to complexation with chloride ions. The species in solution vary primarily based on the concentration of the chloride ion (Winand, 1991). Berger & Winand (1984) proposed the following classification of the strength of Cl^- acceptors:

(Cl^- acceptors) AgCl > CuCl > $PbCl_2$ > $ZnCl_2$ > $CuCl_2$ > $FeCl_3$ > $FeCl_2$ > $NiCl_2$ > HCl, NaCl, KCl (Cl^- donors).

Most chlorides used in hydrometallurgy are soluble in water. The solubility limits are very important, and they are dependent on the concentration of the chloride ion as well as the type of chloride salt added to the solution (Berger & Winand, 1984; Winand, 1991). Cuprous chloride has a low solubility in water due to the successive formation of $CuCl_2^-$ and $CuCl_3^{2-}$ ion complexes. However, its solubility increases with chloride concentration and temperature (Herreros et al., 2005; Lundström, 2009). The

solubility of cupric chloride is the opposite in that its highly soluble in water and the solubility of Cu(II) decreases with increasing Cl^- concentration (Lundström, 2009). Several studies have been conducted on the solubility of Cu(II) at different temperatures. It has been shown that the Cu(II) solubility is not affected by Cl^- concentrations below 4 mol/kg at 50°C, but at Cl^- concentrations higher than 4 mol/kg the solubility of cupric ions decreases considerably (Berger & Winand, 1984; Lundström, 2009).

Figure 2.5 shows the Eh-pH (Pourbaix) diagram of the copper-chlorine-water system. Metallic copper can only be attained at reduced potentials (vs SHE) due to strong complexation, and basic cupric chloride precipitation is observed at a more acidic pH than in sulphate solutions (Winand, 1991).

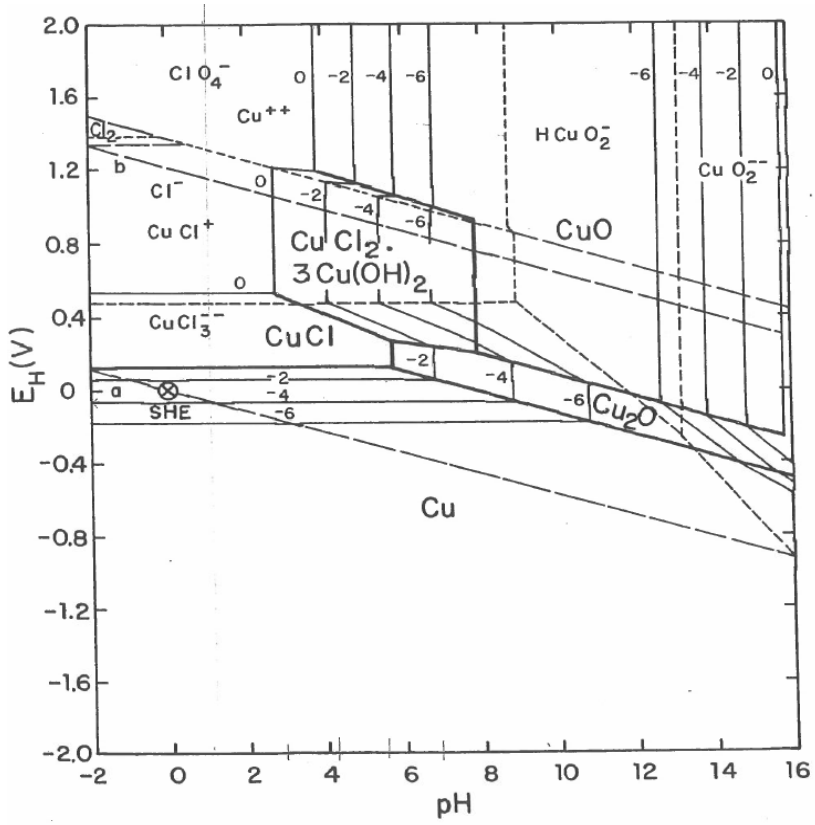

Figure 2.5: Potential-pH Diagram for Copper-Chlorine-Water System at 25°C

(Source: Duby, 1977)

The possible steps in the leaching of metallic copper with Cu(II) in chloride medium are presented in Figure 2.6.

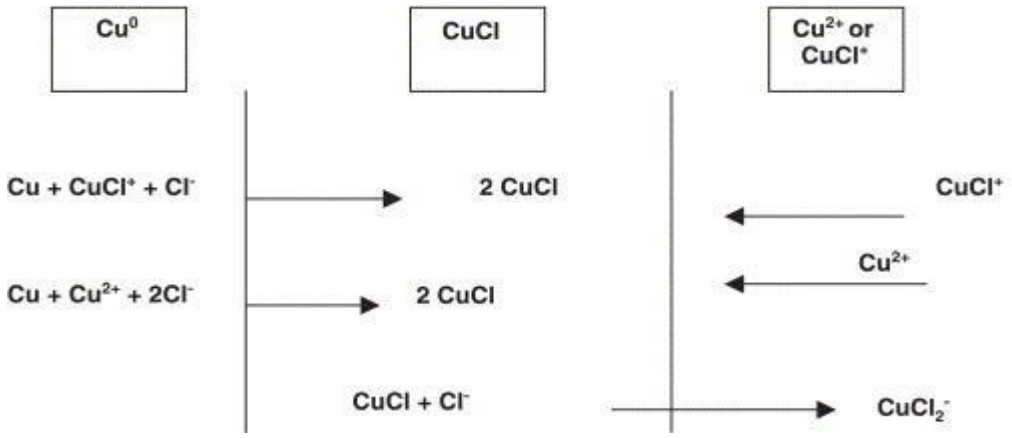

Figure 2.6: Scheme of Possible Steps in the Leaching of Metallic Copper with Cu(II) in Chloride Medium
(Source: Herreros et al., 2005)

The reactions of this process would be:

$$Cu_{(s)} + Cu^{2+}_{(aq)} + 2Cl^{-}_{(aq)} \rightarrow 2CuCl_{(s)} \quad (7)$$

$$Cu_{(s)} + CuCl^{+}_{(aq)} + Cl^{-}_{(aq)} \rightarrow 2CuCl_{(s)} \quad (8)$$

$$2CuCl_{(s)} + 2Cl^{-}_{(aq)} \rightarrow 2CuCl_{2}^{-}{}_{(aq)} \quad (9)$$

The overall reaction from combining (8) and (9) is:

$$Cu_{(s)} + CuCl^{+}_{(aq)} + 3Cl^{-}_{(aq)} \rightarrow 2CuCl_{2}^{-}{}_{(aq)} \quad (10)$$

Following data from standard reduction potentials, Herreros et al. (2005) showed the equilibrium of Cu(II) / Cu(I) in chloride solutions to be:

$$Cu^{2+}_{(aq)} + Cl^{-}_{(aq)} + e^{-} \rightarrow CuCl_{(s)} \quad E° = 0.538\ V\ (vs.\ SHE) \quad (11)$$

And the reduction of Cu(I) to Cu(0) as:

$$CuCl_{(aq)} + e^{-} \rightarrow Cu_{(s)} + Cl^{-}_{(aq)} \quad E° = 0.137\ V\ (vs.\ SHE) \quad (12)$$

Using this data, the dissolution of copper by cupric chloride may be written as:

$$Cu_{(s)} + Cu^{2+}_{(aq)} + 2Cl^{-}_{(aq)} \rightarrow 2CuCl \quad (13)$$

Reaction (13) has E_{cell} = 0.401 V and free energy of formation = -38.7 kJ/mol (-9.25 kcal/mol) (Herreros et al., 2005).

2.4.2. Application to Ores, Concentrates and Waste PCBs

Numerous chloride-based leach processes have been developed for treating copper sulphide concentrates (*e.g.* by agitated tank and pressure oxidation) and low-grade ores (*e.g.* by heap leaching). These processes employ various oxidants such as cupric, cupric chloride, ferric chloride, oxygen or chlorine. Proven chloride leaching processes include Cymet (Cyprus Metallurgical Processes Corporation), HydroCopper™ (Outokumpu, now Metso Outotec), CLEAR (Duval corporation), CUPREX (Hydrometals JV), Cuprochlor® (Minera Michilla, now owned by Antafogasta plc) and SAL (BHP) (Watling, 2014).

There are limited studies on the leaching of copper from waste PCBs by chloride leaching, particularly in cupric chloride media with sulphuric acid. Ping *et al.* (2009) evaluated the leaching of copper from mechanically upgraded waste PCB metal powder (containing 86% Cu) in H_2SO_4-$CuSO_4$-NaCl media with air at room temperature (25°C). Complete dissolution of copper from a 20 g metal powder was achieved after 5.5 hours with 110 g/L H_2SO_4, 7.8 g/L Cu(II) and 18.2 g/L Cl^-; at a solids concentration of 6% w/w. It is not clear whether the acidity was kept constant during the leach and the corresponding acid consumptions were not reported. Yazici and Deveci (2013) also studied the leaching of copper as well as other metals (Fe, Ni, Ag, Pb and Au) from a -250 µm waste PCB sample in H_2SO_4-$CuSO_4$-NaCl media. The effect of initial concentration of cupric ions (0.5-7.5 g/L Cu(II)), chloride (4.7-46.6 g/L Cl^-) and temperature (20-80°C) on the dissolution of metals was investigated using a Box-Behnken experimental design. The effect of solids concentration (1-15% w/w) and air / oxygen (2-4 L/min) were also demonstrated. It was found that the highest levels of all the parameters tested should be selected to achieve above 90% dissolution of Cu, Fe, Ni and Ag from a 5 g waste PCB sample at 1% w/w solids concentration in 120 min. A summary of cupric chloride based leaching studies for metal recovery from PCBs is presented in Table 2.4.

Table 2.3: Summary of Optimal Cupric Chloride Leaching Parameters from Previous Studies

Feed Material	Leaching Reagent	[Solids] (% w/w)	Temperature (°C)	Extent of Leach (%)	Reference
PCBs powder 86% Cu	H_2SO_4-$CuSO_4$-NaCl + Air (110 g/L H_2SO_4, 7.8 g/L Cu(II) and 18.2 g/L Cl^-)	6	25	100% Cu	(Ping et al., 2009)
PCBs (-250 µm) 18.5% Cu	H_2SO_4-$CuSO_4$-NaCl + Oxygen (0.5 M H_2SO_4, 7.5 g/L Cu(II) and 46.6 g/L Cl^-)	1	80	≥ 91% Cu, Fe, Ni and Ag 58% Pd	(Yazici & Deveci, 2013)
PCBs (-250 µm) 18.5% Cu	HCl-$CuCl_2$-NaCl + Oxygen (1 M HCl, 10 g/L Cu(II) and 1.3 M NaCl)	1	80	≥ 98% Cu, Fe, Ni and Ag 90% Pd 14% Au	(Yazici & Deveci, 2015b)
PCB powder 73.3% Cu	0.3 M HCl-0.5 M NaCl +0.2 M H_2O_2	6	65	96% Cu	(Wang et al., 2016)

2.5. REACTION KINETICS

The two most important considerations in leaching (as in all hydrometallurgical reactions) are: (i) the extent to which a reaction will proceed, and (ii) the rate at which the reaction will proceed (Marsden & House, 1992). The former depends on the thermodynamic properties of the chemical system, which determines the overall reaction driving force. The latter, the reaction kinetics, depends on a combination of physical, chemical and mass transport factors, which can be controlled to some extent by appropriate process selection and plant design (Marsden & House, 1992).

The dissolution of a solid is a heterogenous process (solid-liquid interface) and therefore the rate can be expected to be governed by one or more of the following steps (Nicol, 2008):

a. Mass transport of the lixiviant from the bulk solution to the particle surface
b. Mass transport of the products away from the particle surface
c. Mass transport within pores and cracks to the desired mineral surface
d. Mass transport within a reaction product layer around the particle
e. Chemical reaction at the particle surface

These steps can be illustrated as shown in Figure 2.7 for the dissolution of metallic copper in cupric chloride reaction.

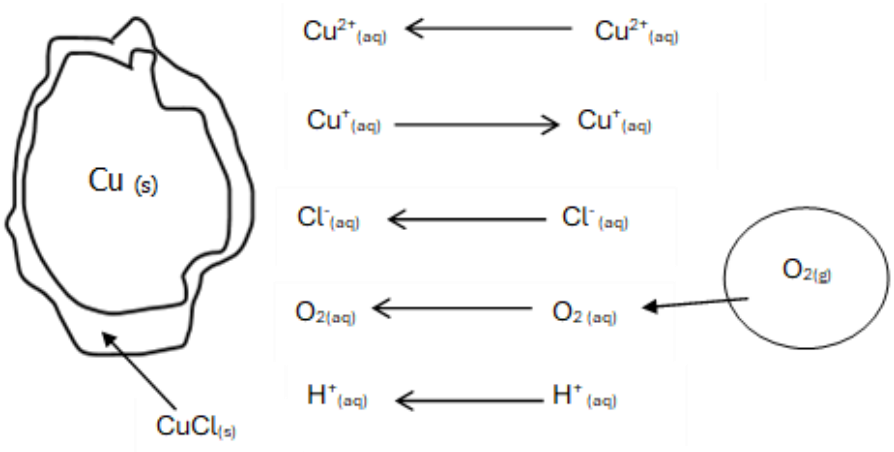

Figure 2.7: Schematic of the Steps in the Dissolution of Metallic Copper in Solutions
(Adapted from Nicol, 2008)

The slowest of the steps, mentioned above, controls the rate of the overall reaction. Any one or more of these steps can be rate-limiting, depending on the reaction conditions and can change as the reaction progresses. If steps (a) to (d) are the rate limiting steps, then the reaction is mass transfer controlled. If step (e) is the rate limiting step, then the reaction is said to be chemical reaction controlled.

For example, in the H_2SO_4-$CuSO_4$-NaCl leaching system, Cu(II) is the primary oxidant which is regenerated by the back oxidation of Cu(I) to Cu(II) with dissolved oxygen. The transfer of oxygen from gaseous phase to aqueous phase could dictate the rate at which the reaction will occur. The rate of oxygen transfer from the gaseous phase into solution is dependent on a variety of factors. These include the reactor configuration, agitation speed, flow rate of the gas, and the solubility of oxygen in solution. Figure 2.8 shows normally dissolved oxygen from air in fresh water and sea water (salinity ~ 35 ppt) at pressures ranging from 1 to 4 bar abs. As seen in Figure 2.8, the concentration of dissolved oxygen in solution increases with increasing partial pressure. At 25°C, the solubility of oxygen in water at a partial pressure of 1 bar is 8.3 mg/L, compared to 25.3 mg/L at a partial pressure of 4 bar. It is also shown that oxygen solubility decreases with increasing temperature and solute concentrations as solutes take up a fraction of the water molecules available to interact with oxygen (Narita et al., 1983).

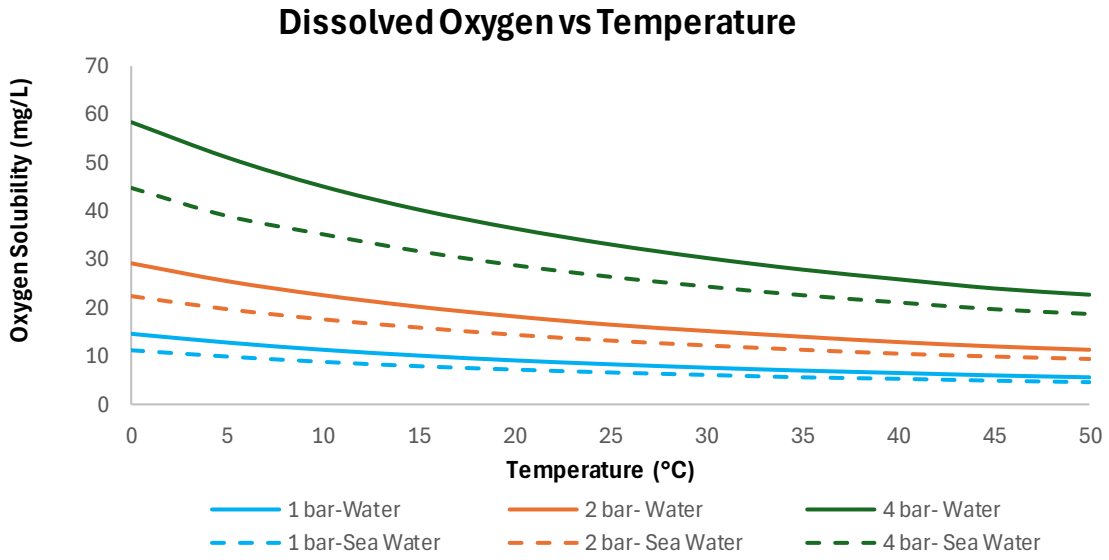

Figure 2.8: Solubility of Oxygen in Pure and Sea Water
(adapted from The Engineering ToolBox, 2005)

Mass transfer-controlled processes are strongly dependent on agitation rate, and largely independent of temperature. Whereas a process controlled by chemical reaction is highly dependent on temperature, but independent of agitation speed. The most reliable (but not conclusive) method of distinguishing between mass transport and chemical reaction as the rate limiting step is the activation energy (E_a) obtained from measurement of the rate at different temperatures. Values of E_a greater than 25 kJ/mole indicate a rate determining step involving a slow chemical reaction (Nicol, 2008).

2.6. PARAMETERS AFFECTING THE RATE AND EXTENT OF LEACHING

A summary of studies where acidic cupric chloride media was used for the leaching of copper and other base metals is given in Table 2.3 (Section 2.4.2). The effects of process variables on the leaching of copper as reported in these studies are discussed here.

2.6.1. Particle Size

The particle size of a material plays an important role in the leaching process, influencing the rate and extent of dissolution. In metal dissolution processes, a finer particle size generally lead to a higher dissolution rate due to increased surface area. Most previous studies have been conducted on ultra-fine PCB samples, which somewhat enhanced the dissolution rates. However, this comes at the cost of higher energy consumption required for fine grinding. There are a few studies where the metal dissolution was conducted on PCB plates without size reduction, and these do not involve leaching in agitated reactors. The finer particle sizes improve the mixing efficiency and are easier to transport around the leaching circuit, *e.g.* by pumping.

2.6.2. Solids Concentration

Generally, the rate of dissolution increases with decreasing solids concentration (pulp density). It has been shown that higher solids concentrations can hamper the mass transfer whilst low solids concentrations can result in higher reagent consumptions and low throughput which may affect the economics of the process. A trade-off between these two effects must be achieved and solid-liquid ratios less than 10% w/w have been found effective (Wang et al., 2016; Yazici & Deveci, 2013).

2.6.3. Temperature

At higher temperatures, reactions normally have faster kinetics due to the highly energised molecules. Wang et al. (2016) investigated the dissolution of copper at temperatures ranging from 25 to 65°C in a HCl-$CuSO_4$-NaCl system and found that the dissolution was highly sensitive to temperature. The high dissolution of copper at high temperature may be attributed to the increase of mass transfer coefficient and the diffusivity as the temperature increases (Wang et al., 2016). The effect of temperature on diffusivity can be modelled using the Arrhenius relationship described as follows:

$$D = D_0 e^{(-E_D/RT)} \quad (14)$$

Where D is the diffusion co-efficient, D_0 is a pre-exponential factor, E_D is the activation energy for diffusion, R is the gas constant, and T is temperature in K.

Yazici and Deveci (2013) observed the importance of temperature in the H_2SO_4-$CuSO_4$-NaCl system and noted that at low temperatures, an even higher initial Cl^-/Cu^{2+} ratio

should be maintained to prevent the precipitation of CuCl as suggested by their speciation calculations. This could explain the consistently lower copper dissolutions they achieved at 20°C. In a similar manner, the beneficial effect of temperature was apparent at high concentrations of copper, and the activation energy was calculated to be ≈46 kJ/mol suggesting that the leaching process was chemically controlled. Fritz (1982) noted that the solubility of CuCl (at 1 M NaCl) decreases by 3.7-fold with decreasing temperature from 80 to 20°C. Similarly, Hayes (1993) reported that a critical Cl^-/Cu^{2+} ratio for the formation of CuCl is 3.8 at 90°C compared with 8 at 10°C.

2.6.4. Reagent Concentration

2.6.4.1. Oxygen/Air

As discussed in Section 2.5. oxygen/air is commonly used as an oxidant in cupric chloride leaching, facilitating the regeneration of Cu(II), which is the primary oxidant. The rate of copper dissolution could be limited by the mass transfer of oxygen in solution due to the low solubility in water, which further decreases with an increase in solute concentrations and temperature (see Figure 2.8). The oxygen limitation has been shown to hinder the regeneration of the oxidant Cu(II). This results in lower rates of dissolution of copper, where the copper does not go into solution due to low solution potentials (reductive conditions). This effect is aggravated at higher solids concentrations (Yazici & Deveci, 2013). Others have improved the concentration of dissolved oxygen by increasing air flow rate, using pure oxygen instead of air (increasing the partial pressure of oxygen) and with vigorous agitation (Wang et al., 2016; Yazici & Deveci, 2013).

2.6.4.2. Cupric ion

Cu(II) is the primary oxidant in the cupric chloride leach system. Herreros *et al*. (2005) observed that the rate of copper dissolution increased with increased total copper concentration. However, when the concentration of chloride is kept constant, an increase in the total copper concentration brings an almost proportional increase in concentrations of the various Cu species present.

Work done by Yazici & Deveci (2013, 2015) showed the positive effect of Cu^{2+} particularly at high concentrations of Cl^-. Similarly, Herreros *et al.* (2005) reported that, in the HCl-$CuSO_4$-NaCl system, the rate and extent of dissolution of metallic copper increased with the increase in the initial copper concentration (*i.e.*, 2.2-5.2 g/L). It was also observed that, at a low concentration of Cl^-, the increase in the concentration of Cu^{2+} (particularly above 4 g/L), *i.e.*, the decrease in Cl^-/Cu^{2+} ratio, adversely affected the leaching process. These findings suggest that, at low initial Cl^-/Cu^{2+} ratios, the dissolution of copper is controlled apparently by the formation of CuCl (Yazici & Deveci, 2013). Herreros *et al.* (2005) determined an initial Cl^-/Cu^{2+} ratio greater than 8 to be critical for the dissolution of metallic copper under the

conditions they tested. They confirmed the formation of CuCl on metallic copper surfaces, using SEM-EDS analysis at Cl^-/Cu^{2+} ratios less than 8.

2.6.4.3. Acidity

Wang *et al.* (2016) found that the rate of dissolution of copper from a waste PCB sample increased with an increase in the concentration of H^+ ions from 0.05 M to 0.3 M when leaching in HCl-NaCl-H_2O_2 media. This agrees with findings by Ping et al. (2009) who observed that the rate of dissolution of copper increased with increased H_2SO_4 addition up to 1.1 M in a H_2SO_4-$CuSO_4$-NaCl + air system. However, the dissolution decreased with H_2SO_4 concentrations above 1.1 M (≈1.5 M).

The effect of acidity on the rate of dissolution of copper cannot be established with confidence since the pH of the leaching medium was not maintained constant in the above studies to the author's knowledge.

2.6.4.4. Chloride ion

Wang et al. (2016) investigated the effect of Cl^- ion on the rate of dissolution of copper from PCBs in HCl-NaCl-H_2O_2 solutions by addition of 0 M, 0.1 M, 0.3 M and 0.5 M NaCl at 25°C. They found that the rate of dissolution increased significantly with increased Cl^- concentration, with the extent of overall dissolution increasing from 55% at 0 M NaCl to 92% at 0.3 M in 90 min. This is contrary to findings by Yazici & Deveci (2015) who found that the increase in the concentration of chloride (0.7-2.0 M NaCl) slowed down the leaching of copper in HCl-$CuCl_2$-NaCl system at 80°C. Herreros *et al.* (2005) also reported the adverse effect of increasing chloride concentration in the range of 0.56-1.43 M Cl^- on the rate and extent of dissolution of metallic copper. They attributed this effect to the decrease in the activity of free Cu^{2+} within the medium.

2.6.4.5. Ferrous ion

A positive effect of adding ferrous in the lixiviant has been reported when leaching chalcopyrite in sulphate solutions containing cupric ions (Hiroyoshi et al., 1997, 2000) and in H_2SO_4-NaCl solutions (Sepúlveda et al., 2023). Hiroyoshi et al. (1997) claimed that adding ferrous sulphate resulted in higher utilisation of dissolved oxygen on the mineral surface. Sepúlveda et al. (2023) reported a slight increase in copper dissolution from chalcopyrite using H_2SO_4-NaCl-$FeSO_4$ compared to H_2SO_4 and H_2SO_4-NaCl media. These findings were contrary to those by Velásquez Yévenes (2009), who found that the addition of ferrous appeared to decrease the rate of dissolution of copper from chalcopyrite in acidic cupric chloride media.

2.7. SUMMARY

The literature review examined copper recovery from waste PCBs in acidic cupric media. It highlighted the growth of e-waste and the environmental and economic importance of recovering valuable metals. Various recovery approaches were reviewed, with a focus on cupric chloride leaching of copper. Key factors affecting leaching rate and extent include solids concentration, pH, temperature, particle size, chloride, cupric and ferrous ion concentrations.

Most previous studies were limited to micro-scale tests at low solids concentrations. These studies often did not monitor elemental mass balances or reagent consumption. Such conditions do not reflect practical processing environments, where PCB heterogeneity and high reagent use are significant challenges. This study investigates copper dissolution at higher solids concentrations. Mass balances and reagent consumption were carefully monitored. The best conditions were also evaluated at pilot scale, providing realistic insights into copper recovery from waste PCBs.

CHAPTER 3: EXPERIMENTAL METHODS AND MATERIALS

3.1. EXPERIMENTAL PLANNING

Agitated reactor leach tests were conducted at bench scale to evaluate the effect of the following parameters on the rate and overall extent of copper dissolution:

a. Particle size: -1 mm, -3+1 mm , -8+3 mm and +8 mm
b. Solids concentration: 6, 10 and 15%
c. Chloride concentration: 10, 20, 30, 50, 80 and 100 g/L
d. Temperature: 25, 50, 60, 70 and 80°C
e. pH (acidity): 1, 1.5 and 2
f. Initial cupric concentration: 0, 0.5 and 1 g/L
g. Initial ferrous concentration: 0, 1, 3 and 5 g/L

A "one-at-a-time" (OAT) experimental approach was followed where one parameter was tested at a time while the other parameters were fixed at baseline conditions. After determining the "best" value for each parameter, leach conditions were recommended for the mini pilot leach test.

The optimal conditions were also tested using calcined samples to assess copper dissolution after the removal of volatile organic materials, such as plastics and resin.

Baseline conditions are presented in Table 3.1 and were tested in duplicate to confirm reproducibility.

Table 3.1: Baseline Conditions

Test ID	Size (mm)	[Solids] (% w/w)	[Cl^-] (g/L)	Temp. (°C)	[Cu(II)] (g/L)	pH	[Fe(II)] (g/L)
T1 (a&b)	-1	6	20	50	0.5	1.0	0

A full experimental matrix for the bench-scale tests is presented in Table 3.2.

A mini pilot-scale test was conducted under recommended conditions established from the bench-scale leach tests to evaluate the scalability of the leach results.

Table 3.2: Experimental Matrix for Bench-Scale Leach Tests

Parameter	Test ID	Particle Size (mm)	[Solids] (% w/w)	[Cl^-] (g/L)	Temp. (°C)	[Cu(II)] (g/L)	pH	[Fe(II)] (g/L)
Particle Size	T1 (Baseline)	-1	6	20	50	0.5	1.0	-
	T2	-3+1	6	20	50	0.5	1.0	-
	T3	-8+3	6	20	50	0.5	1.0	-
	T4	+8	6	20	50	0.5	1.0	-
Solids Concentration	T5	-1	10	20	50	0.5	1.0	-
	T6	-1	15	20	50	0.5	1.0	-
Chloride Concentration	T7	-1	6	10	50	0.5	1.0	-
	T8	-1	6	30	50	0.5	1.0	-
	T9	-1	6	50	50	0.5	1.0	-
	T10	-1	6	80	50	0.5	1.0	-
	T11	-1	6	100	50	0.5	1.0	-
Temperature	T12	-1	6	20	25	0.5	1.0	-
	T13	-1	6	20	60	0.5	1.0	-
	T14	-1	6	20	70	0.5	1.0	-
	T15	-1	6	20	80	0.5	1.0	-
Initial Cu(II) Concentration	T16	-1	6	20	50	0	1.0	-
	T17	-1	6	20	50	1.0	1.0	-
pH	T18	-1	6	20	50	0.5	1.5	-
	T19	-1	6	20	50	0.5	2.0	-
Initial Fe(II) Concentration	T20	-1	6	20	50	0.5	1.0	1.0
	T21	-1	6	20	50	0.5	1.0	3.0
	T22	-1	6	20	50	0.5	1.0	5.0

3.2. RATIONALE

3.2.1. Lixiviant Selection

$CuSO_4$-NaCl-H_2SO_4 with air was selected as the leaching system because Cu^{2+} acts as an effective oxidant for metallic copper. Air provides additional oxidation, helping regenerate Cu^{2+} during leaching. Chloride ions form soluble Cu-Cl complexes, which enhance copper dissolution. Sulphuric acid provides the acidic medium needed to maintain copper solubility and fast reaction rates. This combination has been shown in the literature to achieve high copper extraction from ores and waste PCBs.

A chloride concentration of 20 g/L, which is close to the chloride concentration of seawater (roughly 19 g/L) and 0.5 g/L cupric were chosen as baseline conditions. Higher chloride and cupric ion concentrations may enhance the dissolution rate of copper but significantly increase reagent costs and may be challenging from a practical viewpoint. Maintaining a high copper 'inventory' in the operational circuit also has a negative impact on cash flow.

Iron is a common impurity in copper solvent extraction processes and its presence in high concentrations can adversely affect the efficiency of copper extraction. Also, when present as ferric ions, it is unwanted in electrowinning since ferric ions consume current in the reduction process and thus reduce overall current efficiency. Therefore, no ferrous was added for the baseline test.

For the baseline conditions, the pH was controlled at 1 to limit ferric precipitation which becomes significant above pH 2-2.5.

3.2.2. Particle Size

The selection of -1 mm as the baseline crush size was a compromise between maximising leaching efficiency and minimising operational challenges (sample variability, agitation efficiency, metal losses and filtration). Several studies were conducted on PCB 'powders' or ultra- fine material (-250 µm) (Ping et al., 2009; Yazici and Deveci, 2013, 2015).

3.2.3. Solids Concentration

Ping *et al.* (2009) and Yazici and Deveci (2013) reported the detrimental effect of increased solids concentration on the leaching of copper from waste PCBs in H_2SO_4–$CuSO_4$–NaCl solutions. Optimal rates of copper dissolution were achieved at solid concentrations of 3% w/w (Ping et al., 2009) and 1% w/w (Yazici & Deveci, 2013). These are lower than typical solids concentrations in industrial agitated tank copper leaching operations which range from 10 to 40% w/w (Nezungai et al., 2013). The selection of a 6% solids concentration baseline was based on optimizing the trade-

offs between copper recovery, reagent efficiency, mixing effectiveness and operational challenges.

3.2.4. Temperature

A baseline operating temperature of 50°C provided a compromise between the energy required for heating and the improved leaching performance (*i.e.* the rate and extent of dissolution of copper. Higher temperatures (*e.g.* above 50°C) might further enhance kinetics but significantly increase energy costs and water losses due to evaporation.

3.3. MATERIALS AND REAGENTS

3.3.1. PCB Sample

A ton of high-grade PCB sample was obtained from Desco Electronic Waste Recyclers in Kempton Park, Johannesburg. The PCBs came mainly from personal computers and mobile phones, which are known to have a high content of base and precious metals such as copper and gold. Desco prepared the sample as illustrated in

Figure 3.1.

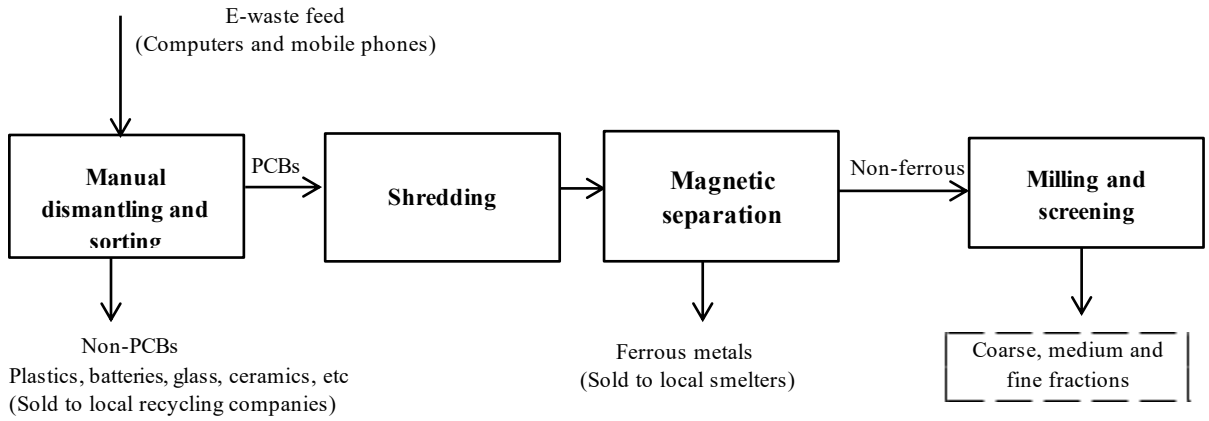

Figure 3.1: Preparation of PCB Samples

PCB sorting involves the classification of PCBs into high, medium and low-grade PCBs based on their metal content, with high-grade PCBs having the highest metal content. After manual dismantling and sorting, the PCBs were shredded with a two-shaft shredder and passed through a magnetic belt to remove loose pieces of magnetic, ferrous metals. The non-magnetic fraction was then ground further with a hammer mill and screened into three fractions, *i.e.* coarse, medium and fines / dust with a rotary drum screen. Figure 3.2 shows the PCB sample fractions received from Desco.

Figure 3.2: PCB Fractions As-Received

Upon receipt, a bulk particle size distribution (PSD) analysis was performed on the sample by dry screening on the following sieve sizes: 8, 3 and 1 mm. Each of the size fractions (+8 mm, -8+3 mm, -3+1 mm and -1 mm) was split into 20-25 kg batches using a rotary splitter and then plastic bagged. Two 20-25 kg bags from each size were further split into 10 sub-samples (2-2.5 kg). The 2-2.5 kg sub-samples were further split into 250 g batches for chemical analysis and leach experiments. A rotary splitter was used for the -3+1 mm and -1 mm fractions, and the -8+3 mm and +8 mm fractions were split by cone and quartering. The different size fractions are presented in Figure 3.3.

Figure 3.3: PCB Sample Size Fractions

3.3.2. Working Solutions

The chemical reagents used for make-up of leaching media are presented in Table 3.3. All solutions were made with reagent grade (AR) chemicals and de-ionised water. Chloride (Cl^-) was added as sodium chloride (NaCl). Initial copper was added as cupric sulphate pentahydrate ($CuSO_4 \cdot 5H_2O$) and iron (where required) was added as ferrous sulphate heptahydrate ($FeSO_4 \cdot 7H_2O$). The initial pH was adjusted by the addition of 98% sulphuric acid (H_2SO_4). A solution of 7.5 M H_2SO_4 was prepared and used for pH adjustment during the leach.

Table 3.3: Chemical Reagents

Chemical Reagent	Formula	Purity	Supplier
Sodium chloride	NaCl	AR, 99.5%	ACE*
Ferrous sulphate heptahydrate	$FeSO_4 .7H_2O$	AR, 99%	ACE
Copper sulphate pentahydrate	$CuSO_4 .5H_2O$	AR, 99%	ACE
Sulphuric acid	H_2SO_4	AR, 98%	ACE

Note:
* ACE: Associated Chemical Enterprises

Example calculations for make-up and analysis of working solutions are presented in Appendix B.

3.4. ANALYTICAL METHODS

All the chemical analyses were done at Mintek, Analytical Chemistry Division (ACD) except for the intermediate ("kinetic" leach samples) copper and iron solution assays, as well as the H_2SO_4, Fe(II) and Cl^- titrations. These were performed by the Biometallurgy Division (BMD).

3.4.1. Solid Head and Residue Samples

All the aliquots were ashed in a muffle furnace at 900°C for 6 hours to remove volatile material. The ashed aliquots were then milled to ensure homogeneity.

The samples were analysed by inductively coupled plasma-optical emission spectroscopy (ICP-OES; ICP_base metal) for: aluminium (Al), calcium (Ca), cobalt (Co), chromium (Cr), copper (Cu), iron (Fe), magnesium (Mg), manganese (Mn), nickel (Ni), lead (Pb), silicon (Si), titanium (Ti), vanadium (V) and zinc (Zn), as well as tin (Sn) by ICP-OES (ICP10). Silver (Ag) and antimony (Sb) were determined by atomic absorption spectroscopy (AAS). Gold (Au), palladium (Pd) and platinum (Pt) were analysed by fire assay and total carbon (C) was determined by a combustion technique (Leco).

3.4.2. Solution Samples

Working and kinetic leach solutions as well as wash water samples were analysed for copper and iron by AAS. Final filtrate solutions were analysed by ICP-OES for: Al, arsenic (As), Ca, Cu, Cr, Fe, lithium (Li), Mg, molybdenum (Mo), Ni, Pb, Si, Ti, V and Zn as part of the ICP_base metal suite. Sn was analysed by inductively coupled plasma-mass spectrometer (ICP-MS), and gold and silver were analysed by AAS.

Descriptions of analytical methods are presented in Appendix B.

3.5. EQUIPMENT

3.5.1. Bench-Scale Leach Tests

3.5.1.1. Experimental Set-up

A schematic diagram of the experimental set-up for bench-scale tests is presented in Figure 3.4. This shows a glass reactor (2 or 4 L working volume). The reactor has a multi-port lid which allows for the fitting of an impeller shaft, pH sensor, condenser, air sparger, acid dosing tube as well as an available port for sampling and portable sensor readings.

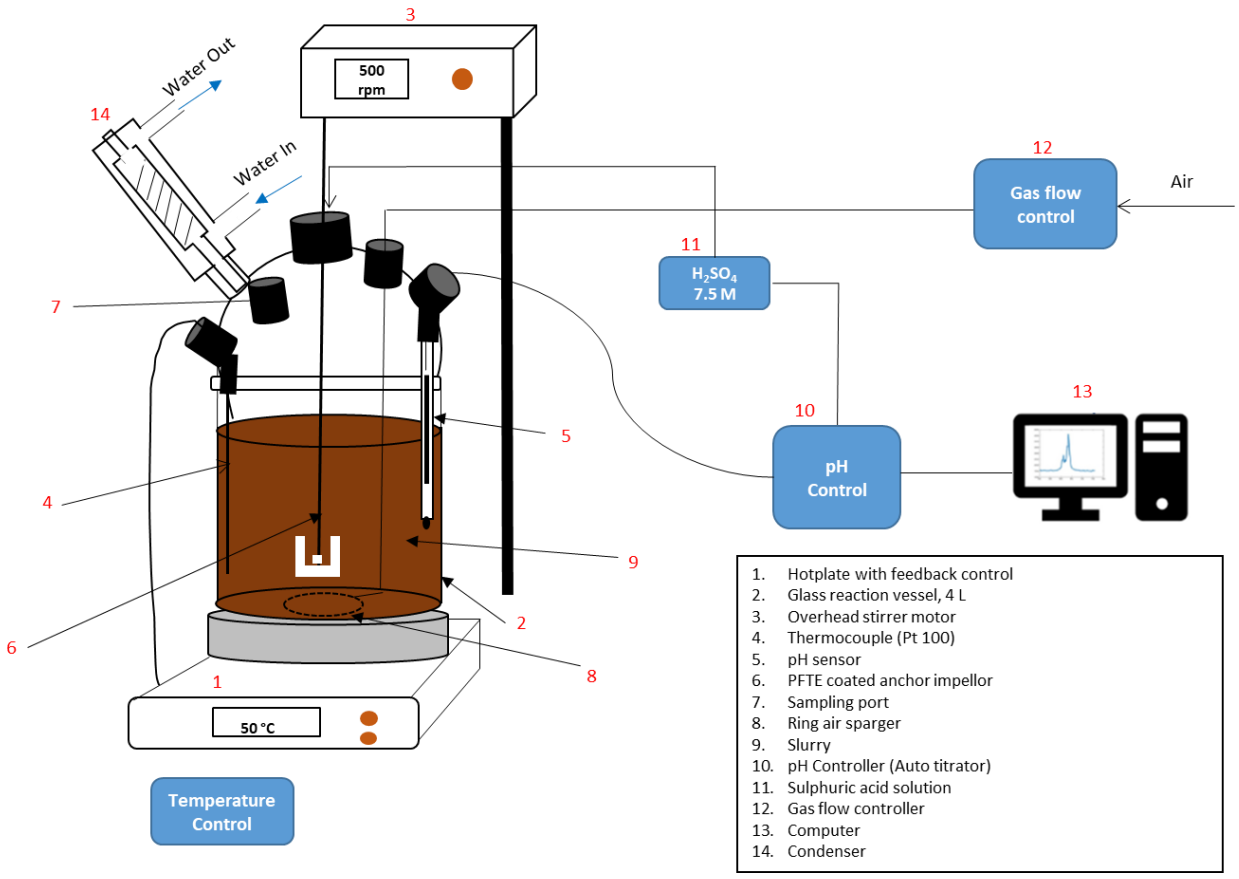

Figure 3.4: Schematic Diagram of the Experimental Set-Up

3.5.1.2. Air flowrate control

The air flowrate was controlled using a gas flow meter from ALICAT™ Scientific. The gas flow meter received air from a compressed air line with the gas pressure regulated at 2 bar (200 kPa). A ¼ in. ID polyethylene tube was connected to the gas flow meter with a perforated ring sparger underneath the impeller.

The air flow rate for all the tests was kept constant at 500 standard cubic centimetres per minute (SCCM) at standard temperature and pressure (STP) of 25°C and 101.325

kPa, respectively. This flow rate was selected based on the dispersion of small air bubbles observed at an agitation speed of 500 rpm. The latter rotation speed was selected to ensure complete suspension of the PCB samples in the agitated slurry over the entire range of 6% to 15% solids.

3.5.1.3. Agitation

The reactor contents were agitated using a Heidolph RZR-2021 overhead stirrer and a polytetrafluoroethylene (PTFE) coated, anchor-type impeller (shaft diameter: 8 mm, length: 350 mm; blade size: 60 (diameter) x 40 (height) x 5 mm (width). The agitation speed was kept constant at 500 revolutions per minute (rpm), which was sufficient for full suspension of solids up to 15% solids.

3.5.1.4. Temperature Control

The slurry temperature was achieved and controlled using a Heidolph MR Hei-Tec heating plate connected to a Pt1000 temperature sensor. The temperature sensor was encapsulated in a polyethylene tube (I.D. x O.D.: 3/16 in x 5/16 in), with the end closed off, to minimise corrosion by chloride ions. The pH probe used for continuous measurement and pH control had a built-in temperature sensor which served as a check for temperature measurement to ensure that the hot plate / sheathed Pt1000 sensor controlled the temperature satisfactorily.

3.5.1.5. pH Control

The slurry pH was measured using a combined Ag/AgCl reference electrode (3 M KCl) with integrated Pt1000 temperature sensor, installation length 43.8 cm (Metrohm pH electrode model: 6.00249.600). The pH was kept constant during the leach by use of an auto titration system (Metrohm, model 907 Titrando, operated on Tiamo™ version 2.3 software). The pH was controlled by dosing with 7.5 M H_2SO_4 solution, and the acid additions were recorded and used to calculate the acid consumption during the leach. The automated pH measurements were verified periodically with a portable pH meter (Metrohm pH meter model: 914 and pH electrode model: 6.0220.100) for quality control.

3.5.2. Mini-Pilot Leach Test

The experimental set-up of the mini-pilot leach test is presented in Figure 3.5. The test was conducted in an agitated, polypropylene batch reactor with an operating volume of 24 L and dimensions: 310 mm (diameter), 320 mm (active height). The vessel had three equally spaced baffles and was sealed with a multi-port lid.

The vessel was equipped with a double impeller system (150 mm diameter) for agitation. The bottom impeller was a six-bladed (flat blade) Rushton turbine and the

top impeller a six-bladed (pitch blade) impeller. The agitation speed was kept at 350 rpm.

The reactor was also equipped with a temperature control system, consisting of a resistance temperature device (RTD) and titanium sleeved hot rod for heating of the slurry.

Air was supplied via a sparger tube (ID: 6 mm), with an open end situated underneath the bottom impeller. The air pressure was controlled at 2 bar using a regulator and the air flow rates were controlled at 200 L/h (ATP: 25°C and 0.86 atm), using a calibrated rotameter.

The pH was measured with a portable pH meter (Metrohm pH meter model 914 and pH electrode model 6.0220.100) and adjusted manually with 98% H_2SO_4 when required.

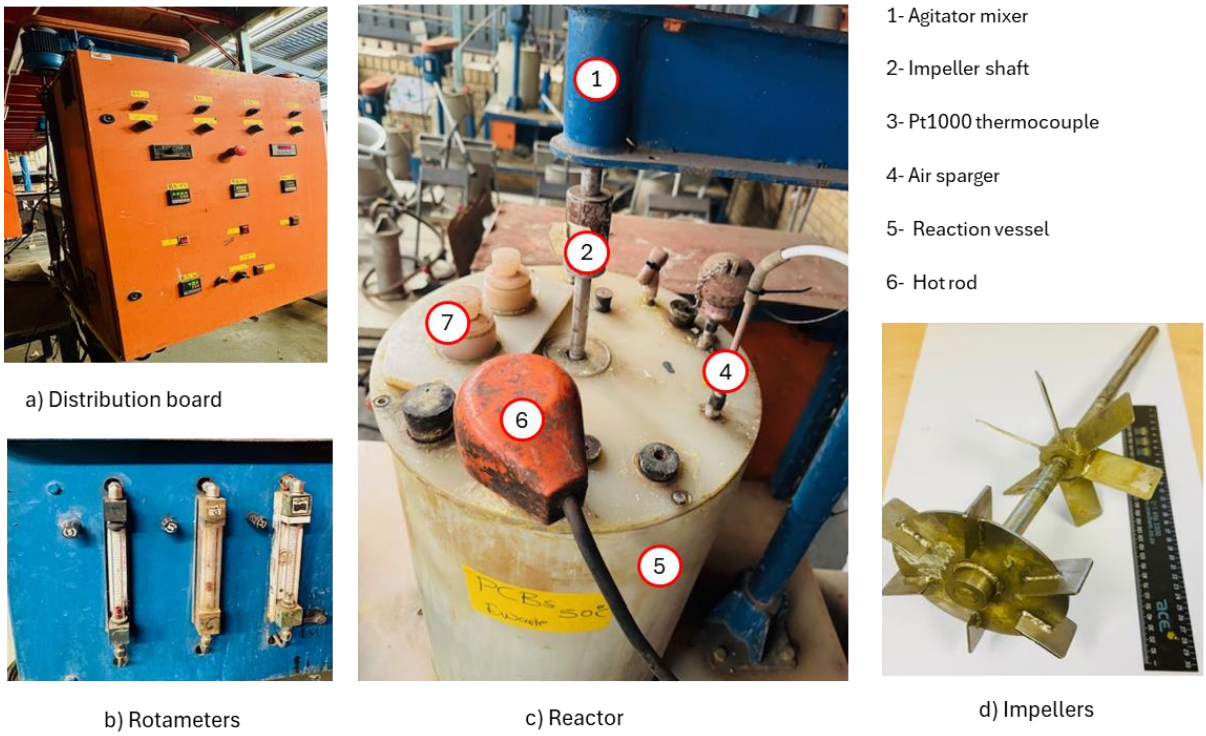

Figure 3.5: Mini-Pilot Experimental Set-Up

3.5.3. Experimental Procedure

3.5.3.1. Bench-Scale Leach Tests

A volume of lixiviant solution of the concentrations stipulated by the experimental design was poured into either a 2 L or 4 L reaction vessel. The solution was heated to the target temperature under continuous agitating and air sparging. Once the target temperature was reached, the initial pH and redox potential of the solution were measured. Then, the solid sample was added into the vessel. The pH control system was then started at t=0.

Samples of 20 mL were taken at 30 min, 1 h, 2 h, 4 h, 6 h, 8 h and 24 h. The solutions were filtered immediately with a Millipore vacuum filtration system. The following parameters were monitored:

a. Temperature and pH: as described in Sections 3.5.1.4. and 3.5.1.5.
b. Solution / slurry potential: all potential measurements were performed and reported against a 3 M KCl, combined Ag/AgCl electrode (Knick pH meter model 902, Hamilton ORP sensor 238145) and converted to the Standard Hydrogen Electrode scale (SHE). A conversion table can be found in Appendix B.
c. Cu and Fe: kinetic leach solution samples were analysed for Cu and Fe by AAs.

All experiments were run for 24 h. Upon completion of the leach, the overheard stirrer, air flow, pH and temperature control systems were switched off and the reactor was allowed to cool down. The reactor contents were poured into a beaker and filtered using a pressure filter. The filter cake was repulped and washed first with a dilute sulphuric acid solution at pH 1.5, and with the same volume as final filtrate. Thereafter, washed again with tap water at half the final filtrate volume.

Filtrate solutions were analysed as per Section 3.4.2. Acid and water wash solutions were analysed for Cu and Fe by AAS.

Solid residues were analysed as per Section 3.4.1.

3.5.3.2. Mini-Pilot Leach Test

The experimental procedure for the mini pilot leach test was the same as described in Section 3.5.3.1. except that the pH was adjusted manually with 98% H_2SO_4. Also, the solution samples were analysed for Cu, Fe and other base metals by ICP-OES. The dissolved oxygen concentrations were also measured using a Knick Portavo 907 multi-parameter transmitter with SE715 amperometric oxygen sensor.

3.6. DATA PROCESSING AND INTERPRETATION

3.6.1. Statistical Analysis

Head sample chemical analyses were performed in triplicate to account for sample heterogeneity and variability. A two-tailed Student's t-test was applied to assess variability among replicates. Negative lower bounds were reported as zero, since negative concentrations are physically impossible, ensuring reported ranges remain realistic while reflecting measurement uncertainty.

The mean ($\bar{X}$) and standard deviation (SD) were calculated as:

$$\bar{X} = \frac{\sum X_i}{n} \tag{15}$$

$$SD = \sqrt{\frac{\sum (X_i - \bar{X})^2}{n-1}} \tag{16}$$

The standard error (SE) was calculated as:

$$SE = \frac{SD}{\sqrt{n}} \tag{17}$$

The 95% confidence interval (CI) was calculated using:

$$CI = t_{0.05,n-1} \times SE \tag{18}$$

The lower and upper bounds of the CI were calculated as:

$$Lower\ bound = \bar{X} - CI \tag{19}$$

$$Upper\ bound = \bar{X} + CI \tag{20}$$

Where:

n=number of replicate measurements (here, n = 3 for triplicates)

X_i=individual measurement in the set of replicates

$t_{0.05,n-1}$=critical t-value from Student's t-table (t=4.303 for n=3, 95% confidence level)

3.6.2. Metal Dissolutions

The copper and iron dissolution profiles were plotted using the respective recalculated copper and iron head and solution analyses. The use of the recalculated instead of the assayed head is for consistency and quality purposes since the resulting metal dissolutions then all correspond to a 100% metal mass balance (with respect to solid and solution phases). This allows for direct comparison between different test results.

For example, the recalculated Cu head is defined as:

$$Recalc.\ head\ Cu_{(g)} = Cu_{leached\,(g)} + Cu_{Solid\ residue\,(g)} \tag{21}$$

Where:

$$Cu_{leached\ (g)} = Cu_{Solution\ (g)} - Cu_{lixiviant\ (g)} \quad (22)$$

$$Recalc.head\ Cu_{\ (\%)} = \frac{Recalc.head\ Cu_{\ (g)}}{Sample\ mass_{\ (g)}} \times 100 \quad (23)$$

The percentage dissolution of copper at a given time could be determined as:

$$Cu\ Diss._{\ (\%)} = \frac{Cu_{leached\ (g)}}{Recalc.head\ Cu_{\ (g)}} \times 100 \quad (24)$$

The metal accountabilities (*i.e.* mass balances) were defined as:

$$Metal\ Mass\ Balance_{\ (\%)} = \frac{Recalc.head_{\ (g)}}{Assayed\ head_{\ (g)}} \times 100 \quad (25)$$

3.6.3. Acid Consumptions

The total acid consumption (TAC), in kg H_2SO_4 / t (dry) PCB sample at a given time was defined as the total mass of acid added to maintain the pH at the desired level.

$$TAC\left(\frac{kg\ Acid}{t\ Sample}\right) = \frac{mass\ H_2SO_4\ added\ (kg)}{mass\ sample\ (t)} \quad (26)$$

The net acid consumption, which discounts for acid consumed to dissolve copper (*i.e.* acid recovered by solvent extraction of copper).

$$NAC\left(\frac{kg\ Acid}{t\ Sample}\right) = TAC\left(\frac{kg\ Acid}{t\ Sample}\right) - \frac{net\ mass\ Cu\ in\ Soln\ (g) \times 98\frac{g}{mol}}{63.5\frac{g}{mol} \times sample\ mass\ (g)} \times 1000\frac{kg}{t} \quad (27)$$

$$NAC\left(\frac{kg\ Acid}{kg\ Cu_{leached}}\right) = \frac{NAC\left(\frac{kg}{t}\right) \times Mass\ sample\ (t)}{Mass\ Cu_{leached}\ (kg)} \quad (28)$$

CHAPTER 4: RESULTS

4.1. HEAD SAMPLE CHARACTERISATION

4.1.1. Particle Size Distribution of the Waste PCB Head Samples

The particle size distributions of the various fractions of the PCB sample are presented in Figure 4.1. About 74% of the whole sample passed 8 mm with 24.6% fines (-1 mm). The -1 mm fraction contained about 85% material passing 600 µm and 27% passing 75 µm on a dry basis. The +8 mm, -8+3 mm and -3+1 mm fractions had 80% passing (P_{80}) 12, 6.5 and 2.3 mm, respectively.

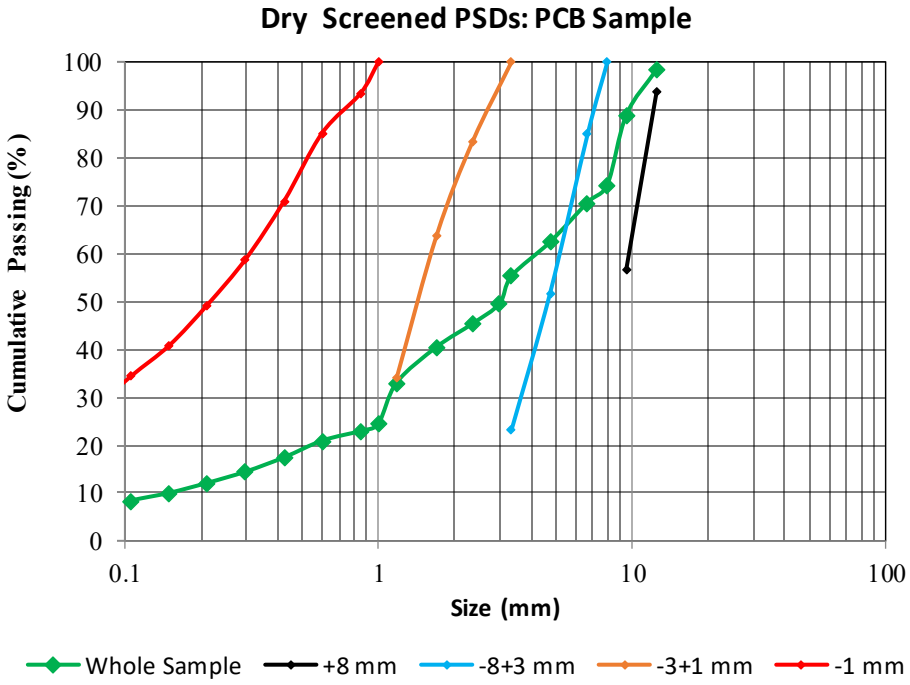

Figure 4.1: Particle Size Distributions of the bulk PCB Sample

4.1.2. Chemical Analysis

The chemical analysis and element distributions for each of the size classes are presented in Tables 4.1 and 4.2, respectively. Each size class was analysed in triplicate to confirm variability and average values are reported.

The reconstituted head assays are within the typical range reported in literature for high-grade PCBs. On average, the sample contains 213 ppm gold (Au), 469 ppm silver (Ag), 23.7% copper (Cu), 3.5% tin (Sn) and 5.9% iron (Fe). Most of the silver (64%) is contained in the -1 mm fraction, while 75% of the gold is in the -8+1 mm size fraction. Copper seems to be distributed evenly between the -8+3 mm, -3+1 mm and -1 mm fractions with only 18% in the +8 mm size fraction.

Table 4.3 presents the statistical analysis of the chemical assays for the -1 mm sample, including the standard deviation and the 95% confidence interval (lower and upper bounds). Statistical analyses of the +8 mm, -8+3 mm, and -3+1 mm samples are provided in Appendix C.

The results show good reproducibility for metals such as Al (5%), Cu (19.3-21.0%), and Fe (9.6-10.1%), while greater variability was observed for Sn (2.4-4.8%), Ag (355-1648 ppm) and Au (128-192 ppm). This variability can be attributed to the heterogeneity of the material. In addition, the small sample sizes used in certain analytical methods present challenges for assay reproducibility.

Table 4.1: Chemical Analysis of the PCB Head Sample by Size (Average Values)

Size (mm)	Mass (%)	Ag (ppm)	Al (%)	Au (ppm)	C (%)	Ca (%)	Co (%)	Cr (%)	Cu (%)	Fe (%)	Mg (%)	Mn (%)	Ni (%)	Pb (%)	Pd (ppm)	Pt (ppm)	Sb (%)	Si (%)	Sn (%)	Ti (%)	V (%)	Zn (%)
+8	15.9	76.8	8.95	32.9	22.7	8.12	< 0.05	0.05	27.0	5.93	0.16	0.05	0.09	0.57	3.5	0.09	0.33	13.2	1.05	0.19	< 0.05	0.38
-8+3	29.7	206	10.09	238	27.3	5.06	< 0.05	0.07	21.2	4.32	0.27	0.08	0.26	1.10	5.8	0.24	1.65	10.9	2.05	0.19	< 0.05	4.83
-3+1	24.3	390	6.66	366	20.3	3.85	< 0.05	0.06	29.1	3.11	0.16	0.22	0.52	3.23	21.5	0.25	0.79	8.3	6.83	0.28	< 0.05	1.32
-1	30.1	1000	5.02	160	16.5	6.70	< 0.05	0.07	20.2	9.82	0.22	0.85	0.64	0.46	60.6	0.96	0.26	12.8	3.63	0.57	< 0.05	0.25
Total	100	469	7.55	213	21.6	5.75	< 0.05	0.07	23.7	5.94	0.21	0.34	0.41	1.34	25.7	0.43	0.81	11.2	3.53	0.32	< 0.05	1.89

Table 4.2: Element Mass Distributions of the PCB Head Sample

Size (mm)	Mass (%)	Ag (%)	Al (%)	Au (%)	C (%)	Ca (%)	Cr (%)	Cu (%)	Fe (%)	Mg (%)	Mn (%)	Ni (%)	Pb (%)	Pd (%)	Pt (%)	Sb (%)	Si (%)	Sn (%)	Ti (%)	Zn (%)
+8	15.9	2.6	18.9	2.5	16.7	22.5	12.0	18.1	15.9	12.1	2.3	3.3	6.8	2.2	3.3	6.5	18.9	4.8	9.2	3.2
-8+3	29.7	13.1	39.7	33.2	37.5	26.1	32.6	26.5	21.6	37.9	7.2	19.1	24.3	6.7	16.1	60.4	28.9	17.2	17.4	75.9
-3+1	24.3	20.2	21.4	41.8	22.8	16.3	23.4	29.8	12.7	19.0	15.7	31.0	58.6	20.3	13.9	23.7	17.9	47.1	21.2	17.0
-1	30.1	64.1	20.0	22.6	23.0	35.1	32.1	25.6	49.8	31.0	74.8	46.6	10.3	70.8	66.8	9.5	34.3	31.0	52.3	3.9
Total	100	100	100	100	100	100	100	100	100	100	100	100	100	100	100	100	100	100	100	100

Table 4.3: Chemical Analysis of the - 1 mm Head Sample (Statistical Analysis)

Element			Ag (ppm)	Al (%)	Au (ppm)	Ca (%)	Cu (%)	Fe (%)	Mg (%)	Mn (%)	Ni (%)	Pb (%)	Pd (ppm)	Pt (ppm)	Sb (%)	Si (%)	Sn (%)	Ti (%)	Zn (%)
Mean			1000	5.02	160	6.70	20.15	9.82	0.22	0.85	0.64	0.46	60.6	0.96	0.26	12.75	3.63	0.57	0.25
Standard Deviation			261	0.010	12.8	0.175	0.333	0.108	0.005	0.010	0.028	0.102	3.726	0.074	0.015	0.176	0.487	0.005	0.070
n	**3**	**95% CI**	648	0.03	31.9	0.43	0.83	0.27	0.01	0.03	0.07	0.25	9.26	0.18	0.04	0.44	1.21	0.01	0.17
df	**2**	**Lower**	352	4.99	128.1	6.27	19.32	9.55	0.20	0.82	0.57	0.21	51.3	0.78	0.22	12.31	2.42	0.55	0.07
t	**4.303**	**Upper**	1648	5.05	191.9	7.13	20.98	10.09	0.23	0.87	0.70	0.71	69.9	1.14	0.29	13.19	4.84	0.58	0.42

4.2. BENCH-SCALE LEACH TESTS

The copper and iron dissolution profiles presented hereafter have been plotted using the recalculated head and solution analysis (see Section 3.6.2).

4.2.1. Baseline Conditions

Figure 4.2 shows the redox potential, copper and iron dissolutions as well as the acid consumptions for the two tests conducted under baseline conditions *i.e.* 6% solids, 20 g/L Cl^-, 0.5 g/L Cu(II), pH 1.0 at 50°C.

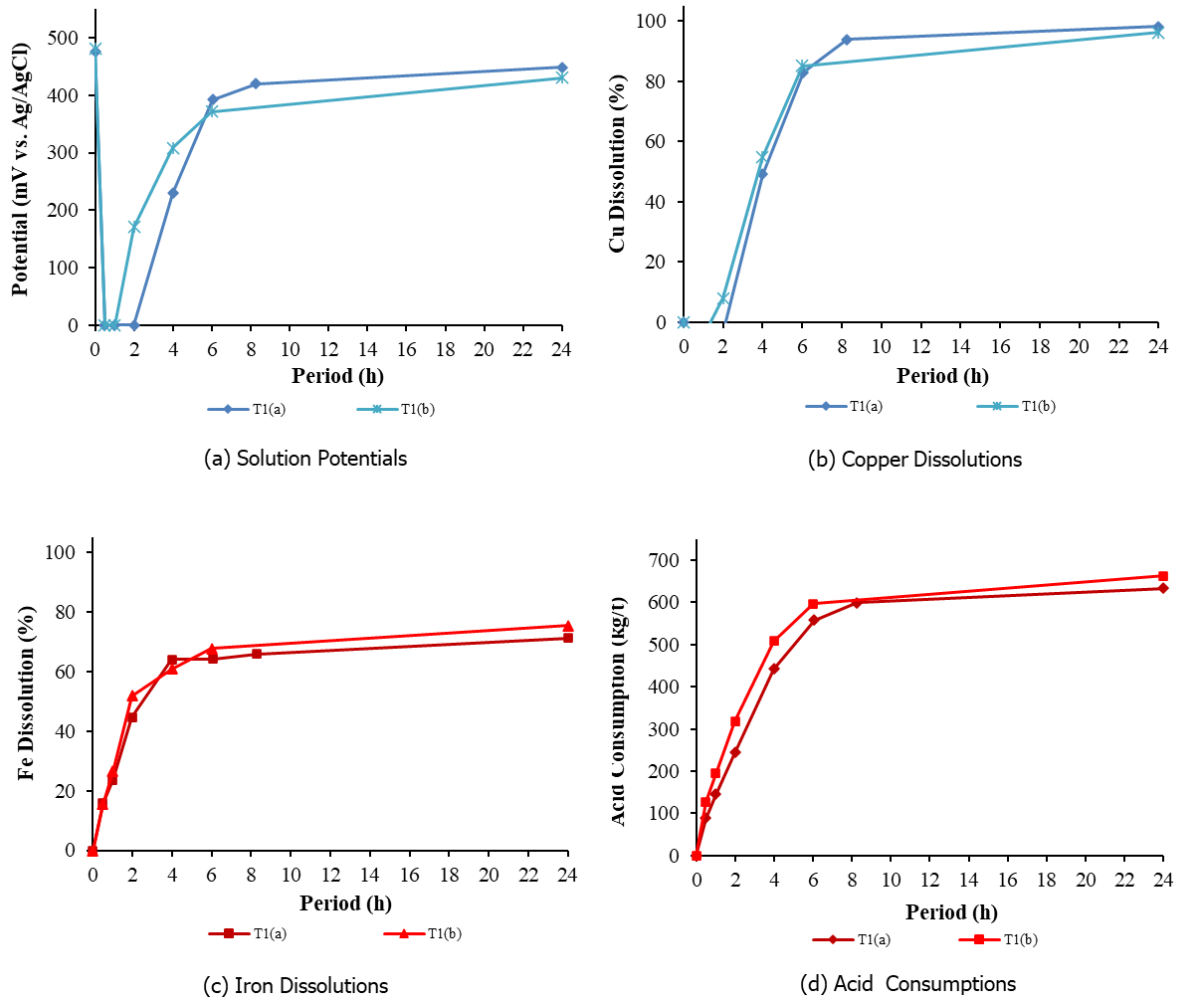

Figure 4.2: Leach Profiles at Baseline Conditions

(a) Solution Potential (b) Copper and (c) Iron Dissolutions (d) Total Acid Consumption at: 6% Solids; 20 g/L Cl^-; 0.5 g/L Cu(II); pH 1.0 and 50°C

Figure 4.2 shows good reproducibility of the baseline conditions, with leach profiles *i.e.* solution potentials, Cu and Fe dissolution and well as acid consumptions of the

two tests in good agreement. The initial reduction in potential was observed in both tests, with a final potential of 430-448 mV after 24 h.

The copper dissolution profile aligns with the potential trend, with low initial dissolution rate owing to the reductive potentials. The dissolution of iron, particularly the accumulation of ferrous ions, adversely affects copper leaching efficiency by lowering the redox potential and thereby slowing the dissolution process. The respective extent of overall dissolution of copper and iron were 97 and 75% on average.

The total acid consumption was between 634 and 663 kg/t.

4.2.2. Effect of Particle Size

The redox potential, copper and iron dissolution and acid consumption profiles at different particle sizes are presented in Figure 4.3. The initial solution potentials for all fractions dropped sharply within the first 1-3 hours, reaching near zero (actual potentials were negative and unstable). This indicates that the reactor conditions were largely reductive. Final potentials stabilized between 380 and 448 mV.

Copper dissolution was strongly influenced by particle size. The +8 mm and -8+3 mm fractions exhibited slower initial leaching compared to the finer -3+1 and -1 mm fractions. For example, after 6 hours, copper dissolution reached 83% for -1 mm, 79% for -3+1 mm, negative for -8+3 mm, and 27% for +8 mm material. Overall copper extraction after 24 hours was similar for the -1 mm and -3+1 mm fractions (98-99%), while the -8+3 mm and +8 mm fractions achieved lower overall dissolution (52% and 66%, respectively). The slower copper leaching from coarser fractions can be attributed to copper being embedded in the PCB matrix, making it more dependent on particle surface area.

In contrast, iron dissolution increased with particle size. The +8 mm fraction exhibited the highest iron leaching, consistent with the presence of loose, liberated iron pieces in coarser PCB particles. After 24 hours, overall iron dissolution reached 71% for -1 mm, 74% for -3+1 mm, 91% for -8+3 mm, and 99% for +8 mm.

Acid consumption trends mirrored iron dissolution. The +8 mm fraction showed the highest total acid consumption at 1360 kg/t, corresponding to the high iron dissolution, while the -1 mm fraction had the lowest at 634 kg/t. The -3+1 mm and -8+3 mm fractions had similar acid consumptions of 1032 and 1002 kg/t, respectively.

These results highlight the contrasting dissolution behaviour of copper and iron in PCB samples, which is influenced by their physical association within the material and the resulting exposure to the leach solution. These results are consistent with previous studies on metal recovery from PCBs.

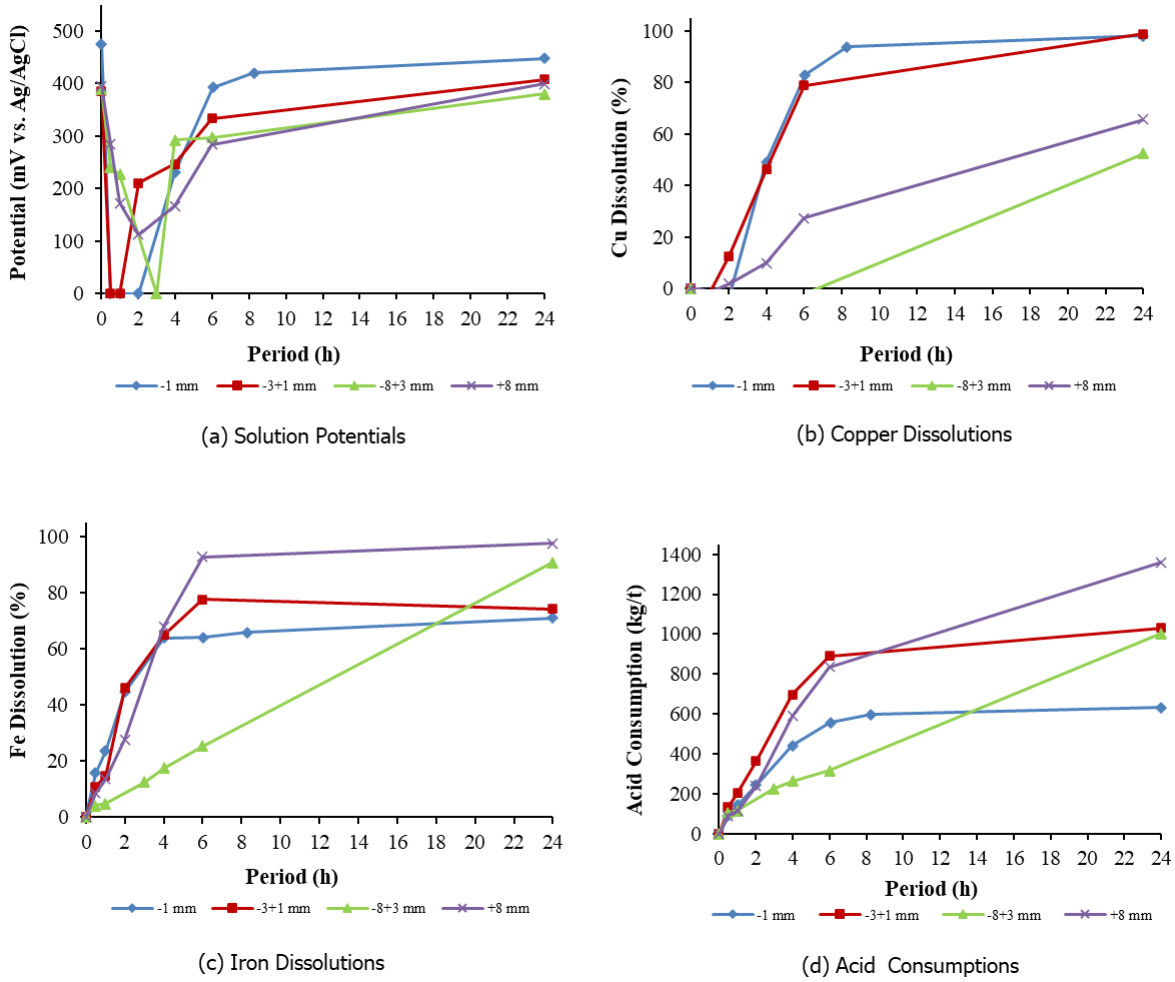

Figure 4.3: Leach Profiles at Different Particle Sizes

(a) Solution Potential (b) Copper and (c) Iron Dissolutions (d) Total Acid Consumption at: 6% Solids; 20 g/L Cl^-; 0.5 g/L Cu(II); pH 1.0 and 50°C

4.2.3. Effect of Solids Concentration

The solution potentials at different solids concentrations are presented in Figure 4.4 (a). Again, these show that the solution potentials stayed lower or negative for longer periods with increasing solids concentration. For example, the potential was less than 0 mV at 15% solids, 300 mV at 10% solids and 400 mV at 6% solids after 6 hours. The maximum potentials achieved were: 354 mV at 15% solids, 423 mV at 10% solids and 448 mV at 6% solids, after 24 hours. Figures 4.7 and 4.8 show the copper and iron dissolution profiles at different solids concentrations, respectively.

Figure 4.4(b) shows an improvement in copper leaching kinetics with the reduction in solids concentration. For example, the copper dissolutions were 83% at 6% solids, 62% at 10% solids and no copper was leached at 15% solids after 6 hours. The reason for this is that higher solution potentials were achieved earlier in the case of the lower

solids concentration as evident in Figure 4.4(a). The extents of overall copper dissolution were: 98% at 6% solids; 87% at 10% solids and 73% at 15% solids. Iron went rapidly into solution, with extents of overall dissolution reaching 71% at 6% solids, 79% at 10% solids and 84% at 15% solids as shown in Figure 4.4(c).

The total acid consumptions were: 634 kg/t at 6% solids, 555 kg/t at 10% solids and 478 kg/t at 15% solids as shown in Figure 4.4(d).

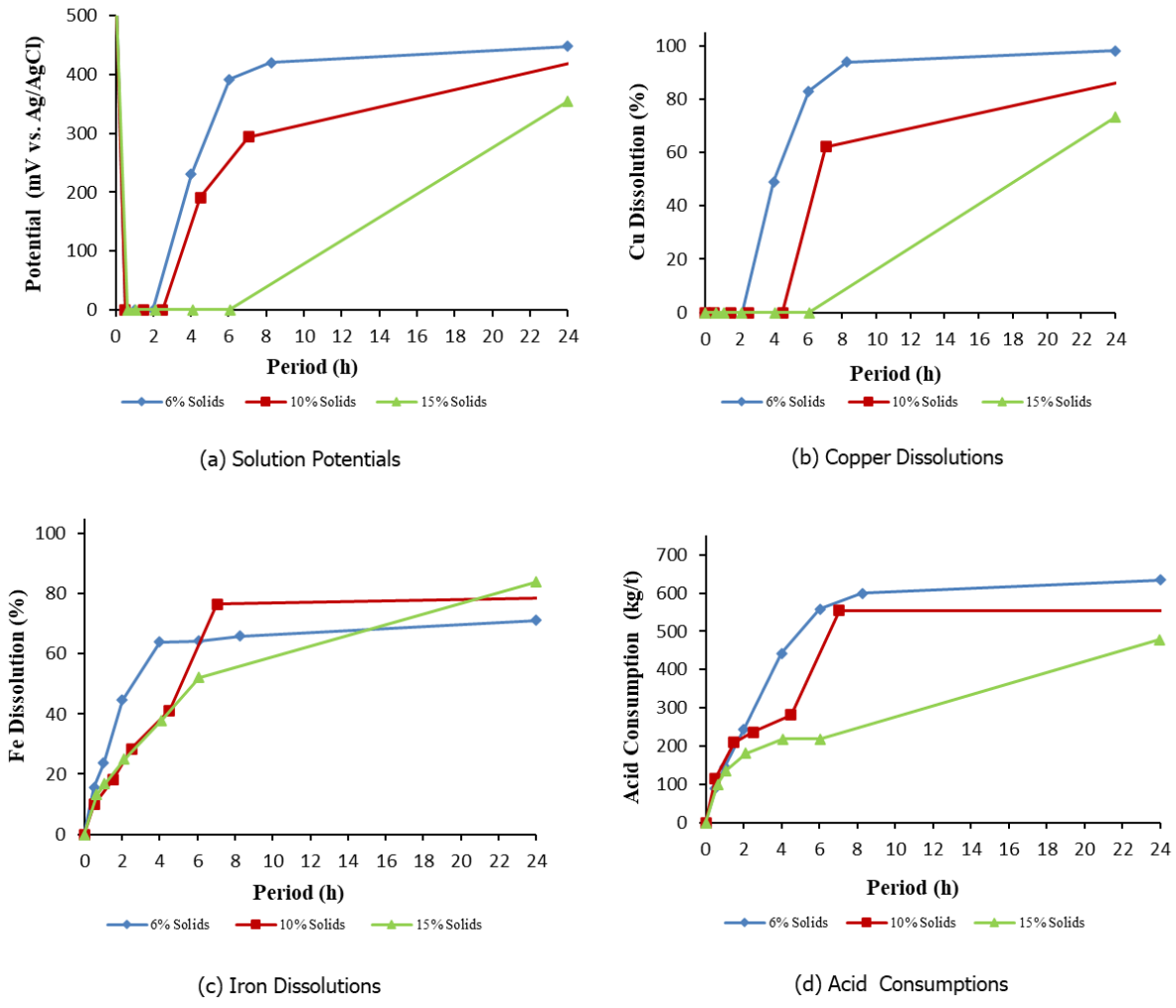

Figure 4.4: Leach Profiles at Different Solids Concentrations

(a) Solution Potential (b) Copper and (c) Iron Dissolutions (d) Total Acid Consumption at: 20 g/L Cl^-; 0.5 g/L Cu(II); pH 1.0 and 50°C

4.2.4. Effect of Chloride Concentration

The solution potentials at varied chloride concentrations are presented in Figure 4.5(a). Similar solution potential profiles were obtained for the 10 g/L to 50 g/L chloride concentrations. A positive, stable potential was only measured after 6 hours at 80 g/L and 100 g/L chloride concentrations compared to 4 hours at lower chloride concentrations. The maximum solution potentials were between 400 mV and 486 mV.

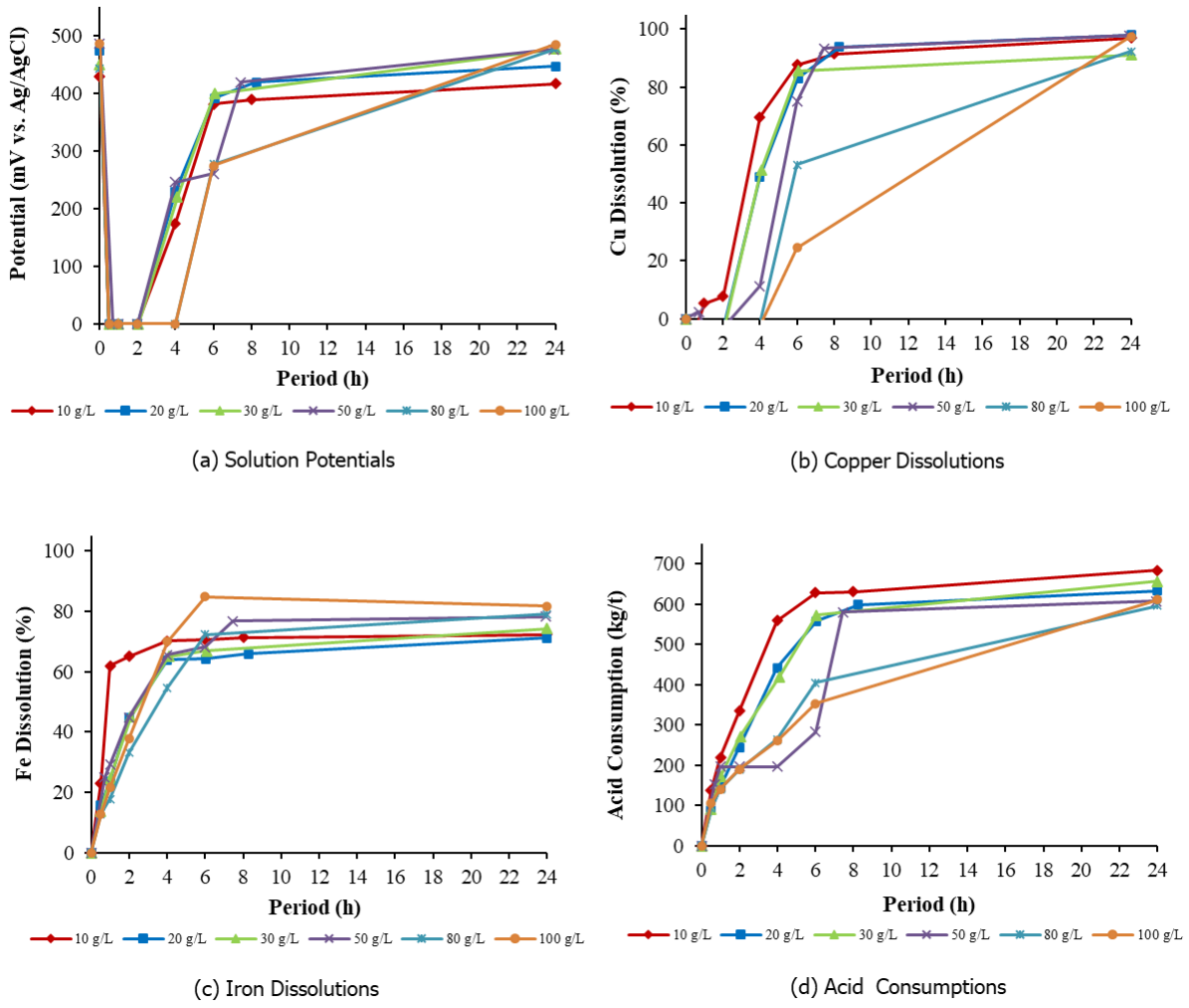

Figure 4.5: Leach Profiles at Different Chloride Concentrations

(a) Solution Potential (b) Copper and (c) Iron Dissolutions (d) Total Acid Consumption at: 6% Solids; 0.5 g/L Cu(II); pH 1.0 and 50°C

Figures 4.5(b) and 4.5(c) show the copper and iron dissolution profiles at different chloride concentrations, respectively.

Figures 4.5(b) and 4.5(c) show that increasing the chloride concentration from 10 g/L to 100 g/L did not have a significant effect on the extents of overall copper and iron dissolutions. The extents of overall copper dissolution ranged from 92 to 98%.

However, the copper leaching rates were significantly slow at 80 and 100 g/L chloride. For example, the dissolution was 88% at 10 g/L, 83% at 20 g/L, 86% at 30 g/L, 75% at 50 g/L, 53% at 80 g/L and 24% at 100 g/L after 6 hours. From a copper leaching point of view, 10 g/L of chloride seems to be sufficient unless any benefit of using higher chloride concentrations is established with respect to other metals.

The iron dissolution profiles were also similar with extents of overall iron dissolution of between 71% and 82% achieved.

Figure 4.5(d) shows the acid consumption profiles at varied chloride concentrations.

The total acid consumptions were between 597 kg/t and 684 kg/t, the highest being at 10 g/L chloride. The slightly lower acid consumption at higher chloride concentrations could be attributed to the improved extent of proton (H^+) dissociation at higher chloride concentrations resulting in a lower pH.

4.2.5. Effect of Temperature

The redox potential profiles at different temperatures are presented in Figures 4.6(a).

The profiles indicate a lower potential (175 mV) at 25°C after 6 hours compared to 392 mV to 441 mV at 50°C to 80°C. The maximum potential measured at 25°C was 335 mV after 24 hours compared with 448 mV at 50°C, 487 mV at 70°C and 500 mV at 80°C.

The copper and iron dissolution profiles are presented in Figures 4.6(b) and 4.6(c).

Relatively slow rates of copper dissolution were evident at 25 °C with 22% achieved after 6 hours compared to 83% achieved at 50 °C. The extent of overall copper dissolution was 51% at 25°C compared with 98% at 50 °C to 80 °C.

The iron dissolution profile at 25°C was similar to those at higher temperatures with 77% achieved after 24 h compared to an average of 78% at 50 °C to 80 °C.

The acid consumption profiles are presented in Figure 4.6(d) and indicate a lower overall acid consumption at 25°C, corresponding with a lower copper dissolution. The total acid consumptions were 485 kg/t at 25°C and 634 kg/t to 782 kg/t at 50°C to 80°C.

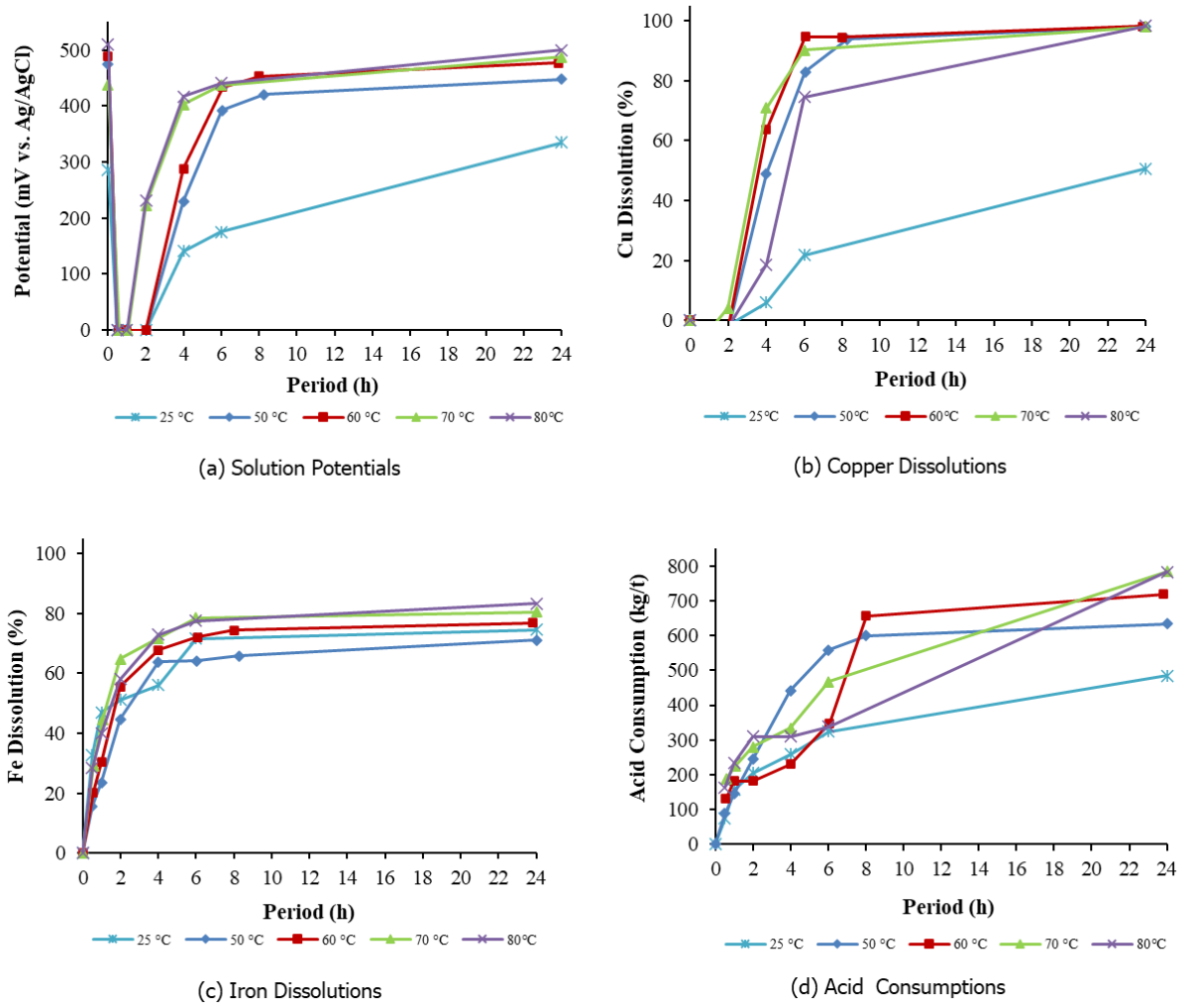

Figure 4.6: Leach Profiles at Different Temperatures

(a) Solution Potential (b) Copper and (c) Iron Dissolutions (d) Total Acid Consumption at: 6% Solids; 20 g/L Cl^-; 0.5 g/L Cu(II) and pH 1.0

4.2.6. Effect of pH

Figures 4.7(a) to (d) presents the solution potentials, copper dissolution profiles, iron dissolution profiles and acid consumption profiles at different operating pHs.

Higher solution potentials were obtained at pH 1.0 compared with pHs 1.5 and 2.0 (Figure 4.7(a). After 6 hours, the potentials were 392 mV (pH 1.0), 182 mV (pH 1.5) and 244 mV (pH 2.0), respectively. The solution potentials increased further to 448 mV (pH 1.0), 402 mV (pH 1.5) and 367 mV (pH 2.0) after 24 hours.

The copper dissolution rates were slower at pHs 1.5 and 2.0 than at pH 1.0. Extents of overall copper dissolution were 98% (pH 1.0), 92% (pH 1.5) and 45% (pH 2.0) after 24 hours (Figure 4.7(b)).

Extents of overall iron dissolution were similar at 72% (pH 1.0), 68% (pH 1.5) and 74% (pH 2.0) after 24 hours (Figure 4.7(c)).

Figure 4.7(d) shows lower total acid consumptions at pHs 1.5 and 2.0. This reduction in acid consumption corresponds with lower copper dissolutions. The total acid consumptions were 634 kg/t (pH 1.0), 487 kg/t (pH 1.5) and 327 kg/t (pH 2.0), respectively.

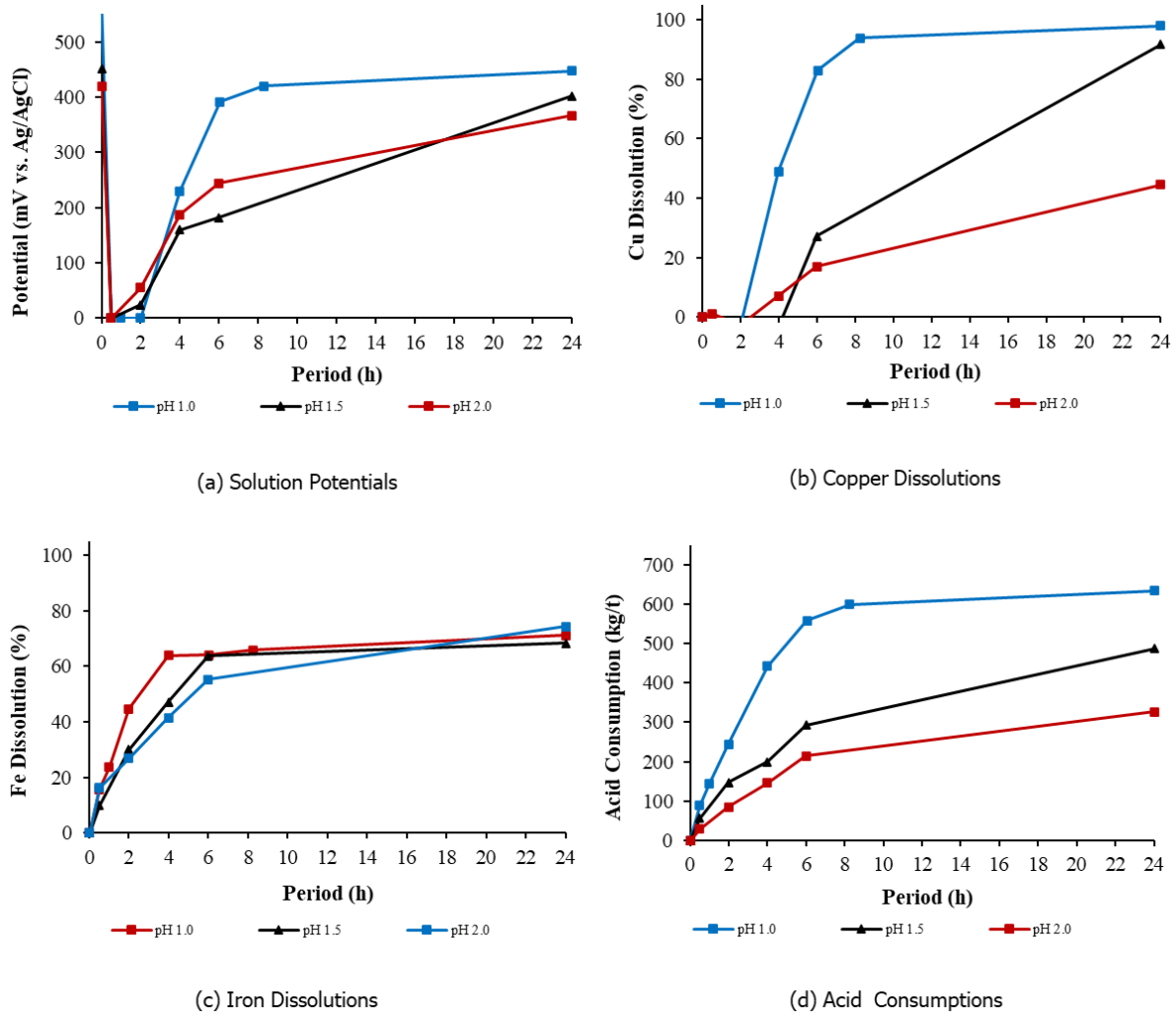

Figure 4.7: Leach Profiles at Different pH Levels

(a) Solution Potential (b) Copper and (c) Iron Dissolutions (d) Total Acid Consumption at: 6% Solids; 20 g/L Cl^- and 0.5 g/L Cu(II)

4.2.7. Effect of Initial Cupric Concentration

The solution potentials at varied initial Cu(II) concentrations are presented in Figure 4.8(a).

Varying the initial Cu(II) concentration did not have a significant effect on the solution potential, the initial conditions were reductive at all concentrations tested with the 1 g/L Cu(II) showing a positive potential within 2 hrs. The maximum potentials measured were similar at 441 mV, 448 mV and 440 mV at initial Cu(II) concentrations of 0 g/L, 0.5 g/L and 1 g/L, respectively.

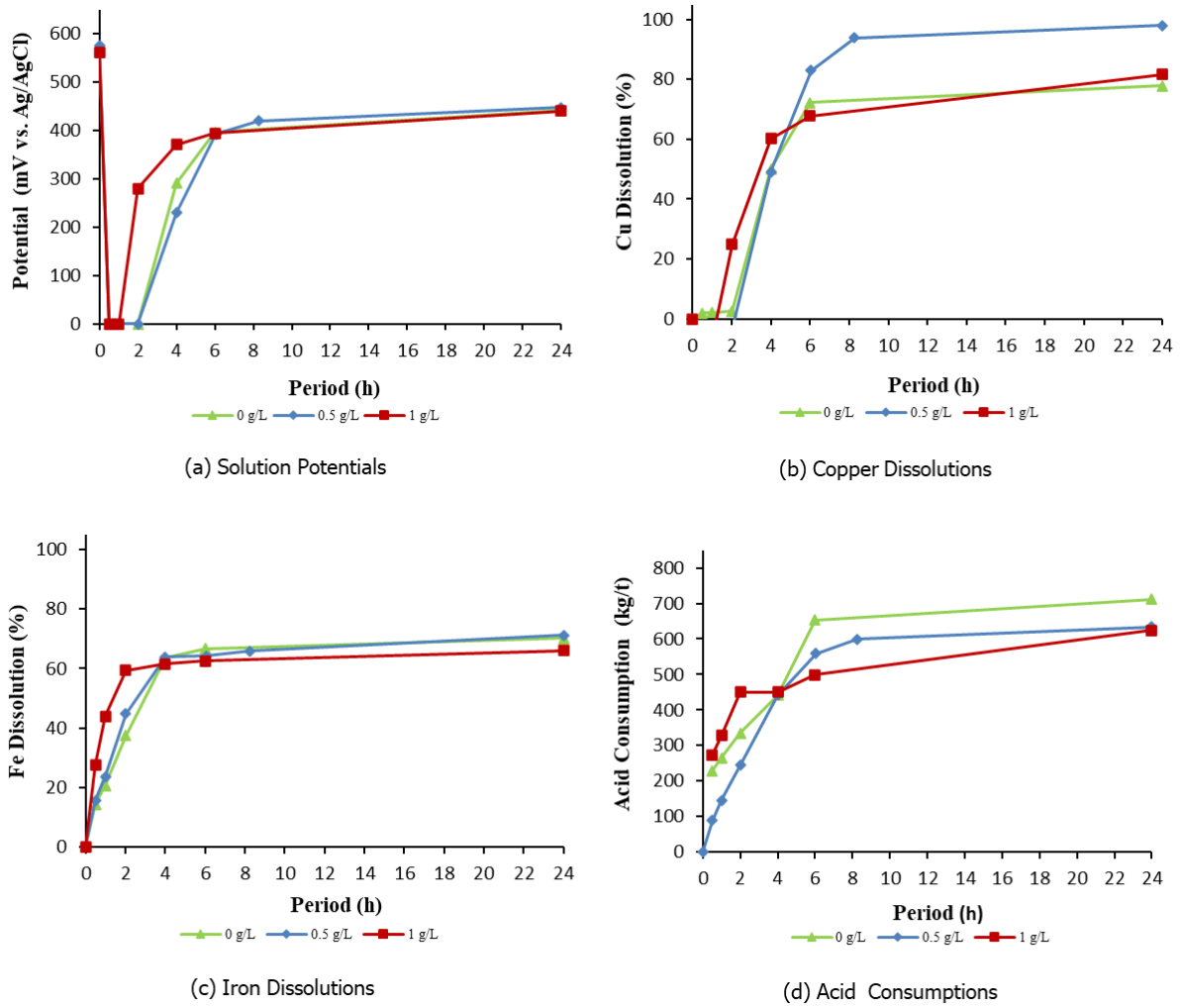

Figure 4.8: Leach Profiles at Different Initial Cupric Concentrations

(a) Solution Potential (b) Copper and (c) Iron Dissolutions (d) Total Acid Consumption at: 6% Solids; 20 g/L Cl⁻; pH 1.0 and 50°C

Figures 4.8(b) and 4.8(c) show the copper and iron dissolution profiles at varied initial Cu(II) concentrations, respectively.

As shown in Figure 4.8(b), varying the initial cupric concentration had little effect on the initial copper leaching kinetics. During the first 1-2 h, the cupric ions in the lixiviant were reduced and plated as metallic copper due to the reductive conditions. After 24 hours, overall copper dissolution reached 78% without initial copper in solution, 98% with 0.5 g/L Cu^{2+}, and 82% with 1 g/L Cu^{2+}. The overall iron dissolutions achieved were similar between 66% and 71% as shown in Figure 4.8(c).

Figure 4.8(d) shows the acid consumption profiles at varied initial cupric concentrations. The total acid consumption was 806 kg/t without initial cupric in solution, 634 kg/t at 0.5 g/L copper and 624 kg/t at 1 g/L cupric.

4.2.8. Effect of Initial Ferrous Concentration

The solution potentials at varied initial ferrous concentrations are presented in Figure 4:9(a).

The addition of ferrous in the lixiviant did not make a significant improvement in the initial solution potentials as seen in Figure 4:9(a). The potential profiles were similar for the ferrous concentrations tested with a maximum average potential of 436 mV measured after 24 hours.

Figures 4.9(b) and 4.9(c) show the copper and iron dissolution profiles at varied initial ferrous concentrations, respectively.

Figure 4.9(b) shows similar copper dissolution kinetics at the ferrous concentrations tested, owing to similar solution potential profiles. The extents of overall copper dissolution were similar at 98% without ferrous, 92% at 1 g/L ferrous, 95% at 3 g/L ferrous and 98% at 5 g/L ferrous.

The overall iron dissolutions were 71% without ferrous, 70% with 1 g/L ferrous, 76% with 3 g/L ferrous and 82% with 5 g/L ferrous.

Figures 4.9(d) shows the acid consumption profiles at varied initial iron concentrations. The total acid consumptions were 634 kg/t without ferrous, 696 kg/t with 1 g/L ferrous, 670 kg/t with 3 g/L and 667 kg/t with 5 g/L ferrous.

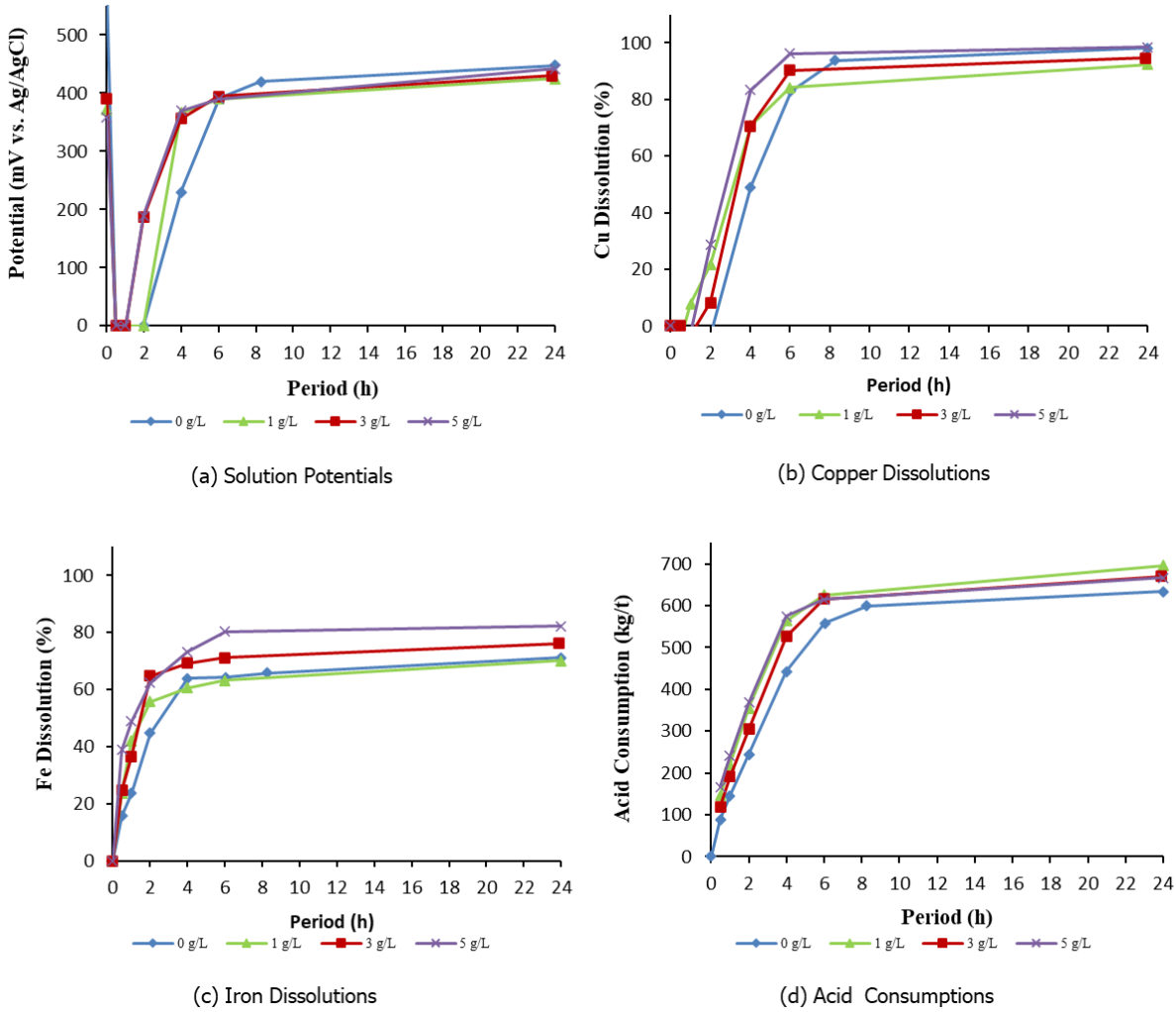

Figure 4.9: Leach Profiles at Different Initial Ferrous Concentrations

(a) Solution Potential (b) Copper and (c) Iron Dissolutions (d) Total Acid Consumption at: 6% Solids; 20 g/L Cl⁻; pH 1.0 and 50°C

4.2.9. Effect of Pre-leach Calcination

Figures 4.10 shows the leach profiles of tests conducted on calcined samples. One sample was milled to 90% passing 75 µm after calcination. The sample tested 'As is' is also plotted for comparison.

As evident in Figure 4.10(a), the initial potential for calcined samples did not decrease as low as the sample leached as is. For example, the potential decreased from 432 mV (starting solution) to 253 mV after 1 h, compared to negative potentials observed on the samples tested as is. However, similar potentials (above 400 mV) were achieved for both samples from 6 h onwards.

The copper leaching kinetics were more rapid in the calcined samples, owing to the higher initial redox potentials prevalent in these tests. For example, the dissolution

was 93% for calcined samples compared to 7% for the 'As is' sample after 2 hours (Figure 4.10(b)). The extents of overall copper dissolution were similar at 96-97%.

The calcined samples yielded lower overall iron dissolutions (31% to 49%) compared with the 'As is' sample (72%) (Figure 4.10(c)). This suggests that iron may form insoluble alloys or more refractory phases during calcination, reducing its leachability.

The calcined and milled sample yielded the highest acid consumption (821 kg/t) compared with the calcined sample (695 kg/t) and the 'As is' sample (634 kg/t).

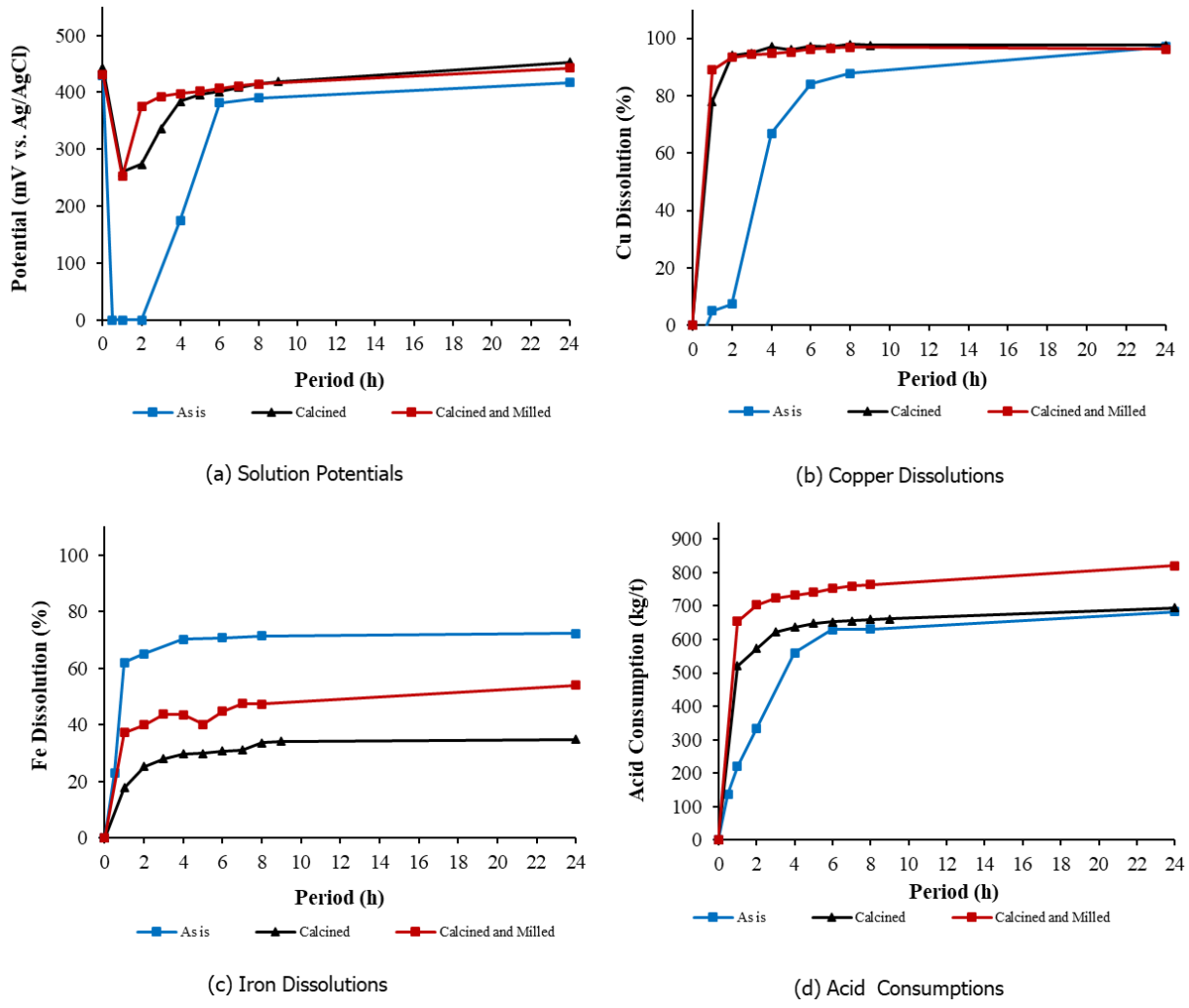

Figure 4.10: Leach Profiles for Calcined Samples

(a) Solution Potential (b) Copper and (c) Iron Dissolutions (d) Total Acid Consumption at: 6% Solids; 10 g/L Cl^-; 0.5 g/L Cu(II); pH 1.0 and 50°C

4.2.10. Summary of Results

Table 4.4 provides a summary of copper and iron dissolution, mass balance results, and the corresponding total and net acid consumptions.

Table 4.4: A Summary of Cu and Fe Dissolutions

Test ID	Size	[Solids]	[Cl⁻]	Temperature	[Cu(II)]	pH	[Fe(II)]	Cu Head		Fe Head		Mass Loss	Out/In		Metal Dissolution [1]		Acid Consumption		
								Assayed	Recalc.	Assayed	Recalc.		Cu	Fe	Cu	Fe	TAC	NAC	
	mm	%	g/L	°C	g/L		g/L	%	%	%	%	%	%	%	%	%	kg/t	kg/t	kg/kg Cu
T1 (a)	-1	6	20.0	50.0	0.5	1.0	0.0	20.15	19.0	9.8	8.9	26	94	91	98	71	635	348	1.9
T1 (b)	-1	6	20.0	50.0	0.5	1.0	0.0	20.15	18.9	9.8	8.4	27	94	86	94	69	663	434	2.5
T2	-3+1	6	20.0	50.0	0.5	1.0	0.0	29.10	35.4	3.1	2.9	40	122	95	96	73	1032	498	1.5
T3	-8+3	6	20.0	50.0	0.5	1.0	0.0	21.20	24.5	4.3	9.8	32	116	227	78	87	1003	707	3.7
T4	+8	6	20.0	50.0	0.5	1.0	0.0	27.00	15.6	5.9	8.1	32	58	137	60	95	1360	1216	13.1
T5	-1	10	20.0	50.0	0.5	1.0	0.0	20.15	22.5	9.8	10.3	25	112	105	87	79	553	251	1.3
T6	-1	15	20.0	50.0	0.5	1.0	0.0	20.15	22.3	9.8	10.6	22	111	107	73	84	479	227	1.4
T7	-1	6	10.0	50.0	0.5	1.0	0.0	20.15	17.2	9.8	8.4	26	85	86	97	72	684	427	2.6
T8	-1	6	30.0	50.0	0.5	1.0	0.0	20.15	19.2	9.8	9.5	24	95	96	91	74	657	387	2.2
T9	-1	6	50.0	50.0	0.5	1.0	0.0	20.15	19.8	9.8	9.1	27	98	93	98	78	608	308	1.6
T10	-1	6	80.0	50.0	0.5	1.0	0.0	20.15	18.1	9.8	10.8	24	90	110	95	82	597	332	1.9
T11	-1	6	100	50.0	0.5	1.0	0.0	20.15	17.8	9.8	7.7	32	89	78	97	81	611	345	2.0
T12	-1	6	20.0	25.0	0.5	1.0	0.0	20.15	19.4	9.8	8.2	20	96	83	51	72	485	332	3.4
T13	-1	6	20.0	60.0	0.5	1.0	0.0	20.15	17.0	9.8	8.7	27	85	88	98	77	719	462	2.8
T14	-1	6	20.0	70.0	0.5	1.0	0.0	20.15	21.2	9.8	8.2	29	105	84	98	81	782	461	2.2
T15	-1	6	20.0	80.0	0.5	1.0	0.0	20.15	23.5	9.8	7.8	29	116	80	98	83	783	427	1.8
T16	-1	6	20.0	50.0	0.0	1.0	0.0	20.15	17.4	9.8	9.5	25	86	97	78	70	805	595	4.4
T17	-1	6	20.0	50.0	1.0	1.0	0.0	20.15	17.9	9.8	7.7	24	89	79	82	66	624	397	2.7
T18	-1	6	20.0	50.0	0.5	1.5	0.0	20.15	17.8	9.8	8.5	21	88	87	86	58	447	211	1.4
T19	-1	6	20.0	50.0	0.5	2.0	0.0	20.15	17.9	9.8	9.6	22	89	97	81	58	409	185	1.3
T20	-1	6	20.0	50.0	0.5	1.0	1.0	20.15	16.9	9.8	8.6	22	84	88	92	70	696	447	2.9
T21	-1	6	20.0	50.0	0.5	1.0	3.0	20.15	21.1	9.8	12.4	25	105	126	95	76	668	360	1.8
T22	-1	6	20.0	50.0	0.5	1.0	5.0	20.15	19.9	9.8	14.2	28	99	144	98	82	664	361	1.8
Incinerated	-1	6	10.0	50.0	0.5	1.0	0.0	32.3	29.5	11.9	7.8	40	91	66	97	40	695	253	0.9
Incinerated & Milled	-1	1	10.0	50.0	0.5	1.0	0.0	32.3	34.6	11.9	8.2	47	107	69	97	51	820.8	305	0.9

Notes:
1) Metal dissolutions by recalculated head and residue (or recalculated head and solution) analyses;
in other words, for a 100% metal mass balance. These are the definitive metal dissolutions

4.3. MINI-PILOT LEACH TEST

The aim of the test was to (i) evaluate the scalability of the test results and (ii) prepare the necessary feed required for the precious metal leach tests, which was not part of this study as indicated in Section 1.6.

4.3.1. Recommended Conditions

The recommended conditions for the pilot experiment are presented in Table 4.5.

Table 4.5: Experimental Matrix for the Pilot Leach Test

Parameter	Bench-scale	Pilot-scale
Particle Size	+ 8 mm to – 1 mm	- 1 mm
Solids Concentration	6-15%	6%
Temperature	25-80°C	50°C
Cl^- Concentration	10-100 g/L	10 g/L
Acidity (pH)	1-2	1
Agitation	500 rpm	350 rpm
Initial Cu(II) concentration	0-1 g/L	0.5 g/L
Initial Fe(II) concentration	0-5 g/L	0 g/L
Air flow rate	500 SCCM (34.9 L/h, ATP)	200 L/h (ATP)
Time	24 h	24 h

4.3.2. pH, Redox and Dissolved Oxygen Profiles

The pH profiles before and after adjustment, redox and DO profiles are presented in Figures 4.11 and 4.12, respectively.

The pH increased to 1.7 in the first 30 minutes and required acid addition for the first 6 h to maintain the pH between 1 and 1.2.

It must be noted that the measured initial potentials (below zero) were very unstable (fluctuated significantly). Attempts were made to record the lowest value measured for the purpose of demonstrating the potential trend.

The sensitivity of the potential to changes in the concentration of dissolved oxygen during the leach is evident in Figure 4.12. For example, the potential decreased from 413 mV (starting solution) to ± - 200 mV in the first 30 minutes. The DO trend was similar, with oxygen limitation observed for the first 4 h. The maximum DO concentration for the conditions tested was 3.28 mg/L. The potential profile is similar to that observed from the bench-scale test at the same conditions, owing to the airflow rates being the same (*i.e.* 34.9 L/h for 4 L reactor vs 200 L/h for 23 L).

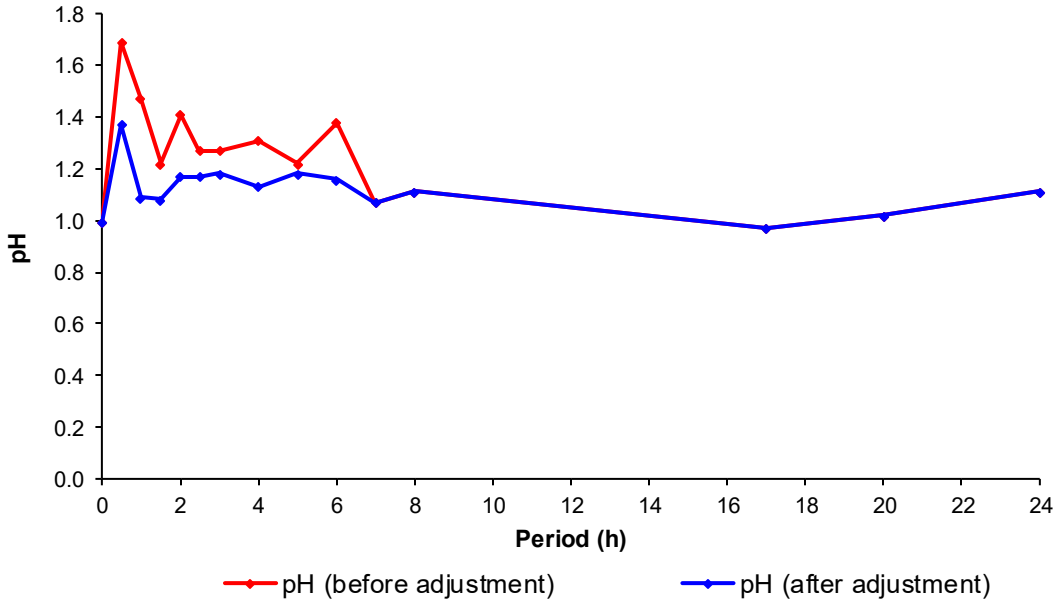

Figure 4.11: pH Profile (Pilot Test)

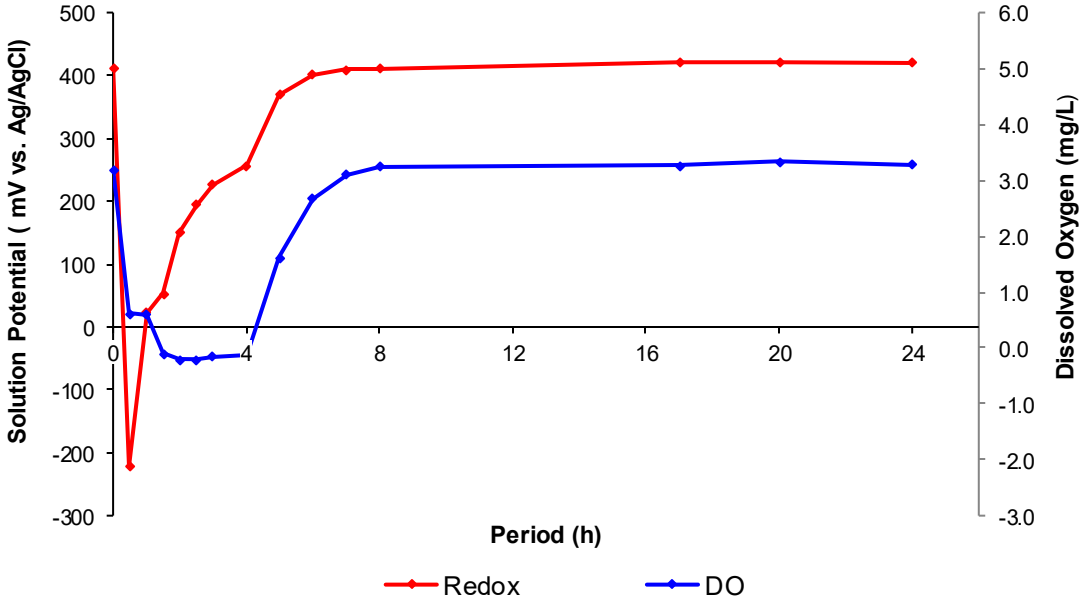

Figure 4.12: Redox and Dissolved Oxygen Profiles (Pilot Test)

4.3.3. Copper and Iron Dissolution Profiles

The copper and iron dissolution profiles are presented in Figure 4.13. These show rapid dissolution of iron, reaching 59% after 3 h. The dissolution of copper was hampered by the low DO concentrations (low potentials) and copper appeared in solution from 2 h, corresponding to a positive measured solution potential, with 97% dissolution of copper achieved after 6 h. Complete dissolution of copper was achieved after 24 h, and the extent of overall dissolution of iron was 65%. These are comparable to the bench scale tests at 97% Cu and 72% Fe dissolutions after 24 h.

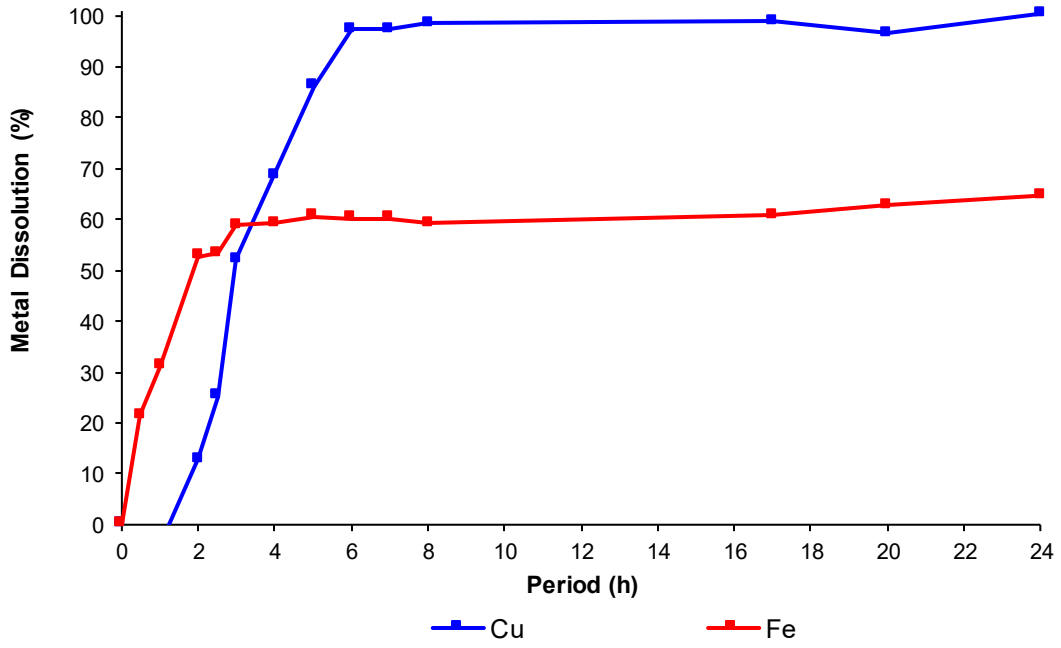

Figure 4.13: Copper and Iron Dissolution Profiles (Pilot Test)

4.3.4. Acid Consumption Profiles

The total and net acid consumption (TAC and NAC) profiles are presented in Figure 4.14. The acid consumption trends were in alignment with metal copper and iron dissolution rates, with no acid consumption observed after 6 h, following nearly complete dissolution of copper. The respective total and net acid consumptions corresponding to the reported metal dissolutions were 676 kg / t and 360 kg/t. These are comparable to those observed from the bench scale test at 684 kg/t TAC and 427 kg/t NAC (Table 4.4, T7).

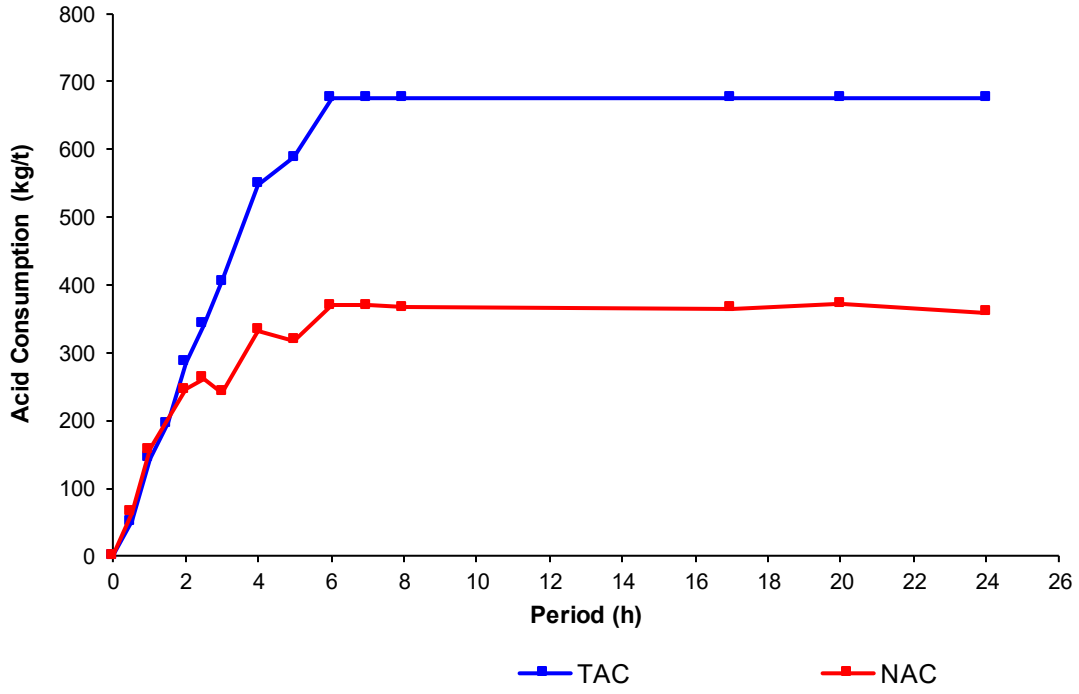

Figure 4.14: Acid Consumption Profiles (Pilot Test)

4.3.5. Dissolution of Other Base Metals and Mass Balances

The concentration profiles of Al, Ca, Cr, Mg, Mn, Ni, Pb and Zn are presented in Figure 4.15. The element mass balances are summarised in Table 4.5. The solution and residue compositions are presented in Appendix C.

Figure 4.15 shows rapid initial dissolution of other base metals, with highest concentrations reached after 8 h. For example, the concentration of Al was 1.08 g/L after 8 h and 1.14 g/L after 24 h, suggesting that there was no further dissolution after 8 h.

Table 4.6 shows satisfactory mass balances (94-110%) for Al, Ca, Cu and Fe. The mass balances of other metals were poor, owing to their low concentrations in the feed sample as well as the non-homogeneity nature of the PCB samples. The definitive dissolutions of other metals were: 31% Al, 70% Ni, 43% Mn, 20% Ti and 4% Pb.

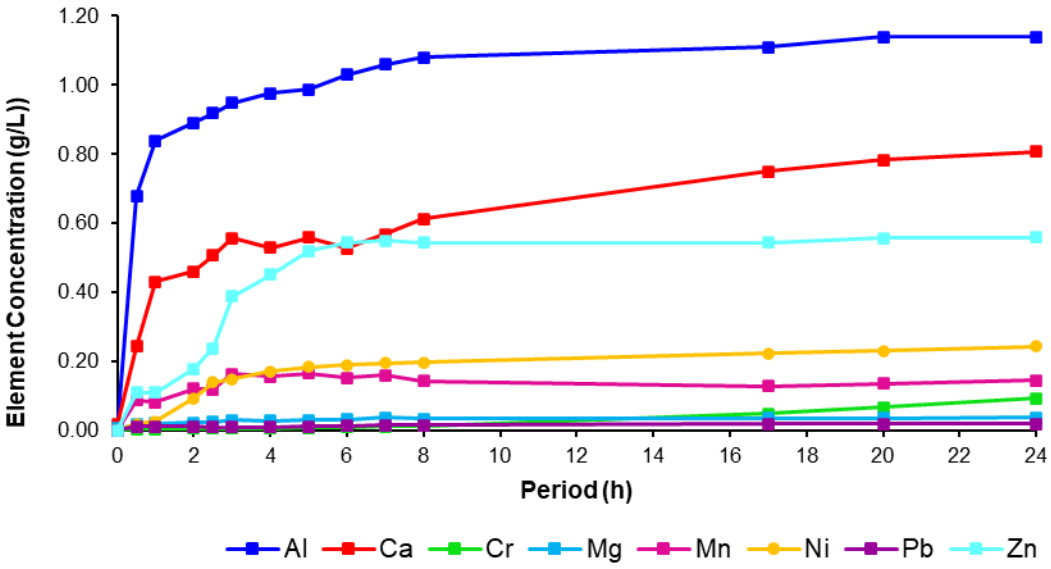

Figure 4.15: Concentrations of Other Metals Over Time (Pilot Test)

Table 4.6: Summary of Dissolutions and Mass Balances for the Pilot Test

Element	Head					Residue			Solution	Metal Dissolution			Out/In (%)
	Feed Mass	Grade		IN head		Residue	Grade	OUT Residue	Mass	Dissolution			
	(kg)	(%) [1]	(%) [2]	(g) [1]	(g) [2]	(kg)	(%)	(g)	(g)	(%) [3]	(%) [4]	(%) [5]	
Al	1.47	5.02	5.53	73.8	81	1.03	5.46	56.2	25.0	33.9	23.8	30.8	110
Ca	1.47	6.70	7.44	98.5	109	1.03	8.66	89.3	20.1	20.4	9.4	18.4	111
Cr	1.47	0.07	0.22	1.0	3	1.03	0.11	1.14	2.2	206.2	-9.4	65.3	316
Cu	1.47	20.15	20.41	296.2	300	1.03	0.62	6.42	294	99.1	97.8	97.9	101
Fe	1.47	9.82	9.26	144.4	136	1.03	4.99	51.4	85	58.7	64.4	62.2	94
Mg	1.47	0.22	0.30	3.2	4	1.03	0.35	3.63	0.8	26.3	-14.7	18.7	141
Mn	1.47	0.85	0.51	12.4	7	1.03	0.41	4.25	3.2	26.1	65.8	43.2	60
Ni	1.47	0.64	0.53	9.3	8	1.03	0.23	2.35	5.5	59.0	74.9	70.1	84
Pb	1.47	1.16	0.82	17.0	12	1.03	1.13	11.6	0.5	2.8	31.8	3.9	71
Si	1.47	12.75	15.46	187.4	227	1.03	22.0	227	0.5	0.3	-21.0	0.2	121
Ti	1.47	0.57	0.78	8.3	11	1.03	0.89	9.18	2.3	28.0	-10.5	20.2	138
Zn	1.47	0.25	0.29	3.6	4	1.03	0.41	4.18	0.1	3.7	-15.9	3.1	120

Notes:

1) Assayed metal head grade
2) Recalculated metal head grade
3) Metal dissolutions by solid head and solution analyses
4) Metal dissolutions by solid head and residue analyses
5) Metal dissolutions by recalculated head and residue (or recalculated head and solution) analyses; in other words, for a 100% metal mass balance. These are the definitive iron dissolutions

CHAPTER 5: DISCUSSION

5.1. DISSOLVED OXYGEN CONCENTRATION AND SOLUTION POTENTIAL

The rate of dissolution of copper was strongly dependent on the solution potential. The initial potential conditions in all the tests became reductive (shortly after solids/solution contact), indicative of weak oxidative strength (*i.e.* absence of Cu(II) which is the primary oxidant). The initial decrease in Cu(II) from starting concentrations of 0.5 g/L-1 g/L to zero is in alignment with the observed oxygen limitation as evident in the DO measurements in the pilot leach test (Figure 4.12). This suggests that a significant decrease in the DO hampers the regeneration of Cu(II), delaying the dissolution of copper until the DO had increased to sufficient levels and most of the more reductive metals had leached which reduces the 'drag' on the potential. Achieving and maintaining higher solution potential is key to the rate of copper dissolution. This aligns with findings by (Yazici & Deveci, 2013), who found that the use of pure oxygen compared to air (higher oxygen partial pressure) achieved and maintained higher potentials from onset, resulting in enhancement of the rate of dissolution of copper.

Increasing the air flowrate, partial pressure of oxygen and agitation speed is recommended to enhance dissolved oxygen levels.

5.2. EFFECT OF PARTICLE SIZE AND SAMPLE HETEROGENEITY

The results showed that the particle size significantly affects copper leaching from PCBs. Finer particle sizes (-3+1 mm and - 1 mm) achieved similar rate and extent of dissolution of copper due to a larger surface area for reaction. The results show that reducing the particle size further than -1 mm may not be necessary as shown by similar rates of dissolution of copper achieved for the calcined samples at -1 mm and - 75 µm (Figure 4.10).

The non-homogenous nature of PCBs also influences how particle size impacts leaching. This variability in material distribution could explain the uneven leaching rates observed. Pre-treatment methods like shredding, milling, sorting and calcination are recommended not only for size reduction but also to improve homogeneity to minimise these effects.

Heterogeneity of sample adversely affects:

a. Assaying, which becomes complex and challenging.
b. Complexity of process (e.g. a copper only process vs. a polymetallic process). For example, a copper only recovery process requires mainly leaching, iron

removal (neutralisation) and SX/EW, whereas a polymetallic sample would require various additional, and often challenging, down-stream processes.

5.3. EFFECT OF SOLIDS CONCENTRATION

The results showed that higher solids concentrations decreased the rate of dissolution of copper significantly (Figure 4.4), primarily due to even lower potentials. This aligns with previous studies, where lower solids concentrations (up to 1% w/w) reduced the leaching time significantly (Yazici & Deveci, 2013, 2015b). However, these low solids concentrations, even though effective lead to low material throughput which could significantly impact the process economics (operating efficiency and cash flow).

The impact on redox potential, which is important for leaching of copper, has already been mentioned above.

5.4. EFFECT OF CHLORIDE AND INITIAL CUPRIC CONCENTRATIONS

An initial decrease of Cu(II) was observed in all the tests (except for calcined samples), suggesting the cementation of copper on more reductive metals. This was caused by the reduced oxidising power because of the oxygen limitation. Previous studies have shown that higher initial Cu(II) concentrations (up to 46.6 g/L) were more effective, provided the Cl^- / Cu(II) ratio was above 8 (Herreros et al., 2005; Yazici & Deveci, 2013). However, such high Cu(II) inventories in the leach circuit are not favourable from a process economics viewpoint. The results also showed that at lower than recommended Cl^- / Cu(II) ratios tested, increasing the chloride concentrations above 10 g/L did not improve the rate and extent of dissolution. Suggesting that copper addition is not required and that a chloride concentration of 10 g/L is sufficient for selective copper dissolution.

5.5. EFFECT OF TEMPERATURE

The results showed that a leaching temperature of 25°C was less effective for the dissolution of copper, yielding an extent of overall copper dissolution of 51% compared to 97% achieved at 50°C after 24 h (Figure 4.6). Temperatures above 50°C did not improve the dissolution rate significantly, and that may be attributed to the decreased solubility of oxygen at higher temperatures which negates the general positive effect of temperature to improve the rate of dissolution under the conditions tested.

5.6. EFFECT OF INITIAL FERROUS CONCENTRATION

The addition of ferrous ion in the lixiviant did not have any impact on the rate and extent of dissolution of copper as observed in Figure 4.9. Therefore, ferrous addition is not required.

5.7. ACIDITY AND ACID CONSUMPTION

High acidity increased the rate of dissolution of copper as shown in Figure 4.7. This is due to the increase in the concentration of H^+ ions, which can enhance the oxidative dissolution of copper since acid is consumed in the re-generation reactions of both Cu(II) and Fe(III). Suggesting that a pH between 1 and 1.5 is conducive for copper leaching. These observations align with findings by previous studies (Ping et al., 2009). However, excessive acidity may also accelerate the consumption of acid as evident in Figure 4.7 (d). Acid can be recovered from solvent extraction of copper which leaves aluminium and iron as the main acid consumers. From an operational point of view, the total acid consumptions were very high and necessitates the removal of aluminium and iron prior to leaching as these, not only have a bearing on the acid consumption, but also on the initial solution potentials.

5.8. CALCINATION

Pre-leach calcination of the samples had the most significant impact on the rate of dissolution of copper as shown in Figure 4.10, with 93% dissolution achieved in 2 hours. This improvement in the rate of dissolution is attributed to the breakdown of polymeric matrices and the liberation of embedded copper particles, which increased the surface area available for leaching. The effectiveness of the calcination explains the preference of processing flowsheets combining both pyro- and hydrometallurgical routes. Milling of the calcined sample did not improve the rate of dissolution, suggesting that the calcination did not result in the encapsulation of copper particles in slag-like residues which could have hindered the dissolution. However, the calcination parameters can be further optimised to reduce energy requirements.

5.9. ELEMENT MASS BALANCES

The copper and iron mass balances were satisfactory, ranging between 84 and 116% for Cu and 66% and 144% for Fe at -1 mm (Tables 4.4 and 4.6). The mass balances were poor for coarser particles and other base metals across the sizes tested. These discrepancies are as a result of a huge variation in PCB composition, which often leads to inaccurate estimation of metal recoveries by most studies.

CHAPTER 6: CONCLUSIONS AND RECOMMENDATIONS

The study demonstrated the effect of several parameters on the dissolution of copper from a waste PCB sample in acidic, cupric chloride medium. It can be concluded from the findings of this study that:

- Copper dissolution is influenced by solution potential, dissolved oxygen concentration, particle size (of the PCB sample), solids concentration and acidity (pH). Up to 98% copper dissolutions were achieved after 24 hrs.
- Balancing solids concentration with the solution potentials is vital for efficient copper leaching.
- PCB heterogeneity affects element mass balances and sample consistency.
- Pre-treatment like calcination can significantly improve the rate of copper dissolution by maintaining more oxidative solution potentials, achieving up to 93% copper dissolution in 2 hours.
- The best conditions identified at lab scale were reproduced at pilot scale, achieving similar copper and iron dissolutions and comparable acid consumption. This demonstrates that the optimized parameters are directly scalable, supporting practical application for larger-scale PCB recycling.

Overall recommendations:

- Optimisation of solution potential by increasing initial cupric ion and dissolved oxygen concentrations (by means of increased air flowrate, higher oxygen partial pressures and higher agitation speed).
- Further evaluation of pre-treatment options like calcination and physical separation to improve sample homogeneity and remove high acid consuming constituents like iron.

CHAPTER 7: REFERENCES

Baldé, C. P., Kuehr, R., Yamamoto, T., McDonald, R., Althaf, S., Bel, G., Deubzer, O., Fernandez-Cubillo, E., Forti, V., Gray, V., Herat, S., Honda, S., Iattoni, G., Khetriwal, D. S., & Luda di Cortemiglia, V. (2024). *The Global E-Waste Monitor*. United Nations Institute for Training and Research (Unitar). https://www.itu.int/itu-d/sites/environment.

Barrueto, Y., Hernández, P., Jiménez, Y., & Morales, J. (2021). Leaching of metals from printed circuit boards using ionic liquids. *Journal of Material Cycles and Waste Management*, *23*(5), 2028–2036. https://doi.org/10.1007/S10163-021-01275-8/FIGURES/3

Berger, J. M., & Winand, R. (1984). Solubilities, densities and electrical conductivities of aqueous copper(I) and copper(II) chlorides in solutions containing other chlorides such as iron, zinc, sodium and hydrogen chlorides. *Hydrometallurgy*, *12*(1), 61–81. https://doi.org/10.1016/0304-386X(84)90048-3

Bhunia, S., & Tehranipoor, M. (2019). Printed Circuit Board (PCB): Design and Test. *Hardware Security*, 81–105. https://doi.org/10.1016/B978-0-12-812477-2.00009-5

Birloaga, I., & Vegliò, F. (2016). Study of multi-step hydrometallurgical methods to extract the valuable content of gold, silver and copper from waste printed circuit boards. *Journal of Environmental Chemical Engineering*, *4*(1), 20–29. https://doi.org/10.1016/j.jece.2015.11.021

Broeksma, C. P. (2018). *Evaluating the applicability of an alkaline amino acid leaching process for base and precious metal leaching from printed circuit board waste. Master of Engineering Thesis, Stellenbosch University*. https://scholar.sun.ac.za

Brožová, S., Lisińska, M., Saternus, M., Gajda, B., Simha Martynková, G., & Slíva, A. (2021). Hydrometallurgical recycling process for mobile phone printed circuit boards using ozone. *Metals*, *11*(5). https://doi.org/10.3390/met11050820

Chehade Y., Siddique A., Alayan H., Sadasivam N., N. S. and I. T. (2012). Recovery of Gold, Silver, Palladium and Copper from Waste Printed Circuit Boards. *International Conference on Chemical, Civil and Environment Engineering*, *1*, 226–234. https://doi.org/10.3390/resources3010152

Cui, H., & Anderson, C. (2020). Hydrometallurgical Treatment of Waste Printed Circuit Boards: Bromine Leaching. *Metals 2020, Vol. 10, Page 462*, *10*(4), 462. https://doi.org/10.3390/MET10040462

Cui J, & Zhang L. (2008). Metallurgical recovery of metals from electronic waste: A review. *Journal of Hazardous Materials*, *158*(2–3), 228–256. https://doi.org/10.1016/j.jhazmat.2008.02.001

Desco Electronic Recyclers - Identify E-Waste - What We Recycle. (2017). https://www.desco.co.za/index.php/e-waste-wall/199-identify-e-waste-what-we-recycle

Duby, P. (1977). *The Thermodynamic Properties of Aqueous Inorganic Copper Systems. International Copper Research Association, Series on the Metallurgy of Copper, National Standard Reference Data System*.

Elomaa, H., Seisko, S., Junnila, T., Sirviö, T., Wilson, B., Aromaa, J., & Lundström, M. (2017). The Effect of the Redox Potential of Aqua Regia and Temperature on the Au, Cu, and Fe Dissolution from WPCBs. *Recycling*, *2*(3), 14. https://doi.org/10.3390/recycling2030014

Eng, J. A. C., Cui, H., & Anderson, C. G. (2016). Literature Review of Hydrometallurgical Recycling of Printed Circuit Boards (PCBs). *Journal of Advanced Chemical Engineering*, *6*(1), 1–11. https://doi.org/10.4172/2090-4568.1000142

Fazari, J., Hossain, M. Z., & Charpentier, P. (2024). A review on metal extraction from waste printed circuit boards (wPCBs). In *Journal of Materials Science* (Vol. 59, Issue 27, pp. 12257–12284). Springer. https://doi.org/10.1007/s10853-024-09941-6

Forti, V., Baldé, C. P., Kuehr, R., & Bel, G. (2020). The Global E-waste Monitor 2020: Quantities, Flows, and the Circular Economy Potential. In *United Nations University (UNU)/United Nations Institute for Training and Research (UNITAR) – co-hosted SCYCLE Programme, International Telecommunication Union (ITU) & International Solid Waste Association (ISWA), Bonn/Geneva/Rotterdam*.

Fritz, J. J. (1982). Solubility of Cuprous Chloride in Various Soluble Aqueous Chlorides. *Journal of Chemical and Engineering Data*, *27*(2), 188–193. https://doi.org/10.1021/JE00028A027/ASSET/JE00028A027.FP.PNG_V03

Gu, F., Summers, P. A., & Hall, P. (2019). Recovering materials from waste mobile phones: Recent technological developments. *Journal of Cleaner Production*. https://doi.org/10.1016/j.jclepro.2019.117657

Hao, J., Wang, X., Wang, Y., Wu, Y., & Guo, F. (2022). *Optimizing the Leaching Parameters and Studying the Kinetics of Copper Recovery from Waste Printed Circuit Boards*. *7*, 3689–3699. https://doi.org/10.1021/acsomega.1c06173

Hayes, P. C. (Peter C.). (1993). *Process principles in minerals and materials production / by Peter C. Hayes ; with contributions from S.H. Algie ... [et al.]*.

Herreros, O., Quiroz, R., Restovic, A., & Viñals, J. (2005). Dissolution kinetics of metallic copper with CuSO4-NaCl-HCl. *Hydrometallurgy*, *77*(3–4), 183–190. https://doi.org/10.1016/j.hydromet.2004.11.010

Hiroyoshi, N., Hirota, M., Hirajima, T., & Tsunekawa, M. (1997). A case of ferrous sulfate addition enhancing chalcopyrite leaching. *Hydrometallurgy*, *47*(1), 37–45. https://doi.org/10.1016/S0304-386X(97)00032-7

Hiroyoshi, N., Miki, H., Hirajima, T., & Tsunekawa, M. (2000). A model for ferrous-promoted chalcopyrite leaching. *Hydrometallurgy*, *57*(1), 31–38. https://doi.org/10.1016/S0304-386X(00)00089-X

International Copper Association. (2024). Copper Demand and Long-Term Availability. *Https://Internationalcopper.Org/*. https://internationalcopper.org/sustainable-copper/about-copper/cu-demand-long-term-availability/

Jackson, E. . (1986). *Hydrometallurgical extraction and reclamation*. 266.

Jadhav, U., & Hocheng, H. (2015). Hydrometallurgical Recovery of Metals from Large Printed Circuit Board Pieces. *Scientific Reports*, *5*(101), 1–10. https://doi.org/10.1038/srep14574

Jha, M. K., Choubey, P. K., Jha, A. K., Kumari, A., Lee, J. chun, Kumar, V., & Jeong, J. (2012). Leaching studies for tin recovery from waste e-scrap. *Waste Management*, *32*(10), 1919–1925. https://doi.org/10.1016/j.wasman.2012.05.006

Kamberovic, Z., Korac, M., & Ranitovic, M. (2011a). Hydrometallurgical Process for Extraction of Metals from Eectronic Waste-Part II: Development of the Processes for the Recovery of Copper from Printed Circuit Boards (PCB). *Metalurgija-MJoM*, *17*(3), 139–149. https://doi.org/628.477.6

Kamberovic, Z., Korac, M., & Ranitovic, M. (2011b). Hydrometallurgical Process for Extraction of Metals from Eectronic Waste-Part II: Development of the Processes for the Recovery of Copper from Printed Circuit Boards (PCB). *Metalurgija-MJoM*, *17*(3), 139–149. https://doi.org/628.477.6

Kamberović, Ž., Korać, M., Vračar, S., & Ranitović, M. (2010). *Preliminary Process Analysis and Development of Hydrometallurgical Process for the Recovery of Copper from Printed Circuit Boards, Going Green-Care Innovation Conference*.

Kaya, M. (2016). Recovery of metals and nonmetals from electronic waste by physical and chemical recycling processes. *Waste Management*, *57*, 64–90. https://doi.org/10.1016/j.wasman.2016.08.004

Khaliq, A., Rhamdhani, M. A., Brooks, G., & Masood, S. (2014). Metal extraction processes for electronic waste and existing industrial routes: A review and Australian perspective. *Resources*, *3*(1), 152–179. https://doi.org/10.3390/resources3010152

Khatri, B. R., Sodha, A. B., Shah, M. B., Tipre, D. R., & Dave, S. R. (2018). Chemical and microbial leaching of base metals from obsolete cell-phone printed circuit boards. *Sustainable Environment Research*, *28*(6), 333–339. https://doi.org/10.1016/j.serj.2018.10.002

Kim, E. Y., Kim, M. S., Lee, J. C., Jeong, J., & Pandey, B. D. (2011). Leaching kinetics of copper from waste printed circuit boards by electro-generated chlorine in HCl solution. *Hydrometallurgy*, *107*(3–4), 124–132. https://doi.org/10.1016/j.hydromet.2011.02.009

Kumar, A., Holuszko, M. E., & Janke, T. (2018). Characterization of the non-metal fraction of the processed waste printed circuit boards. *Waste Management*, *75*, 94–102. https://doi.org/10.1016/j.wasman.2018.02.010

Kumar, A., Holuszko, M., & Espinosa, D. C. R. (2017). E-waste: An overview on generation, collection, legislation and recycling practices. *Resources, Conservation and Recycling*, *122*, 32–42. https://doi.org/10.1016/j.resconrec.2017.01.018

Kumar, M., Lee, J.-C., Kim, M.-S., Jeong, J., & Yoo, K. (2014). *Leaching of Metals From Waste Printed Circuit Boards (WPCBs) Using Sulfuric And Nitric Acids, Environmental Engineering and Management* (Vol. 13, Issue 10). http://omicron.ch.tuiasi.ro/EEMJ/

Lundström, M. (2009). *CHALCOPYRITE DISSOLUTION IN CUPRIC CHLORIDE SOLUTIONS Doctoral Thesis*.

Lydall, M., Nyanjowa, W., & James, Y. (2017). *Mapping South Africa's waste electrical and electronic equipment (WEEE) dismantling, pre-processing and processing technology landscape*. *March*, 1–91. https://doi.org/DOI: 10.1016/j.resmic.2009.12.007

Marsden, J., & House, I. (1992). *The Chemistry of Gold Extraction* (E. West, Ed.; First). Ellis Horwood Limited.

Montero, R., Guevara, A., & De La Torre, E. (2012). Recovery of gold, silver, copper and niobium from printed circuit boards using leaching column technique. *26th International Mineral Processing Congress, IMPC 2012: Innovative Processing for Sustainable Growth - Conference Proceedings*, *2*, 3513–3519.

Moyo, T., Chirume, B. H., & Petersen, J. (2020). Assessing alternative pre-treatment methods to promote metal recovery in the leaching of printed circuit boards. *Resources, Conservation and Recycling*. https://doi.org/10.1016/j.resconrec.2019.104545

Narita, E., Lawson, F., & Han, K. N. (1983). Solubility of oxygen in aqueous electrolyte solutions. *Hydrometallurgy*, *10*(1), 21–37. https://doi.org/10.1016/0304-386X(83)90074-9

Nezungai, D., Crundwell, F. K., Lloyd, J., & Osman, A. (2013). *Analysis of the Effects of Changes in Operating Conditions on the Agitated Leaching of Copper, The Southern African Institute of Mining and Metallurgy Base Metals Conference*.

Nicol, M. J. (2008). *Hydrometallurgy- Theory and Practice- Study Guide, University of Cape Town*.

Nxumalo, D. N. (2016). *Recovery of Copper from Printed Circuit Boards (PCBs) by Leaching in Sulphate Solutions, Mintek Internal Report 42245*.

Nyanjowa, W., & James, Y. (2015). *Material Flow Analysis of Printed Circuit Boards and Lithium Ion Batteries in Gauteng, South Africa, A Contribution to teh Urban Mining Project, Mintek Internal report 41939* (Issue March).

Park, Y. J., & Fray, D. J. (2009). Recovery of high purity precious metals from printed circuit boards. *Journal of Hazardous Materials*, *164*(2–3), 1152–1158. https://doi.org/10.1016/j.jhazmat.2008.09.043

Ping, Z., ZeYun, F., Jie, L., Qiang, L., GuangRen, Q., & Ming, Z. (2009). Enhancement of leaching copper by electro-oxidation from metal powders of waste printed circuit board. *Journal of Hazardous Materials*, *166*(2–3), 746–750. https://doi.org/10.1016/j.jhazmat.2008.11.129

Sepúlveda, R., Martínez, M., Hernández, P., Guzmán, A., & Castillo, J. (2023). Effect of Chloride and Ferrous Ions on Improving Copper Leaching from Black Copper Ores. *Processes 2024, Vol. 12, Page 13*, *12*(1), 13. https://doi.org/10.3390/PR12010013

Sodha, A. B., Tipre, D. R., & Dave, S. R. (2020a). Optimisation of biohydrometallurgical batch reactor process for copper extraction and recovery from non-pulverized waste printed circuit boards. *Hydrometallurgy*. https://doi.org/10.1016/j.hydromet.2019.105170

Sodha, A. B., Tipre, D. R., & Dave, S. R. (2020b). Optimisation of biohydrometallurgical batch reactor process for copper extraction and recovery from non-pulverized waste printed circuit boards. *Hydrometallurgy*, *191*. https://doi.org/10.1016/j.hydromet.2019.105170

Sohaili, J., Muniyandi, S. K., & Mohamad, S. S. (2012). A Review on Printed Circuit Boards Waste Recycling Technologies and Reuse of Recovered Nonmetallic Materials. *International Journal of Scientific & Engineering Research*, *3*(2), 1–7.

Tetronics. (2024). *Electronic waste recycling - Tetronics*. https://tetronics.com/our-solutions/resource-recovery/electronic-waste-recycling/

The Engineering ToolBox. (2005). *Oxygen - Solubility in Fresh and Sea Water vs. Temperature*. https://www.engineeringtoolbox.com/oxygen-solubility-water-d_841.html

Tuncuk, A., Stazi, V., Akcil, A., Yazici, E. Y., & Deveci, H. (2012). Aqueous metal recovery techniques from e-scrap: Hydrometallurgy in recycling. *Minerals Engineering*. https://doi.org/10.1016/j.mineng.2011.09.019

Umicore. (2024). *Our process | Umicore Precious Metals Refining*. https://pmr.umicore.com/en/about-us/process/

Valix, M. (2017). Bioleaching of Electronic Waste: Milestones and Challenges. In *Current Developments in Biotechnology and Bioengineering: Solid Waste Management* (pp. 407–442). Elsevier Inc. https://doi.org/10.1016/B978-0-444-63664-5.00018-6

Velásquez Yévenes, L. (2009). *THE KINETICS OF THE DISSOLUTION OF CHALCOPYRITE IN CHLORIDE MEDIA*.

Wang, Z., Guo, S., & Ye, C. (2016). Leaching of Copper from Metal Powders Mechanically Separated from Waste Printed Circuit Boards in Chloride Media Using Hydrogen Peroxide as Oxidant. *Procedia Environmental Sciences*, *31*, 917–924. https://doi.org/10.1016/j.proenv.2016.02.110

Watling, H. R. (2014). Chalcopyrite hydrometallurgy at atmospheric pressure: 2. Review of acidic chloride process options. In *Hydrometallurgy* (Vol. 146, pp. 96–110). Elsevier. https://doi.org/10.1016/j.hydromet.2014.03.013

Winand, R. (1991). Chloride hydrometallurgy*. In *Hydrometallurgy* (Vol. 27).

Yang, T., Xu, Z., Wen, J., & Yang, L. (2009). Factors influencing bioleaching copper from waste printed circuit boards by Acidithiobacillus ferrooxidans. *Hydrometallurgy*, *97*(1–2), 29–32. https://doi.org/10.1016/j.hydromet.2008.12.011

Yang, Y., Chen, S., Li, S., Chen, M., Chen, H., & Liu, B. (2014). Bioleaching waste printed circuit boards by Acidithiobacillus ferrooxidans and its kinetics aspect. *Journal of Biotechnology*, *173*(1), 24–30. https://doi.org/10.1016/j.jbiotec.2014.01.008

Yazici, E. Y., & Deveci, H. (2013). Extraction of metals from waste printed circuit boards (WPCBs) in H 2SO4-CuSO4-NaCl solutions. *Hydrometallurgy*, *139*, 30–38. https://doi.org/10.1016/j.hydromet.2013.06.018

Yazici, E. Y., & Deveci, H. (2015a). Cupric chloride leaching (HCl-CuCl2-NaCl) of metals from waste printed circuit boards (WPCBs). *International Journal of Mineral Processing*, *134*, 89–96. https://doi.org/10.1016/j.minpro.2014.10.012

Yazici, E. Y., & Deveci, H. (2015b). Cupric chloride leaching (HCl-CuCl2-NaCl) of metals from waste printed circuit boards (WPCBs). *International Journal of Mineral Processing*, *134*, 89–96. https://doi.org/10.1016/j.minpro.2014.10.012

Zhang, L., & Xu, Z. (2016). A review of current progress of recycling technologies for metals from waste electrical and electronic equipment. *Journal of Cleaner Production*, *127*, 19–36. https://doi.org/10.1016/j.jclepro.2016.04.004

Zhang, Y., Liu, S., Xie, H., Zeng, X., & Li, J. (2012). Current Status on Leaching Precious Metals from Waste Printed Circuit Boards. *Procedia Environmental Sciences*, *16*, 560–568. https://doi.org/10.1016/j.proenv.2012.10.077

APPENDIX A : LITERATURE SUPPORTING MATERIAL

Table A1: Common Oxidants Used in Hydrometallurgy

Oxidant	Efficiency and Advantages	Disadvantages	Common Use Case	Reference
Ozone (O_3)	Strong oxidant (E° = 2.07 V), can be used at atmospheric pressure and temperature.	Requires careful handling	Used in acidic (HCl, HNO_3 / H_2SO_4) leach systems	(Brožová et al., 2021)
Hydrogen peroxide (H_2O_2)	Strong oxidant (E° = 1.78 V), highly efficient.	Decomposes easily, leading to reagent loss and operational inefficiencies.	Commonly used in H_2SO_4 leaching. Can also be used with HCl and glycine.	(Birloaga & Vegliò, 2016; Brožová et al., 2021; Hao et al., 2022; Wang et al., 2016)
Pure Oxygen (O_2) / Air	Strong oxidant (E° = 1.23 V) Widely available, cost effective when used as air and environmentally friendly.	Limited oxygen solubility in some systems.	Used in chloride, ammonium and bioleaching.	(Ping et al., 2009; Yazici & Deveci, 2013, 2015b)
Ferric ions (Fe(III))	Moderate oxidant (E° = 0.77 V), widely used for selective copper leaching. Can be regenerated *in situ* by action of iron-oxidising microorganisms.	Requires continuous regeneration. Stable at pH < 2	Used in acidic media as chloride / sulphate for base metals leaching. Used as ferric sulphate with thiourea for gold leaching.	(Birloaga & Vegliò, 2016; Kamberovic et al., 2011a)
Cupric ions (Cu(II))	Efficient for copper leaching. Can be regenerated by oxygen. Has a wider operating pH window compared to Fe(III).	Requires higher copper inventories in solution. Sensitive to dissolved oxygen concentrations	Used in cupric chloride leach systems in the presence of air or oxygen.	(Ping et al., 2009; Yazici & Deveci, 2013, 2015b)
Nitric acid (HNO_3)	Functions as both acid and strong oxidant.	Expensive and produces toxic gases.	Used on its own or in combination with HCl (aqua regia) to recover base and precious metals	(Brožová et al., 2021; Elomaa et al., 2017; Park & Fray, 2009)

APPENDIX B : METHODOLOGY SUPPORTING MATERIAL

Table B1: Description of Analytical Methods (solids)

Analyte(s)	Method(s)	Description	Detection Limit
Al, Ca, Cu, Co, Cr, Fe, Pb, Mg, Mn, Ni, Si, Ti, V and Zn	ICP base metals (ICP-OES) [1]	A mass of solid sample (0.2 g) is fused with a strong alkali flux followed by acidification (HCl / HNO_3) for conversion into solution. The solution is then analysed by ICP-OES.	0.05% - 40%
Ag	AAS [2]	A mass of solid sample (1 g) is digested with acid (HCl / HNO_3) for conversion into solution. The solution is then analysed by AAs.	Lower limit: 2 ppm
Au, Pd and Pt	Fire assay	Standard fire assay with low-temperature cupellation of the silver prill, parting and annealing, followed by gravimetric finish.	Lower limit: 0.08 g/t
C(total)	Combustion (LECO analyzer)	A mass of solid sample is heated in the instrument furnace with an accelerator. Carbon is released and detected by infra-red spectroscopy (IRS).	Lower limit: 0.01%
C(organic)	Extraction / combustion	Carbonate is leached from a mass of solid sample with an acid (HCl). The remaining carbon (graphitic and organic) in the solid residue is determined by combustion.	Lower limit: 0.1%
C(carbonate)	Calculated (by difference)	C(total) - C(organic)	Lower limit: 0.5%
Sn	ICP10 (ICP-MS) [3]	A mass of solid sample (0.2 g) is digested with boric acid, HF, $HClO_4$ and H_2SO_4) for conversion into solution. The solution is then analysed by ICP-MS.	0.05% - 40%

Notes:

1. ICP-OES: Inductively coupled plasma-optical emission spectroscopy
2. AAS: Atomic absorption spectroscopy
3. ICP-MS: Inductively coupled plasma-mass spectrometer

Table B2: Description of Analytical Methods (solutions)

Analyte(s)	Method(s)	Description	Detection Limit
Al, Ca, Cu, Co, Cr, Fe, Pb, Mg, Mn, Ni, Si, Ti, V and Zn	ICP base metals (ICP-OES)	A volume of sample is diluted with acid and water and then analysed by ICP-OES.	Lower limit: 2 ppm
Ag	AAS	A volume of sample is analysed by AAS. The sample may be diluted with a solution of 10% HCl depending on the silver concentration.	Lower limit: 2 ppm
Au	AAS	A volume of sample is analysed by AAS. The sample may be diluted with a solution of sodium cyanide prior to analysis depending on the gold concentration.	Lower limit: 0.1 ppm
	ETA-AAS [4]	A volume of sample is analysed by electrothermal AAS.	0.008 ppm 0.1 ppm
Sn	ICP10 (ICP-MS)	A volume of solution is analysed by ICP-MS.	Lower limit: 2 ppm

Note:

1. ETA-AAS: Electrothermal atomic absorption spectroscopy

Table B3 summarises the values used for conversion of potential (E) vs 3 M KCl, Ag/AgCl) to E_h vs standard hydrogen electrode (SHE).

$$E_h = E + E_{Ag} \quad \text{(B.1)}$$

Where E_{Ag} is the potential of the reference electrode.

Table B3: Conversion of Potential Measurements from 3 M KCl Ag/AgCl to the SHE Scale

Temperature (°C)	**E_{Ag} (mV, Ag/AgCl)**
0	224.2
10	217.4
20	210.5
25	207.0
40	196.1
50	188.4
60	180.3
70	172.1
80	163.1

Working Solutions

Analysis of working solutions are presented in Tables B4 and B5.

Table B4: Analysis of Working Solutions (Bench-scale Tests)

T1-6, T12-15			
Parameter	**Unit**	**Spec**	**Measured**
Temperature	°C		
pH		1.0	1.01
Redox	mV	-	467
$[H_2SO_4]$	g/L		8.94
$[Cl^-]$	g/L	20	20.5
[Cu]	g/L	0.50	0.52
Fe(T)	g/L	0	0.07
Fe(II)	g/L	0	0

T7			
Parameter	**Unit**	**Spec**	**Measured**
Temperature	°C	50.0	50.2
pH		1.0	1.02
Redox	mV	-	448
$[H_2SO_4]$	g/L		10.3
$[Cl^-]$	g/L	10	10.5
[Cu]	g/L	0.50	0.50
Fe(T)	g/L	0	0.04
Fe(II)	g/L	0	0

T8			
Parameter	**Unit**	**Spec**	**Measured**
Temperature	°C	50.0	50.5
pH		1.0	1.02
Redox	mV	-	432
$[H_2SO_4]$	g/L		8.49
$[Cl^-]$	g/L	30	30.2
[Cu]	g/L	0.50	0.48
Fe(T)	g/L	0	0.12
Fe(II)	g/L	0	0.0

T9			
Parameter	**Unit**	**Spec**	**Measured**
Temperature	°C	50.0	49.8
pH		1.0	1.02
Redox	mV	-	496
$[H_2SO_4]$	g/L		7.11
$[Cl^-]$	g/L	50	50.2
[Cu]	g/L	0.50	0.50
Fe(T)	g/L	0	0.09
Fe(II)	g/L	0	0

T10			
Parameter	**Unit**	**Spec**	**Measured**
Temperature	°C	50.0	50.1
pH		1.0	1.02
Redox	mV	-	468
$[H_2SO_4]$	g/L		5.57
$[Cl^-]$	g/L	80	77.5
[Cu]	g/L	0.50	0.49
Fe(T)	g/L	0	0
Fe(II)	g/L	0	0

T11			
Parameter	**Unit**	**Spec**	**Measured**
Temperature	°C	50.0	50.2
pH		1.0	1.01
Redox	mV	-	485
$[H_2SO_4]$	g/L		5.16
$[Cl^-]$	g/L	100	102.5
[Cu]	g/L	0.50	0.50
Fe(T)	g/L	0	0
Fe(II)	g/L	0	0

T16			
Parameter	**Unit**	**Spec**	**Measured**
Temperature	°C	50.0	50.5
pH		1.0	1.01
Redox	mV	-	424
$[H_2SO_4]$	g/L		9.01
$[Cl^-]$	g/L	20	20.5
[Cu]	g/L	0	0
Fe(T)	g/L	0	0.16
Fe(II)	g/L	0	0

T17			
Parameter	**Unit**	**Spec**	**Measured**
Temperature	°C	50.0	50.6
pH		1.0	1.0
Redox	mV	-	465
$[H_2SO_4]$	g/L		9.39
$[Cl^-]$	g/L	20	20.3
[Cu]	g/L	1.0	0.94
Fe(T)	g/L	0	0.05
Fe(II)	g/L	0	0

T18			
Parameter	**Unit**	**Spec**	**Measured**
Temperature	°C	50.0	50.3
pH		1.5	1.5
Redox	mV	-	435
$[H_2SO_4]$	g/L		3.13
$[Cl^-]$	g/L	20	20.7
[Cu]	g/L	0.50	0.53
Fe(T)	g/L	0	0.07
Fe(II)	g/L	0	0

T19			
Parameter	**Unit**	**Spec**	**Measured**
Temperature	°C	50.0	50.2
pH		2.0	2.01
Redox	mV	-	453
$[H_2SO_4]$	g/L		1.04
$[Cl^-]$	g/L	20	20.5
[Cu]	g/L	0.50	0.51
Fe(T)	g/L	0	0
Fe(II)	g/L	0	0

T20			
Parameter	**Unit**	**Spec**	**Measured**
Temperature	°C	50.0	50.6
pH		1.0	1.01
Redox	mV	-	398
$[H_2SO_4]$	g/L		9.52
$[Cl^-]$	g/L	20	20.6
[Cu]	g/L	0.50	0.50
Fe(T)	g/L	1.0	1.01
Fe(II)	g/L	1.0	0.99

T21			
Parameter	**Unit**	**Spec**	**Measured**
Temperature	°C	50.0	50.5
pH		1.0	1.01
Redox	mV	-	378
$[H_2SO_4]$	g/L		10.6
$[Cl^-]$	g/L	20	20.0
[Cu]	g/L	0.50	0.49
Fe(T)	g/L	3.0	2.81
Fe(II)	g/L	3.0	2.78

T22			
Parameter	**Unit**	**Spec**	**Measured**
Temperature	°C	50.0	50.4
pH		1.0	1.0
Redox	mV	-	367
$[H_2SO_4]$	g/L		11.3
$[Cl^-]$	g/L	20	20.5
[Cu]	g/L	0.50	0.50
Fe(T)	g/L	5.0	4.68
Fe(II)	g/L	5.0	4.72

Table B5: Sample of Lixiviant Assays

Test ID	Temp. °C	pH (Auto)	pH (Portable)	H_2SO_4 g/L	Redox mV	E_h mV	Al mg/L	As mg/L	Ca mg/L	Cd mg/L	Cl g/L	Co mg/L	Cr mg/L	Cu (AA) mg/L	Cu (ICP) mg/L	Fe(II) mg/L	Fe(III) mg/L	Fe (AA) mg/L	Fe (ICP) mg/L	Li mg/L	Mg mg/L	Mn mg/L	Mo mg/L	Ni mg/L	Pb mg/L	S mg/L	Si mg/L	Ti mg/L	V mg/L	Zn mg/L
T20 (a)	50.6	1.051	1.01	9.54	398	586	< 2	< 2	< 2	< 2	20.5	< 2	< 2	487	498	981	29.0	953	1010	< 2	< 2	< 2	< 2	< 2	< 2	4305	< 2	< 2	< 2	< 2
T20 (b)				9.49			< 2	< 2	< 2	< 2	20.8	< 2	< 2	488	496	988	29.0	962	1000	< 2	< 2	< 2	< 2	< 2	< 2	4260	< 2	< 2	< 2	< 2
T20 (c)				9.52			< 2	< 2	< 2	< 2	20.6	< 2	< 2	489	499	989	29.0	958	1010	< 2	< 2	< 2	< 2	< 2	< 2	4270	< 2	< 2	< 2	< 2
T20 (d)				9.51			< 2	< 2	< 2	< 2	20.6	< 2	< 2	491	498	988	29.0	961	1010	< 2	< 2	< 2	< 2	< 2	< 2	4280	< 2	< 2	< 2	< 2
Average	50.6	1.051	1.01	9.52	398	586	< 2	< 2	< 2	< 2	20.6	< 2	< 2	489	498	987	29.0	959	1008	< 2	< 2	< 2	< 2	< 2	< 2	4279	< 2	< 2	< 2	< 2

APPENDIX C : EXPERIMENTAL DATA AND RESULTS

Table C1: Chemical Analysis +8 mm Sample (Statistical Analysis)

Element			Ag	Al	Au	Ca	Cu	Fe	Mg	Mn	Ni	Pb	Pd	Pt	Sb	Si	Sn	Ti	Zn
			(ppm)	(%)	(ppm)	(%)	(%)	(%)	(%)	(%)	(%)	(%)	(ppm)	(ppm)	(%)	(%)	(%)	(%)	(%)
Mean			76.8	8.95	32.9	8.12	27.0	0.59	0.16	< 0.05	0.09	0.57	3.52	0.09	0.33	13.2	1.05	0.19	0.38
Standard Deviation			49.7	1.54	20.3	0.19	0.68	0.17	0.02		0.01	0.09	0.65	0.09	0.03	0.12	0.05	0.01	0.21
n	**3**	**95% CI**	123.5	3.83	50.6	0.46	1.69	0.41	0.05		0.02	0.23	1.61	0.23	0.08	0.29	0.12	0.01	0.53
df	**2**	**Lower**	0*	5.12	0*	7.65	25.3	0.18	0.11		0.07	0.34	1.91	0*	0.25	12.9	0.93	0.17	0*
t	**4.303**	**Upper**	200	12.8	83.4	8.58	28.7	1.00	0.21		0.10	0.80	5.12	0.32	0.41	13.5	1.17	0.20	0.90

Table C2: Chemical Analysis -8+3 mm Sample (Statistical Analysis)

Element			Ag	Al	Au	Ca	Cu	Fe	Mg	Mn	Ni	Pb	Pd	Pt	Sb	Si	Sn	Ti	Zn
			(ppm)	(%)	(ppm)	(%)	(%)	(%)	(%)	(%)	(%)	(%)	(ppm)	(ppm)	(%)	(%)	(%)	(%)	(%)
Mean			206	10.1	238	5.06	21.2	4.32	0.27	0.08	0.26	1.10	5.82	0.16	1.65	10.9	2.05	0.19	4.83
Standard Deviation			149	1.17	66.2	0.114	2.35	0.499	0.060	0.029	0.072	0.069	2.46	0.123	0.122	0.787	0.390	0.020	1.80
n	**3**	**95% CI**	371	2.90	164	0.28	5.85	1.24	0.15	0.07	0.18	0.17	6.10	0.30	0.30	1.95	0.97	0.05	4.46
df	**2**	**Lower**	0*	7.19	73.9	4.78	15.3	3.08	0.12	0.01	0.08	0.93	0*	0*	1.35	8.94	1.08	0.14	0.37
t	**4.303**	**Upper**	577	13.0	403	5.34	27.0	5.56	0.42	0.15	0.44	1.27	11.9	0.47	1.95	12.9	3.02	0.24	9.30

Table C3: Chemical Analysis -3+1 mm Sample (Statistical Analysis)

Element			Ag	Al	Au	Ca	Cu	Fe	Mg	Mn	Ni	Pb	Pd	Pt	Sb	Si	Sn	Ti	Zn
			(ppm)	(%)	(ppm)	(%)	(%)	(%)	(%)	(%)	(%)	(%)	(ppm)	(ppm)	(%)	(%)	(%)	(%)	(%)
Mean			390	6.66	366	3.85	29.1	3.11	0.16	0.22	0.52	3.23	21.5	0.25	0.79	8.25	6.83	0.28	1.32
Standard Deviation			366	0.004	12.4	0.223	0.389	0.145	0.004	0.014	0.032	0.046	2.76	0.021	0.011	0.247	0.647	0.007	0.049
n	**3**	**95% CI**	909	0.01	30.7	0.55	0.97	0.36	0.01	0.04	0.08	0.11	6.85	0.05	0.03	0.61	1.61	0.02	0.12
df	**2**	**Lower**	0*	6.65	335	3.29	28.1	2.75	0.15	0.18	0.44	3.12	14.6	0.19	0.76	7.64	5.22	0.27	1.20
t	**4.303**	**Upper**	1299	6.67	397	4.40	30.1	3.47	0.17	0.26	0.60	3.35	28.3	0.30	0.82	8.87	8.43	0.30	1.44

* Values with lower bounds below zero were truncated at zero due to physical constraints.

Table C4: Bench-Scale Test Details

Test ID	Mass Solids (g)	Mass Soln (g)	Residue Mass (g)	Filtrate Vol (L)
T1	253	3964	188	4.13
T2	126	1974	76	2.03
T3	127	1990	86	2.25
T4	135	2115	91	1.97
T5	225	2025	169	1.73
T6	353	2000	276	1.74
T7	244	3823	181	4.00
T8	256	4011	195	3.89
T9	240	3760	175	4.02
T10	126	1974	96	1.95
T11	124	1943	85	2.00

Test ID	Mass Solids (g)	Mass Soln (g)	Residue Mass (g)	Filtrate Vol (L)
T12	124	1943	99	1.95
T13	244	3823	178	3.74
T14	121	1896	85.8	1.94
T15	126	1974	89.7	1.82
T16	125	1958	93.6	2.32
T17	121	1896	91.9	1.96
T18	124	1943	95.5	1.91
T19	124	1943	96.2	1.89
T20	123	1927	96.2	1.98
T21	128	2005	92.5	1.96
T22	126	1974	92.0	1.98

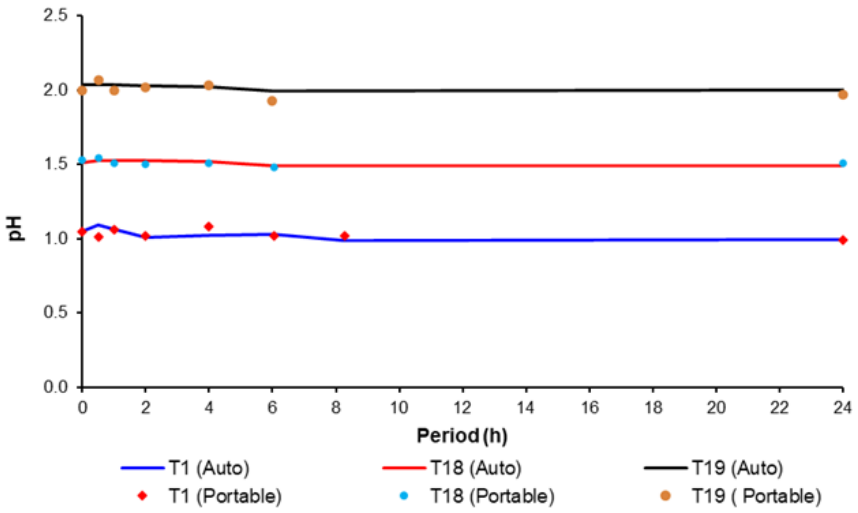

Figure C1: Sample pH Control

Table C5: Final Filtrate Composition (Bench-scale Leach Tests)

Test ID	Au	Ag	Al	As	Ca	Cd	Co	Cr	Cu	Fe	Li	Mg	Mn	Mo	Ni	Pb	S	Si	Sn	Ti	V	Zn
	ppm	ppm	ppm	ppm	ppm	ppm	ppm	ppm	g/L	g/L	ppm	ppm	ppm	ppm	ppm	ppm	g/L	ppm	ppm	ppm	ppm	ppm
T1(a)	< 5	< 2	1020	< 2	909	< 2	< 2	< 2	10.1	3.70	< 2	34.0	274	< 2	267	43.0	16.5	80.0	32.1	3.60	< 2	438
T1(b)			1033	< 2	640	2.58	4.68	5.56	10.6	3.60	6.62	36.8	265	< 2	256	16.2	17.1	115	4.7	< 2	< 2	512
T2			1990	< 2	272	< 2	4.19	3.86	20.0	1.20	< 2	15.5	42.8	<2	300	24.0	24.5	45.7	28.8	2.66	< 2	2830
T3			4030	< 2	107	< 2	5.55	53.3	7.25	4.60	< 2	13.6	58.8	< 2	270	20.9	20.3	109	711	< 2	< 2	1350
T4			10300	< 2	119	< 2	3.86	20.9	6.55	4.95	< 2	51.1	23.6	< 2	63.4	26.6	32.5	123	627	< 2	< 2	560
T5	< 5	< 2	1480	< 2	667	< 2	< 2	< 2	12.6	5.78	6.15	60.0	487	< 2	329	30.5	19.4	184	76.6	4.00	< 2	665
T6	< 5	< 2	2030	< 2	616	< 2	< 2	< 2	17.7	9.82	12.0	58.0	755	< 2	503	22.0	25.9	280	98.4	< 2	< 2	995
T7	< 5	< 2	848	< 2	826	< 2	< 2	< 2	8.79	3.34	< 2	25.0	217	< 2	220	9.5	13.1	67.0	48.5	4.3	< 2	343
T8	< 5	< 2	850	< 2	735	< 2	< 2	< 2	7.87	3.43	< 2	27.0	284	< 2	230	48.0	15.8	135	84.8	6.2	< 2	381
T9	< 5	< 2	616	< 2	411	< 2	< 2	< 2	7.25	2.92	< 2	22.0	231	< 2	188	169	12.6	107	116	3.1	< 2	403
T10			758	< 2	371	3.32	14.85	407	10.6	4.36	< 2	18.4	407	8.20	785	840	20.8	64.0	266	6.36	< 2	599
T11			668	< 2	202	2.52	6.11	10.3	10.4	3.59	< 2	16.6	300	< 2	251	936	15.5	92.8	2431	8.11	< 2	411
T12			906	< 2	816	3.02	5.3	2.34	6.42	3.45	< 2	28.4	258	< 2	195	11.9	18.1	65.1	35.9	2.70	< 2	424
T13	< 5	< 2	1030	< 2	894	< 2	< 2	84	11.3	4.76	2.30	32.0	338	< 2	336	44.0	22.1	107	30.3	7.10	4.2	569
T14	< 5	< 2	782	< 2	750	< 2	< 2	< 2	8.24	3.31	< 2	35.5	270	< 2	220	40.0	16.4	116	15.18	2.30	< 2	395
T15	< 5	< 2	932	< 2	685	< 2	< 2	< 2	8.27	3.56	< 2	45.0	281	< 2	308	34.0	17.6	136	6.50	< 2	< 2	443
T16	< 5	< 2	883	< 2	774	< 2	4.25	9.70	5.86	2.90	< 2	27.0	257	< 2	188	28.0	15.5	76.0	12.3	8.25	< 2	354
T17	< 5	< 2	784	< 2	624	< 2	4.80	4.40	7.66	3.14	< 2	24.0	280	< 2	229	33.0	15.6	68.0	13.0	3.70	< 2	400
T18	< 5	< 2	603	< 2	168	< 2	5.00	2.80	7.28	2.88	4.40	15.0	185	< 2	223	31.0	12.3	31.0	5.82	< 2	< 2	352
T19	< 5	< 2	588	< 2	120	< 2	8.10	3.00	7.43	2.81	5.20	14.0	142	< 2	223	35.0	11.7	25.0	6.14	< 2	< 2	314
T20	< 5	< 2	867	< 2	878	< 2	4.90	41.0	7.79	4.40	< 2	28.0	278	< 2	227	33.0	18.2	76.0	32.8	5.50	< 2	388
T21	< 5	< 2	1040	< 2	954	< 2	5.20	12.0	8.22	5.94	< 2	29.0	298	< 2	252	33.0	20.3	80.0	47.2	8.10	< 2	434
T22	< 5	< 2	833	< 2	825	< 2	5.30	4.50	8.13	7.71	< 2	27.5	292	< 2	256	23.0	20.2	67.5	69.4	8.95	< 2	447
Incinerated			1475	3.64	806	< 2	5.26	10.7	17.5	1.87	4.62	65.0	276	< 2	195	< 2	28.2	446		30.1	< 2	718
Incinerated &Milled			1233	8.95	826	< 2	5.01	20.1	20.1	2.48	3.66	49.7	219	< 2	179	< 2	20.2	820		39.4	< 2	243

Table C6: Residue Composition (Bench-scale Leach Tests)

Test ID	Al	Ca	Co	Cr	Cu	Fe	Mg	Mn	Ni	Pb	Si	Sn	Ti	V	Zn	Ag	Au	Pd	Pt
	%	%	%	%	%	%	%	%	%	%	%	%	%	%	%	ppm	ppm	ppm	ppm
T1(a)	4.88	8.29	< 0.05	0.058	0.495	3.46	0.30	0.29	0.22	0.87	21.3	1.84	0.88	< 0.05	0.26	1175	199	73.2	1.49
T1(b)	2.35	3.75	< 0.05	< 0.05	1.680	3.63	0.25	0.08	0.13	2.00	11.9	1.11	0.52	< 0.05	0.26	1300	220	91.0	1.33
T2	2.01	3.61	< 0.05	0.051	2.28	1.35	< 0.05	0.13	0.21	3.10	9.23	0.01	0.29	< 0.05	0.26	567	862	82.1	0.41
T3	1.87	2.82	< 0.05	0.100	7.90	1.92	0.27	0.23	0.17	1.05	11.5	3.65	0.21	< 0.05	0.32	317	794	14.6	0.56
T4	2.33	3.74	< 0.05	< 0.05	9.25	0.66	0.22	0.05	0.05	2.19	8.97	7.98	0.18	< 0.05	0.12	154	165	12.9	0.32
T5	4.90	9.04	< 0.05	0.090	3.98	2.93	0.28	0.06	0.27	0.13	22.8	1.99	0.91	< 0.05	< 0.05	1100	278	89.4	0.91
T6	4.81	8.94	< 0.05	0.078	7.65	2.18	0.27	< 0.05	0.36	0.12	20.4	3.19	0.84	< 0.05	< 0.05	1100	244	87.7	1.27
T7	4.91	8.57	< 0.05	0.053	0.700	3.16	0.30	0.35	0.24	0.96	22.2	1.91	0.84	< 0.05	0.14	1100	209	88.3	1.49
T8	4.99	9.10	< 0.05	0.074	2.33	3.19	0.29	0.10	0.25	0.12	22.6	1.30	0.88	< 0.05	< 0.05	1000	288	62.3	0.69
T9	5.85	10.8	< 0.05	0.072	0.590	2.71	0.32	0.12	0.20	0.08	23.5	1.03	0.73	< 0.05	< 0.05	940	193	32.7	2.10
T10	5.97	10.2	< 0.05	< 0.05	1.20	2.56	0.32	0.16	0.25	0.05	21.5	0.42	0.92	< 0.05	0.057	572	248	61.4	1.08
T11	7.01	11.1	< 0.05	< 0.05	0.790	2.09	0.33	0.13	0.23	< 0.05	24.3	0.01	0.98	< 0.05	< 0.05	431	295	52.8	1.94
T12	4.63	7.40	< 0.05	< 0.05	11.9	2.86	0.25	0.31	0.46	0.13	19.5	1.13	0.87	< 0.05	0.11	950	221	89.1	1.50
T13	4.95	8.40	< 0.05	0.053	0.520	2.79	0.29	0.15	0.22	1.10	21.4	1.79	0.89	< 0.05	0.44	1050	182	64.9	0.93
T14	5.36	9.45	< 0.05	0.075	0.600	2.26	0.30	< 0.05	0.21	0.16	26.7	1.25	1.06	< 0.05	< 0.05	950	191	66.9	0.81
T15	5.31	9.04	< 0.05	0.076	0.520	1.83	0.29	< 0.05	0.13	0.18	27.5	1.23	1.06	< 0.05	< 0.05	1000	379	81.9	2.02
T16	5.04	9.07	< 0.05	0.077	5.16	3.79	0.37	0.14	0.26	0.14	25.5	1.69	1.00	< 0.05	0.11	925	381	93.8	1.38
T17	5.45	9.91	< 0.05	0.061	4.33	3.46	0.37	0.22	0.26	0.16	25.3	1.73	0.95	< 0.05	0.13	800	301	91.9	7.50
T18	5.99	11.0	< 0.05	0.068	3.09	4.54	0.38	0.59	0.27	0.28	24.3	1.64	0.91	< 0.05	0.23	700	283	79.3	1.11
T19	5.69	10.5	< 0.05	0.067	4.37	5.14	0.37	0.77	0.31	0.23	22.0	1.73	0.90	< 0.05	0.21	700	315	93.4	1.49
T20	5.23	9.10	< 0.05	0.076	1.67	3.31	0.35	0.17	0.26	0.20	26.9	1.63	1.01	< 0.05	0.11	1350	349	84.4	2.07
T21	5.32	9.31	< 0.05	0.097	1.53	3.93	0.36	0.22	0.30	0.15	27.5	1.61	1.10	< 0.05	0.12	842	315	88.0	3.68
T22	5.42	9.23	< 0.05	0.085	0.42	3.48	0.38	0.17	0.21	0.14	29.8	1.41	0.93	< 0.05	0.09	900	261	67.3	1.08
Incinerated	6.19	7.28	<0.05	0.07	1.38	7.85	<0.05	0.6	0.7	1.64	17.60	4.07	0.71	<0.05	1.16	684	109	71	0.75
Incinerated &Milled	5.58	5.99	<0.05	0.12	2.23	7.64	<0.05	0.5	0.8	1.77	15.30	4.89	0.81	<0.05	1.16	1400			

Table C7: Pilot Test Loading Details

Pilot Test Loading Details		
Parameter	**Unit**	
Particle Size	mm	-1
pH		1-1.2
Temperature	°C	50
Solids concentration	% w/w	6.0
Airflow rate	L/h	200
Solution Mass	kg	23.18
Solution SG		1.008
Feed Mass	kg	1.47
Reactor Volume	(L)	23
Impeller Speed	rpm	365
Chloride concentration	g/L	10
Initial Cu(II) concentration	g/L	0.5
Initial Fe(II) concentration	g/L	0

Table C8: Pilot Test Off-loading Details

Pilot Test Off-loading Details		
Parameter	**Unit**	
Filtrate mass	kg	23.27
SG		1.072
Filtrate volume	L	21.71
Acid wash mass	kg	23.15
SG		1.002
Acid wash volume	L	23.10
Water wash mass	kg	11.48
SG		0.994
Water wash volume	L	11.6
Solid residue mass (wet)	kg	1.62
Solid residue mass (dry)	kg	1.03
Solid residue moisture	kg	0.59
Mass loss	(%)	29.9

Table C9: Pilot Test Solution Analysis

Element	Al	As	Ca	Cd	Co	Cr	Cu	Fe	Li	Mg	Mn	Mo	Ni	Pb	S	Si	Ti	V	Zn
Sample	ppm	ppm	ppm	ppm	ppm	ppm	g/L	g/L	ppm	ppm	ppm	ppm	ppm	ppm	g/L	ppm	ppm	ppm	ppm
Feed	< 2	< 2	17.5	< 2	< 2	< 2	0.55	0.005	< 2	6.32	< 2	< 2	< 2	< 2	5.0	< 2	< 2	< 2	< 2
30 min	679	< 2	244	2.51	< 2	4.11	0.01	1.27	5.88	17.40	88.3	< 2	18.6	12.30	3.50	37.6	< 2	< 2	111
1 hr	839	< 2	431	2.62	< 2	4.93	0.02	1.84	5.69	22.00	82.5	< 2	26.2	11.50	6.71	55.2	< 2	< 2	111
2 hr	892	< 2	461	2.71	< 2	6.20	2.21	3.11	5.64	22.60	122	< 2	92.9	11.50	10.1	57.7	< 2	< 2	178
2.5 hr	919	< 2	507	2.68	2.4	6.28	3.81	3.15	5.71	24.00	119	< 2	140	9.28	10.5	63.1	< 2	< 2	239
3hr	948	< 2	558	2.91	< 2	6.47	7.28	3.47	5.78	31.05	164	< 2	149	10.40	11.7	66.5	< 2	< 2	389
4hr	976	< 2	530	2.70	< 2	6.79	9.36	3.49	5.64	29.50	156	< 2	171	10.80	16.0	71.9	< 2	< 2	452
5hr	987	< 2	560	2.72	< 2	7.91	11.6	3.57	5.89	29.90	165	< 2	184	11.90	16.4	74.3	< 2	< 2	520
6hr	1030	< 2	528	2.72	< 2	9.66	13	3.54	5.81	32.00	153	< 2	190	13.60	19.0	76.0	< 2	< 2	544
7hr	1060	< 2	568	2.72	2.11	11.6	13	3.54	5.7	37.50	160	< 2	195	15.50	18.5	80.9	2.52	< 2	550
8hr	1080	< 2	613	2.71	< 2	13.8	13.15	3.48	5.79	34.20	143	< 2	198	16.15	18.5	84.6	2.91	< 2	544
17hr	1110	< 2	751	2.71	2.13	49.8	13.2	3.56	5.65	35.60	129	< 2	224	18.90	18.5	95.1	5.20	< 2	544
20hr	1140	< 2	784	2.73	2.25	68.2	12.9	3.68	5.50	36.20	136	< 2	230	19.40	18.0	96.3	5.76	< 2	557
24hr	1140	< 2	808	2.73	2.38	93.6	13.4	3.79	5.33	37.20	145	< 2	244	19.80	18.7	98.2	6.42	< 2	560
Filtrate	1090	< 2	799	2.66	2.20	92.6	12.7	3.68	5.17	34.70	140	< 2	237	19.50	17.8	96.6	6.15	< 2	542
Acid wash	46.6	< 2	122	< 2	< 2	5.87	0.561	0.18	< 2	6.68	7.59	< 2	14.3	2.15	1.64	7.77	< 2	< 2	25.7
Water wash	< 2	< 2	14.7	< 2	< 2	< 2	0.014	0.004	< 2	5.28	< 2	< 2	< 2	< 2	0.14	2.22	< 2	< 2	< 2

Table C10: Pilot Test Residue Analysis

Sample	Al	Ca	Co	Cr	Cu	Fe	Mg	Mn	Ni	Pb	Si	Ti	V	Zn	Ag	Au	Pd	Pt	Sb	Sn
	%	%	%	%	%	%	%	%	%	%	%	%	%	%	ppm	ppm	ppm	ppm	ppm	ppm
A	5.53	8.70	< 0.05	0.08	0.58	4.94	0.34	0.41	0.21	0.79	22.1	0.90	< 0.05	0.37	786	225	82.8	2.43	3363	2.25
B	5.37	8.70	< 0.05	0.07	0.67	4.64	0.34	0.40	0.20	1.49	21.9	0.86	< 0.05	0.45	602	204	65.1	1.19	3450	2.53
C	5.50	8.59	< 0.05	0.12	0.66	5.03	0.36	0.43	0.23	1.14	21.9	0.91	< 0.05	0.40	821	229	72.2	0.95	3700	2.33
D	5.42	8.64	< 0.05	0.18	0.58	5.34	0.37	0.41	0.27	1.09	22.1	0.89	< 0.05	0.40	496	215	65.2	1.25	3500	2.50
Average	**5.46**	**8.66**	**< 0.05**	**0.11**	**0.62**	**4.99**	**0.35**	**0.41**	**0.23**	**1.13**	**22.0**	**0.89**	**< 0.05**	**0.41**	**676**	**218**	**71.3**	**1.45**	**3503**	**2.40**